

Sheffield Hallam University

The effect and interactions of interstitial hydrogen and nitrogen in ferritic steels.

HIGGINS, Andrew D.

Available from the Sheffield Hallam University Research Archive (SHURA) at:

<http://shura.shu.ac.uk/19790/>

A Sheffield Hallam University thesis

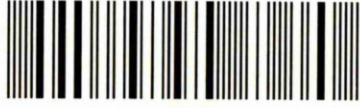
This thesis is protected by copyright which belongs to the author.

The content must not be changed in any way or sold commercially in any format or medium without the formal permission of the author.

When referring to this work, full bibliographic details including the author, title, awarding institution and date of the thesis must be given.

Please visit <http://shura.shu.ac.uk/19790/> and <http://shura.shu.ac.uk/information.html> for further details about copyright and re-use permissions.

101 927 432 8



REFERENCE

ProQuest Number: 10697092

All rights reserved

INFORMATION TO ALL USERS

The quality of this reproduction is dependent upon the quality of the copy submitted.

In the unlikely event that the author did not send a complete manuscript and there are missing pages, these will be noted. Also, if material had to be removed, a note will indicate the deletion.



ProQuest 10697092

Published by ProQuest LLC (2017). Copyright of the Dissertation is held by the Author.

All rights reserved.

This work is protected against unauthorized copying under Title 17, United States Code
Microform Edition © ProQuest LLC.

ProQuest LLC.
789 East Eisenhower Parkway
P.O. Box 1346
Ann Arbor, MI 48106 – 1346

The Effects and Interactions of Interstitial Hydrogen and Nitrogen in Ferritic Steels

by
Andrew D. Higgins

A thesis submitted in partial fulfilment of the requirements of
Sheffield Hallam University
for the degree of Doctor of Philosophy

June 2009

Supervisor:- Professor J. D. Atkinson

The Effects and Interactions of Interstitial Hydrogen and Nitrogen in Ferritic Steels

Thesis presented for a Doctorate in Philosophy

by

Andrew D. Higgins

Abstract

This thesis details work that has been carried out in three main areas, these are:
The evaluation of a physical as opposed to a chemical method for measuring the quantity of ammonia formed when hydrogen is reacted with the free nitrogen in a steel sample. Unfortunately the work has shown that due to the very small quantities of ammonia produced this is not a viable technique. The findings also indicate that any method using hydrogen to extract nitrogen as ammonia will give an over estimate of the free nitrogen content.

The commissioning of a Vibran Interstitial Analyser and the design and development of a mathematical model which allows the free (uncombined) nitrogen and carbon contents to be determined from the measured data. The results from this work have been used to produce a modified equation for the predicting of the Impact Transition Temperature. There is also the possibility of developing a new method for measuring hydrogen in steel

In the third section of the work experimental evidence has been produced to show that hydrogen in iron at low temperatures can show metallic behaviour. Further testing of hydrogen treated materials has shown that at temperatures in the range -56 to -20°C hydrogen reduces the work hardening coefficient of Armco iron and mild steels with both low and high free nitrogen contents.

CONTENTS

	Page
Acknowledgements	4
1.0 Introduction	6
1.1 Objectives	10
2.0 Literature Review	11
2.1 Effects of Nitrogen in Steel	11
2.2 Measurement of Free Nitrogen	22
2.3 Effect of Hydrogen in Steel	28
2.4 Metallic Hydrogen	37
3.0 Experimental Work	43
3.01 Experimental Materials	43
3.1 Evaluation of the Feasibility of using a Thermistor Bridge to Measure a Small Concentration of Ammonia in a Hydrogen Gas Stream.	44
3.2 The Measurement of Internal Friction using the Vibran Interstitial Analyser.	55
Observations on the effect of Free Nitrogen on the Impact Transition Temperature	82
The Effects of Hydrogen dissolved in Armco Iron.	93
3.3 Experiment to examine the Nature of Hydrogen dissolved in Iron.	93
3.4 Experiment to ascertain if Hydrogen gives rise to Dynamic Strain Ageing in Iron.	110
4.0 General Discussion	127
5.0 Conclusions	143
6.0 Recommendations	145
7.0 References	146
Appendices	

Acknowledgements

I would like to thank the following people without whose help this project would have been either much more difficult or much more expensive. Professor John Atkinson, Professor Mike Bramhall, Keith Wright, Tim O'Hara and Tony Earnshaw at Sheffield Hallam University, Stuart Southeran at Corus Swinden Technology Centre and my friend Dr Paul Roebuck who patiently let me try out ideas on him. And finally to my wife Heather and Mark and Rachael my children for listening to my arguments, challenging my ideas, correcting my English and putting up with me.

Andrew D. Higgins
June 2009

Declaration

No material contained in this thesis has been used in any other submission for an academic award.

Some results from the Internal Friction work are now in the public domain in the following papers:

J.D. Atkinson, M.R. Corrigan and A.D. Higgins, *Presentation at the International .Co-operative Group on Environmentally Assisted Cracking Annual Meeting*. Antwerp, April 2005.

J.D. Atkinson, M.R. Corrigan, A.D. Higgins and Z.J. Zhao, *The Interaction of EAC and DSA in C-Mn Piping Steels*, 13th Environmental Degradation of Water Reactor Materials Conference, August 2007.

“If, in some cataclysm, all of scientific knowledge were to be destroyed, and only one sentence passed on to the next generations of creatures, what statement would contain the most information in the fewest words? I believe it is the *atomic hypothesis* that *all things are made of atoms – little particles that move around in perpetual motion, attracting each other when they are a little distance apart, but repelling upon being squeezed into one another.* In that one sentence, you will see, there is an *enormous* amount of information about the world, if just a little imagination and thinking are applied.”

Richard P. Feynman
Lectures on Physics, June 1963

1.0 Introduction

Due to the massive economic importance of steel in modern society, the role of the interstitial element carbon has been extensively studied for over a hundred years. By contrast for many years the role of nitrogen in steel was virtually ignored, yet steels produced by Bessemer converters, where air was blown through the molten steel, had significant nitrogen contents. With the introduction of oxygen steelmaking, the loss of the effects of nitrogen became apparent and this led to various major investigations into the roles of carbon and nitrogen being carried out in the 1950s and 60s.

As a result of the problems of brittle failure that had occurred in large welded structures this work tended to concentrate on the deleterious effects of nitrogen (and carbon) on both fracture properties and the problems caused by yielding. This led to the introduction of various techniques for removing or tying up interstitial elements and the development of the Interstitial Free Steels (IFS). This particular aspect of the work being primarily driven by the needs of the car manufacturers for formable sheet steel for body panels.

Another area where the damaging effects of nitrogen (and carbon) has led to on going investigations is in Dynamic Strain Ageing (DSA) where at temperatures in the region of 250°C slow strain rate tensile testing results in a peak in the tensile strength and a corresponding drop in ductility (normally measured as reduction of area). This drop in ductility at the temperature at which the blue patina forms on tempering a ground steel surface was first reported by Stromeyer in the 1880s and gave rise to the term 'blue brittleness'⁽¹⁾. The problem had almost certainly been known to blacksmiths for many years, but not recorded until Stromyer's paper in 1885.

Le Chatelier's work in 1909 showed that at slow strain rates there was a corresponding increase in the tensile strength of mild steel when tested in this blue brittle temperature region⁽²⁾.

In 1919 Fettwiess showed that this behaviour and the multiple or serrated yielding that accompanied it was related to the static ageing phenomena and this gave rise to the term 'dynamic strain ageing'⁽³⁾ i.e. this appeared to be the same mechanism but due to the increased temperature was occurring continuously rather than after a period of hours.

The work by Taylor⁽⁴⁾, in 1934, on the concept of slip occurring as a result of the movement of dislocations within a crystal along with the experimental work of Davenport and Bain⁽⁵⁾, in 1935, laid the foundation for Nabarro's 1948 paper⁽⁶⁾ proposing that serrated yielding in steel occurred when the temperature was high enough to allow carbon and nitrogen atoms to diffuse sufficiently fast to allow strain ageing to take place during plastic deformation⁽⁷⁾. Cottrell and Bilby's work⁽⁸⁾ refined this concept of carbon (and later nitrogen) atmospheres locking dislocations.

Carbon tended to feature as the prime interstitial atom for dislocation locking probably because carbon contents in steel were much easier to measure than nitrogen contents.

The value of nitrogen was recognised in the nineteen sixties particularly in the aluminium killed C-Mn steels where aluminium nitride pinned austenite grain boundaries giving a refined ferrite grain size on transformation⁽⁹⁾ and the additional benefit when coupled with controlled rolling⁽¹⁰⁾. However, relatively little attention was paid to the role of 'free' or uncombined nitrogen.

In the nineteen nineties nitrogen's value in producing fine alloy carbo-nitrides as compared to the coarser more brittle alloy carbides started to be appreciated⁽¹¹⁾. Further

studies on the beneficial effects of nitrogen, with particular emphasis on corrosion resistance, have continued and led in the 1990's to the development by several European steel makers of new hard stainless steels where carbon, which degrades the corrosion resistance, was partially replaced with nitrogen, which enhances corrosion resistance. These steels, in replacing some of the carbon with nitrogen, form nitrogen rich martensites and fine carbo-nitrides rather than big brittle carbides. An example of this type is Cronidur 30 made by a subsidiary of Krupps and Thyssen which only contains 0.3% carbon but can be hardened to 700HV as a result of the 0.4% nitrogen it contains. However, getting this high level of nitrogen into the steel requires remelting using a Pressurised Electro Slag Reactor (PESR). Silicon nitride is added during the electro slag remelting and breaks down releasing nitrogen into the steel. The whole process being carried out under nitrogen at a pressure of ~10 bar.

The French steelmakers Aubert and Duval have also developed a high nitrogen stainless steel which does not require the use of a PESR. These developments have been mainly driven by the needs of the aerospace industry.

Despite the promise shown by nitrogen in these more esoteric materials, relatively little work has been done on the potential benefits of increased nitrogen levels in non-stainless steels or on how the deleterious effects of nitrogen may be moderated.

The other major interstitial element that occurs in steel is hydrogen. Unlike the other interstitial elements hydrogen does not appear to have any benefits and all the major research has been on its removal, usually at the liquid steel stage, or on the production of hydrogen resistant steels. However, the actual behaviour of hydrogen in steel still presents some anomalies, a more detailed study of which may give a better understanding of the mechanisms of hydrogen degradation.

Similarly the interaction of relatively low levels of nitrogen and hydrogen in steel is a relatively unexplored area of metallurgy with possible new applications to be discovered.

1.1 Objectives of the Present Work

The initial objectives of this work were;-

- 1) Develop two separate methods for the determination of free nitrogen in steel, one by hydrogen extraction and one by internal friction.
- 2) Use the free nitrogen values obtained to determine if an improved equation for predicting Impact Transition Temperatures could be developed.
- 3) To determine the nature of hydrogen dissolved in iron.
- 4) To see if there was any evidence of Dynamic Strain Ageing, in steels with high and low nitrogen contents, due to Hydrogen at temperatures below 0°C.

The experimental work for this project has divided down to four main areas;-

- i) Determining the feasibility of using a thermistor bridge to measure the ammonia produced when using hydrogen extraction to measure the nitrogen content of a steel sample.
- ii) Measurement of the free nitrogen content by internal friction.
- iii) Investigation of the behaviour of dissolved hydrogen.
- iv) Low strain rate tests to look for evidence of DSA due to hydrogen and to determine if hydrogen produces a work hardening effect.

2.0 Literature Review

2.1 Effects of Nitrogen in Steel

Early in the 20th century nitrogen's fate might have appeared to have been settled; *"The injurious influence of nitrogen on the mechanical properties of iron is now firmly proved. As shown by its position in Mendeleeff's periodic system, nitrogen would necessarily be an injurious impurity."*⁽¹²⁾

Whilst the benefits of carbon in giving steel its useful properties were recognised, for nitrogen it would appear to be a case of 'give a dog a bad name' syndrome (as nitrogen was in the same group as phosphorus this 'proved' it must be bad). Tschischewski's paper, of which the above quote is the opening statement, dealt entirely with the loss of ductility caused by nitrogen but with no mention of an increase in tensile strength. This was probably the result of the very high quantities of nitrogen (the lowest level mentioned in the paper is 0.025%) used in his experiments which produced brittle coatings of iron nitride on the surface of the iron wires used for determining the ductility (measured as % strain). It should be pointed out however, that in the subsequent discussion of the paper, Dr W. H. Hatfield felt Tschischewski had gone 'a great deal too far' in his denunciation of nitrogen. However, the paper went on to examine how nitrogen got into iron and the effects it had on the main alloying additions but again only in very large amounts. The effects of this 'bad name' have been slow to disappear and Tschischewski's results were still being cited as late as the 1950's⁽¹³⁾.

Nitrogen, like carbon, when in solution as an interstitial in steel results in increases in hardness and yield strength in the temperature range 100 – 200°C and a corresponding decrease in toughness⁽¹⁴⁾. Various workers^(15,16) have also shown that nitrogen increases the Impact Transition Temperature (ITT) in Charpy tests and high levels of uncombined

nitrogen can result in a change in the fracture energy to occur above room temperature with a resultant change from ductile to brittle behaviour. In pure body centred iron it has been shown that nitrogen segregates to the grain boundaries and that this segregation can result in intergranular embrittlement^(17,18). This mechanism probably occurs in steels, as killed steels where nitrogen is tied up by silicon or aluminium show improved impact properties compared to un-killed or semi-killed steels⁽¹⁹⁾. Bramhall showed that additions of titanium and aluminium, in an 8%Mn steel, reduced the Ductile Brittle Transition Temperature (DBTT) presumably by tying up free nitrogen but also reduced the hardness in both the air cooled and the water quenched condition⁽²⁰⁾.

However, it is the effect on the yield that for many commercial steel applications has resulted in nitrogen being simply regarded as an 'undesirable residual' due to the phenomenon of strain ageing. Strain ageing is the reappearance of a yield point in steel that has previously been deformed beyond the yield point into the plastic region. The current interpretation for this phenomena was first put forward by Cottrell and Bilby in 1948⁽⁸⁾. Their paper specifically dealt with carbon but they pointed out that the arguments could '*with very little modification*' be applied to nitrogen. Nitrogen, and to a lesser extent carbon, gradually diffuse to the preferential sites around the new dislocations that have formed when the steel initially yielded. This leads to the reappearance of the yield phenomena and the associated problems this causes when attempting to produce smooth cold formed shapes. Normally this only occurs after the steel has been allowed to stand at room temperature for a period of several weeks or months⁽²¹⁾ but even a small rise in temperature can significantly speed up the diffusion and so shorten this time. As a result, a lot of work has been carried out on producing 'interstitial free' steels, such that bulk steels with <20ppm of nitrogen are now routinely produced for use in the automobile sector, for pressed body and chassis components⁽²²⁾.

Nitrogen generally causes more of a problem with strain ageing than carbon as a result of its higher solubility in ferrite⁽²³⁾, the carbon being precipitated out on existing carbides whilst the nitrogen is still free to migrate to new dislocations.

At temperatures above ambient but below $\sim 400^{\circ}\text{C}$ the return of the yield point occurs much more rapidly and yielding becomes a continuous event known as dynamic strain ageing as nitrogen (and some of the carbon) rapidly migrates to the preferential sites around new dislocations as they form. This results in an increase in the tensile strength of the steel, and a drop in the ductility and fracture toughness. These effects tend to peak at temperatures around 250°C . This was explained (for carbon) by Cottrell and Bilby as the formation of saturated atmospheres around new dislocations which would only require a carbon level of $0.003\text{wt}\%$ ⁽⁸⁾ (or a similar level of nitrogen). However, Gladman has pointed out that the interstitial levels associated with strain age hardening and strain age embrittlement are well in excess of this level⁽²⁴⁾. His suggested explanation being that carbide (and nitride) precipitation occurs on the dislocations giving an additional precipitation strengthening effect. Work initially by Baird and MacKenzie⁽²⁵⁾ and later by Baird and Jamieson⁽²⁶⁾ showed that whilst nitrogen alone in pure iron gave a high rate of strain hardening (a symptom of dynamic strain ageing) up to 225°C a manganese and nitrogen addition to iron continued this effect up to 450°C . Baird and Jamieson suggested that this effect was due to pairs or small clusters of manganese and nitrogen atoms where the presence of the manganese restricted the mobility of the nitrogen atoms around moving dislocations.

Nitrogen can exist in steel, either as uncombined 'free' nitrogen (sometimes called lattice nitrogen), or chemically combined with other elements in the form of nitrides or carbo-nitrides. The strain ageing effects are due to free nitrogen which is why they can

be removed from low nitrogen steels by the addition of strong nitride formers such as titanium which ties up any free nitrogen, preventing its migration to sites around dislocations. However this is not a straight forward phenomena as Brindley and Barnby have shown that in coarse grained low nitrogen mild steel strained in the temperature range 200 – 300°C new dislocations form at such a rate that yielding, as evidence by a drop in the stress without a previous rise, occurs repeatedly but this phenomena does not occur in a similar steel with a high free nitrogen content ⁽²⁷⁾ (see figures 2.1 and 2.2).

Their explanation is that in the low nitrogen steel there is insufficient nitrogen to lock the newly forming dislocations immediately, whereas in the high nitrogen steel the dislocations are locked as they form and remain locked. This is reflected in the greater capacity for work-hardening in the high nitrogen steel.

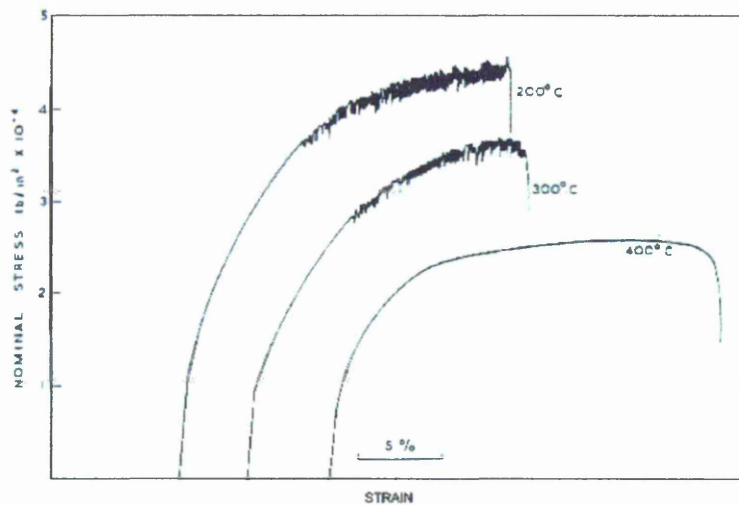


Fig. 2.1 Stress – Strain curves for coarse grained low nitrogen material as a function of temperature. (from Brindley and Barnby ⁽²⁷⁾)

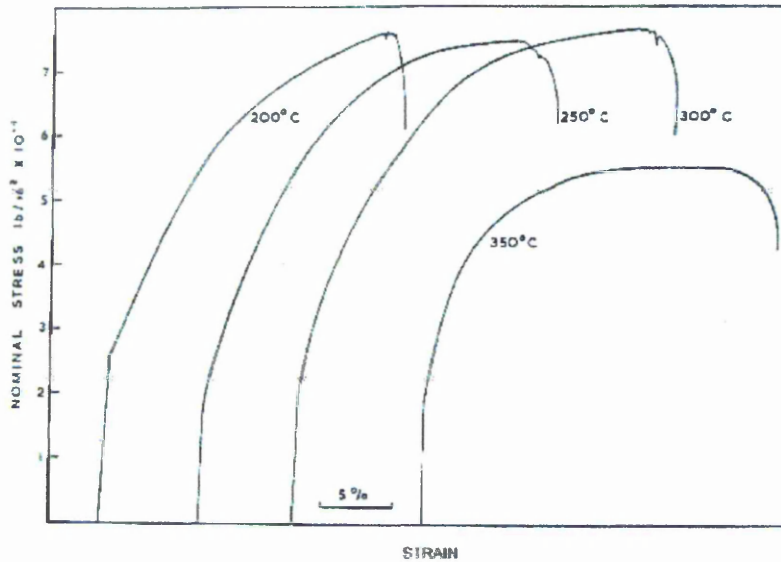


Fig. 2.2 Stress – Strain curves for coarse grained high nitrogen material as a function of temperature. (from Brindley and Barnby⁽²⁷⁾)

2.1.1 Interaction Effects

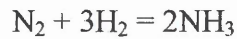
Work has been carried out by various groups on combined nitrogen and the benefits it gives in terms of fine precipitates and improved corrosion resistance. Pickering has produced a review of much of this work⁽²⁸⁾.

Gavriljuk et al. have shown that nitrogen in austenitic stainless steel reduces the damaging effects of hydrogen⁽²⁹⁾ but the main mechanism appears to be the stabilisation of the γ phase(austenite) which hydrogen would normally cause to transform to the ϵ (epsilon) phase.

Plasma nitriding has been shown to reduce the absorption of hydrogen in both Armco iron and austenitic stainless steel^(30,31). Various workers have also shown that nitriding, and carbo-nitriding, give beneficial effects in fatigue^(32,33,34,35) and moreover, nitrogen whether from nitriding or in the bulk steel has been shown to reduce corrosion fatigue⁽³⁵⁾. However, relatively little work has been done on understanding the mechanisms governing the effect of ‘free’ nitrogen and in particular, on how it interacts

with interstitial hydrogen, and on the role of possible precipitates of nitrides and hydrides acting as nuclei for brittle fracture.

Hydrogen does react with nitrogen in the presence of iron to form ammonia;



And whilst the equilibrium constant, at room temperature, for the reaction is high (6×10^5) the process is extremely slow at room temperature⁽³⁶⁾.

Rogers⁽³⁷⁾, working with Armco iron specimens, showed that the yield point could be removed when high levels of hydrogen were introduced into the specimen by electrolytic charging. He postulated that hydrogen did not displace the carbon and nitrogen atmospheres attached to dislocations but attached itself to loops of dislocations which were released from carbon and nitrogen atoms by thermal fluctuations, lowering the energy, and thereby the stress, necessary for the formation of a critical-size loop. This was based on internal friction measurements that showed there was no increase in free nitrogen after hydrogen charging.

However, later work suggested that the loss of the yield point was not due to the hydrogen *per se* but probably a result of the plastic strain caused by the hydrogen charging which gives hydrogen contents equivalent to those produced by exposure to very high pressure hydrogen gas.

The explanation for the yield point at that time (~1950) was that yielding occurred when the stress was sufficient to break the dislocation from its carbon and nitrogen atmosphere. The current view, based on Cottrell and Bilby's work⁽⁸⁾, that yielding is due to the formation of new dislocations which on subsequent ageing collect their own atmospheres, would tend to support Rogers' original postulate.

The possibility still exists that hydrogen may affect the yield behaviour as Ferreira et al⁽³⁸⁾ demonstrated that hydrogen reduced the elastic interactions between dislocations and elastic centres which act as barriers, such as nearby dislocations and solute pinning points. Based on the fact that this occurred in various crystal structures they suggested that this was a general mechanism. The experimental work that they carried out supported a 'hydrogen shielding mechanism' previously proposed by Sofronis and Birnbaum^(39,40,41) where the presence of a hydrogen atmosphere around a dislocation 'shields' its interaction with other elastic centres such as dislocations and solute atoms. However, Ferreira's experimental materials, pure aluminium and stainless steel containing molybdenum and vanadium, would have had very low levels of free interstitials such as nitrogen for dislocation pinning.

Work has also been carried out which suggests that the peak conditions for stress corrosion cracking, a hydrogen related phenomena, correspond to the peak conditions for dynamic strain ageing⁽⁴²⁾, an effect known to be due to nitrogen, yet the two effects are apparently due to two different mechanisms.

2.1.2 Impact Transition Temperature

Free nitrogen is known to increase the Impact Transition Temperature (ITT) and various models have been proposed for estimating ITT⁽¹⁶⁾, the most widely used of these being that due to Pickering and Gladman^(9, 43):-

$$ITT = - 19 + 44*(Si\%) + 700*\sqrt{N_f} + 2.2*(Pearlite \%) - 11.5*d^{-1/2}$$

Where N_f = free nitrogen content, and d = average grain diameter in millimetres.

However, this equation was a development of an equation for a simple plain carbon steel produced by multiple regression analysis of a range of test results ⁽⁹⁾. There appears to be no theoretical basis for the factor of $700x\sqrt{N_f}$ (N_f = free nitrogen content) and the equations given in Pickering's Kyoto paper⁽⁴³⁾ for flow stress and fracture stress use straight free nitrogen values. (Brittle failure will occur when the flow stress, which increases with decreasing temperature exceeds the fracture stress, which is relatively unaffected by temperature.) Data generated by Mintz⁽¹⁶⁾ indicated that the $700x\sqrt{N_f}$ factor only fitted steels with a low (<0.1%) silicon content and that for steels with a silicon content of >0.1% a factor of $2750 \times \%N_f$ gave a better fit.

From figure 2.3 it can be clearly seen that the square root of the free nitrogen content gives a reasonable linear fit to the low silicon steels but not to the silicon killed steels. Mintz's equation for the silicon killed steels is ;

$$ITT = 15 + 50*(Si\%) + 2750*N_f\% + 2.2*(Pearlite \%) - 11.5*d^{-1/2} + 70*Al\%$$

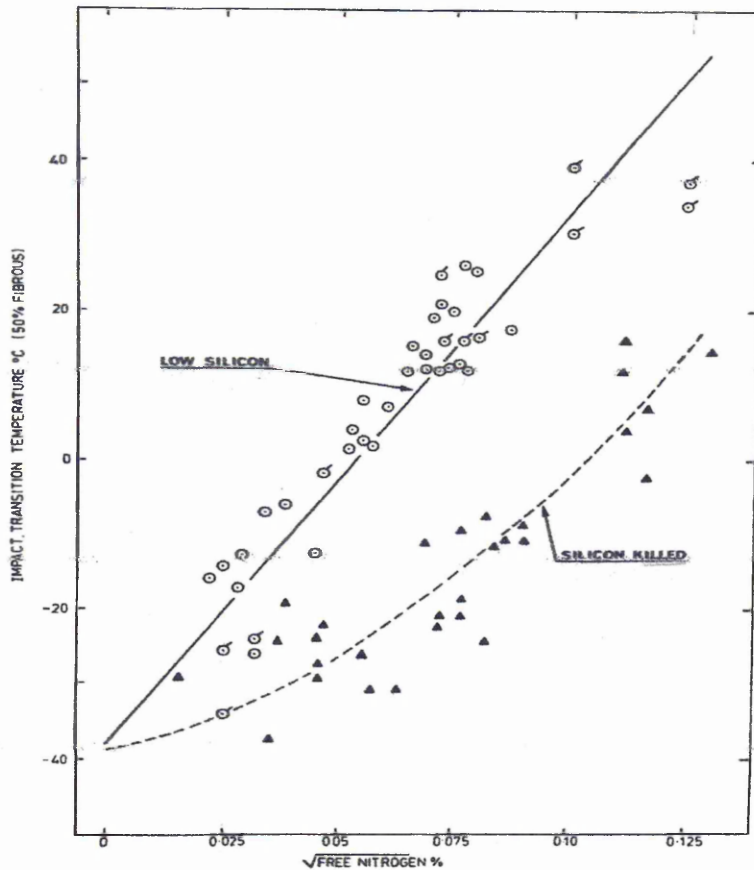


Fig. 2.3 Influence of free nitrogen on impact temperature of low-silicon (~0.03%) and silicon-killed (~0.3%), 0.6%Mn steels Data standardized to grain size of $d^{-1/2} = 8 \text{ mm}^{-1/2}$ and to zero Al and Si levels using calculated correction factors and a Pearlite volume fraction of $16 \pm 2\%$ ⁽¹⁶⁾

Similarly Bucher et al. (quoted in ref. 16) had found the following formula fitted their data for as-rolled steels:

$$\text{ITT} = 60 + 1500 \cdot N_f\% + 2 \cdot P\% - 191 \cdot d^{-1/2} - 48 \cdot \text{Mn}\%$$

Again this formula uses the free nitrogen weight percentage rather than the square root value. (It should also be noted that in both these equations the constant has a positive value and is much larger than in the Pickering Gladman equation.)

Figure 2.4 shows the data for the silicon-killed steels replotted against % free nitrogen.

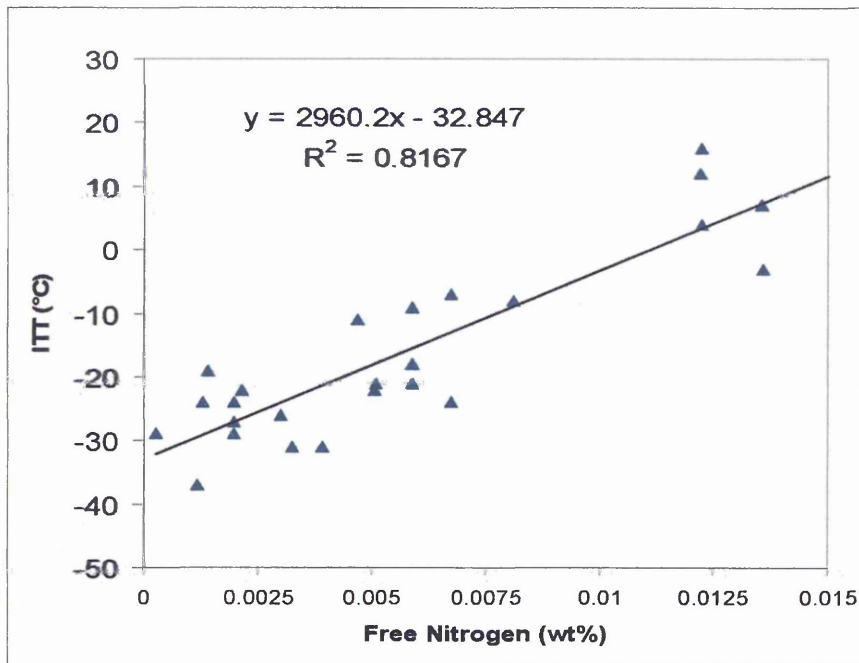
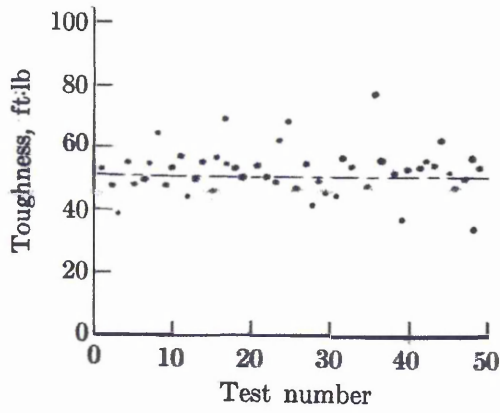


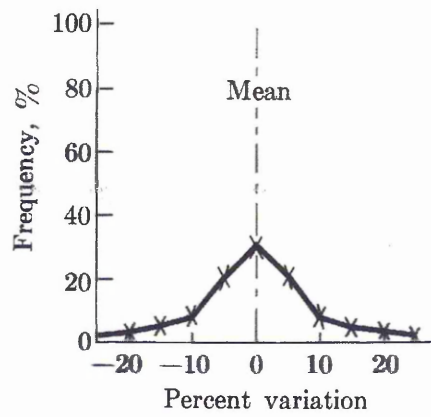
Fig. 2.4 Data for silicon-killed steels plotted against % free nitrogen

Based on a Microsoft Excel plot the replotted values give a nitrogen factor of 2960 which is similar to the value of 2750 used in Mintz's equation. (The plot shown in figure 6 of Mintz's 1973 paper⁽¹⁹⁾ actually gives a factor of 2570 for the free nitrogen but this is probably a typing error.)

However, any attempt to model impact transition temperatures run into the problem that the Charpy test has a very high level of variance⁽⁴⁴⁾, i.e. poor reproducibility. Figures 2.5a and 2.5b show the scatter and the variance for Charpy and tensile results from 50 identically tested samples of SAE 1040 steel.

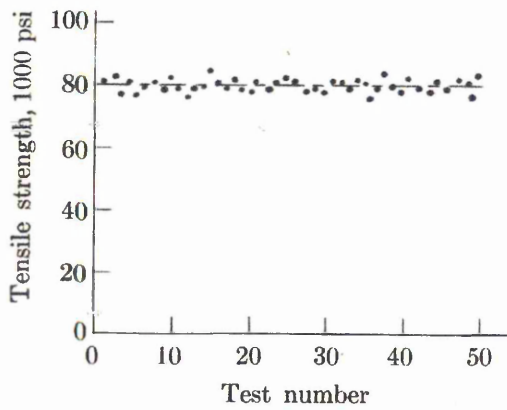


(a)

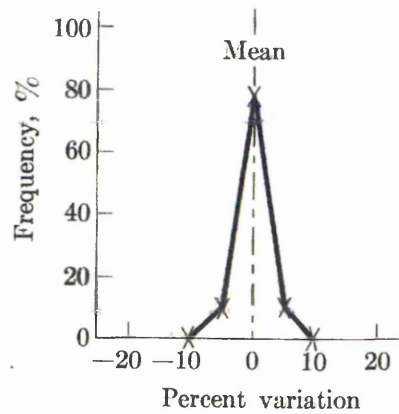


(b)

Fig. 2.5a Variance encountered with Charpy impact testing of SAE 1040 at 21°C (70°F). All tests were identical. (a) Scatter data. (b) Frequency distribution.
(from Van Vlack⁽⁴⁴⁾)



(a)



(b)

Fig. 2.5b Variance encountered with tensile testing of SAE 1040 at 21°C (70°F). All tests were identical. (a) Scatter data. (b) Frequency distribution.
(from Van Vlack⁽⁴⁴⁾)

2.2 Measurement of 'Free' Nitrogen

Measurements of nitrogen in steel can be either, total nitrogen which includes free or lattice nitrogen, nitrogen combined as nitrides and carbo-nitrides and nitrogen in pores or separate measurements of free, combined or pore nitrogen⁽⁴⁵⁾. Nitrogen can also be measured in the liquid steel by the Nitris® technique where a mixture of nitrogen and helium of known composition is bubbled through the liquid steel and the gas collected and the composition compared with that of the original mixture⁽⁴⁶⁾.

The aim of this work is the effect of free nitrogen in solid steel and there are three main methods for determining free nitrogen;-

- i) Hydrogen carrier gas method.
- ii) Internal Friction measurements.
- iii) Total nitrogen figure minus chemically insoluble fraction.

2.2.1 Hydrogen Carrier Gas Method

This method effectively uses the Haber Bosch process to react the free nitrogen with hydrogen to form ammonia at around 450°C, the steel acting as a catalyst. The quantity of ammonia formed is measured by a chemical titration. This method was refined by Headridge and Long but requires the use of standardising solutions which have to be freshly prepared for each set of measurements^(47,48). However, the method assumes that any combined nitrogen (nitrides) will not break down at the temperature at which the extraction is carried out. For instance manganese forms a range of compounds with nitrogen (MnN , Mn_6N_5 , Mn_3N_2 , Mn_2N , Mn_4N and M_xN ($9.2 < x < 25.3$)⁽⁴⁹⁾). (This supports the idea put forward by Baird and Jamieson⁽²⁶⁾). These have varying stability and along with iron nitrides can start to decompose at temperatures above 400°C. In fact some

metallic azides (AgN_3 , $\text{Cu(N}_3)_2$ and $\text{Pb(N}_3)_2$) are unstable to the point of being shock-sensitive and will detonate readily⁽⁴⁹⁾.

2.2.2 Internal Friction

There are two possible sites in a BCC alpha iron lattice that a small interstitial atom could occupy; these are the tetrahedral and the octahedral sites. The average radii of these sites are 0.36\AA for the tetrahedral and 0.19\AA for the octahedral. The common interstitial elements all have larger radii than these sites, carbon 0.77\AA , nitrogen 0.72\AA and hydrogen 0.46\AA . It would appear then that the tetrahedral sites would be the ones most likely to be occupied. However, interstitial atoms such as carbon and nitrogen occupy octahedral positions in body centred cubic iron, as in order to occupy a tetrahedral site would involve displacing four surrounding atoms, whereas only two nearest neighbour atoms need to be displaced in order to fit an interstitial atom into an octahedral site⁽⁵⁰⁾. This results in distortion in the structure, causing an elongation in a tetrad direction and a small contraction in the corresponding diad axes, see figure 2.6⁽⁴⁹⁾.

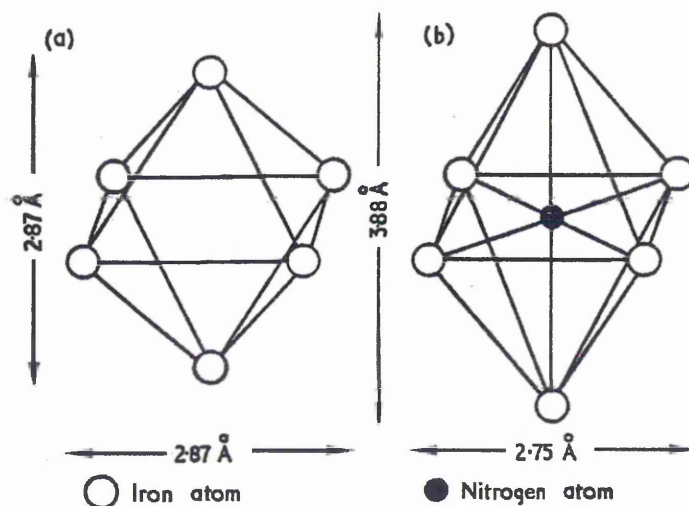


Fig. 2.6 Octahedral Interstice in Body Centred Cubic Iron
(from Leak⁽⁵¹⁾)

In the absence of stress all the octahedral sites are equivalent and will be randomly occupied. If a tensile stress is applied to the crystal these interstitial atoms will tend to move to sites where the tetragonal extension is in line with the stress. This will occur over a period of time dependant on the diffusion coefficient of the solute atoms.

If an oscillating stress is applied to the iron the solute atoms will move to preferred sites with each alternate half cycle. This will take a finite time and so result in a phase lag between stress and strain and energy will be absorbed by the system; this damping is referred to as 'internal friction'. The amount of damping will be proportional to the number of solute atoms and the frequency of the maximum damping will vary with the type of solute atom and the temperature.

The internal friction is normally expressed as the logarithmic decrement δ which is given by;-

$$\delta = \log(A_n/A_{n+1}) \quad (1)$$

Where A_n and A_{n+1} are the amplitudes of successive oscillations. If the system is not allowed to freely decay, but driven at constant amplitude, then δ is given by;-

$$\delta = \frac{\Delta W}{2 W} \quad (2)$$

Where ΔW is the energy lost (to heat) per cycle and W is the maximum amount of energy stored in the sample during an oscillation. The phase angle α , between stress and strain is directly related to the logarithmic decrement by;-

$$\tan \alpha = \delta/\pi \quad (3)$$

It is normal practice to express the magnitude of the damping (internal friction) in terms of $\tan \alpha$; in analogy to the damping in an electrical circuit this is termed $1/Q^{(52)}$. For a

given metal sample at a given temperature $\tan \alpha$ is strongly frequency dependant and can be expressed by;-

$$\tan \alpha = A \frac{\tau\omega}{(1 + (\tau\omega)^2)} \quad (4)$$

Where A is the relaxation strength of the process and is directly proportional to the number of solute atoms taking part, ω is the frequency of vibration and τ is the relaxation time for the mechanism⁽⁵²⁾. τ is related to the diffusion coefficient D, for the solute atoms in a body centred cubic lattice, by;-

$$\tau = \frac{a^2}{36D} \quad (5)$$

Where a is the lattice parameter and the diffusion coefficient is given by;-

$$D = D_0 \exp (-Q/RT) \quad (6)$$

Where R is the gas constant, T the absolute temperature, D_0 a constant and Q the activation energy for the diffusion process. From equation 4 it can be seen that the damping is a maximum when $\tau\omega = 1$ giving

$$\tan \alpha_{(max)} = \frac{1}{2} A \quad (7)$$

$\tan \alpha_{(max)}$ can be determined by plotting $\tan \alpha$ against temperature for a constant frequency or $\tan \alpha$ against frequency for a constant temperature. Normally a fixed frequency is used as this is easier experimentally. The maximum damping, $\tan \alpha_{(max)}$ is directly proportional to the number of solute atoms taking part in the damping process.

The most common form of apparatus for measuring internal friction is the torsion pendulum. The test specimen is in the form of a wire attached to a pendulum bob which imparts rotary oscillation. The dimensions are such that frequency of oscillation is

around 1 Hertz (1 cycle per second). The specimen is enclosed in an oven so that the temperature can be varied. Full details of the standard apparatus are given in reference 52.

Using a torsion pendulum Gladman and Pickering⁽⁵³⁾ showed that manganese influenced the position of the nitrogen peak and suggested that the displacement was in direct relation to the manganese content. They concluded that the jump of a nitrogen atom between equivalent positions relative to a pair of manganese atoms would occur at a lower temperature than a jump from such a position to a position between two iron atoms. Further work by Couper and Kennedy⁽⁵⁴⁾ using a more advanced computer analysis of the nitrogen peaks for several manganese contents showed that the peak was actually made up of three (and in the case of high nitrogen levels four) peaks, which corresponded to jumps in a pure iron lattice (Fe – Fe), a peak due to nitrogen jumping around equivalent sites in a iron –manganese lattice (Fe-Mn) and a third peak equating to a jump from a Fe-Mn site to a Fe-Fe site.

This effect of manganese may be due to the distortion of the lattice caused by the presence of a manganese atom (manganese has an atomic radius of 0.137nm compared to 0.124nm for iron). It could also be due to a chemical attraction forming manganese nitrides. In either case atoms such as silicon (0.1273nm), molybdenum (0.136nm), and possibly chromium, should show similar effects. In the case of chromium which has a radius of 0.125nm, there is no significant distortion of the lattice, as evidenced by the fact that chromium additions to pure iron do not cause an increase in strength, however, a chemical effect is likely as all three elements form stable nitrides. (Atomic radii taken from L.H. Van Vlack ref. 44 Appendix D)

It is of interest to note that in the discussion following the presentation of Tschischewski's 1915 paper⁽¹²⁾ several speakers noted that the presence of manganese appeared to increase the nitrogen retained in a steel.

In 1960 Heller, using a torsion pendulum operating at ~1Hz inside a Collins liquid helium cryostat, showed that hydrogen gave an internal friction peak at 30K (-243°C) and deuterium gave a broader peak around 37K (-236°C)⁽⁵⁵⁾.

Questions were raised as to whether this was a true internal friction peak but Gibala and Kumnick⁽⁵⁶⁾ argued that whilst it was small it was a true internal friction peak .

2.3 Effects of Hydrogen in Steel

The way that hydrogen is taken up by a metal depends upon a range of factors but generally the metals can be divided into two main groups; the endothermic occluders, where solubility increases with temperature and the exothermic occluders that form pseudo-metallic hydrides and show decreasing solubility with increasing temperature⁽⁵⁷⁾. The first group the endothermic occluders include iron, cobalt, nickel, copper, silver and gold and the Group VIa metals. These metals only form solid solutions or very unstable hydrides.

Iron will form a complex organic molecule with carbon, hydrogen and nitrogen,⁽⁵⁸⁾ however the very large size of the molecule ($\text{FeC}_{32}\text{H}_{16}\text{N}_8$) and its planar structure containing benzene rings would preclude its formation within a steel.

The presence of hydrogen in ferritic steel, in virtually every instance, results in a degradation of the steel's mechanical properties. This is normally seen as an increased tendency to cracking and this led to the use of the term 'hydrogen embrittlement'.

However, with hydrogen the degradation is not a typical embrittlement which would normally imply an increase in yield strength as well as a reduction in toughness, and various workers have shown that for a range of different steels there is either no increase in yield strength or a slight drop⁽⁵⁹⁻⁶⁷⁾. Furthermore hydrogen embrittlement is enhanced by slow strain rates, unlike normal carbon and nitrogen embrittlement, and by elevated temperatures⁽⁶⁸⁾. Beachem⁽⁶⁹⁾ suggested that rather than embrittlement, the basic hydrogen - steel interaction appeared to be an easing of dislocation motion and / or generation. This is supported by fractographic evidence for plastic flow and the lowering of the torsion flow stress in AISI 1020 samples subjected to hydrogen pick up⁽⁶⁰⁾. Ferreira et al.⁽³⁷⁾ have shown that solute hydrogen reduces the elastic interactions

between dislocations and elastic centres such as nearby dislocations and solute pinning points in fcc structures, which act as barriers to slip. A similar effect was observed by Matsumoto et al.⁽⁷⁰⁾ when low pressure hydrogen was admitted into an HVEM containing a thin foil of high purity iron under a fixed strain: '*An extremely rapid dislocation motion and generation occurred resulting in a very high density of dislocations in the form of tangles*'. This did not occur when the experiment was repeated with helium or air. Hänninen et al.⁽⁷¹⁾ has also shown that hydrogen causes movement of dislocations in specimens of A533B under strain. In view of this Hydrogen Assisted Cracking (HAC) is probably a better term to describe the phenomenon. However, Hirth⁽⁷²⁾ suggested that enhanced dislocation motion is not the complete solution but simply a contributory factor to the overall degradation process. Mathematical analysis of the concentration of hydrogen at dislocations and cracks⁽⁷³⁾ has given results that suggest unstable hydrides may form at such locations. This has also been supported by other workers⁽⁷⁴⁾.

Hydrogen does appear to show a yield point effect at sub zero temperatures but there is some question as to the actual temperature; some workers have suggested that it only occurs below -120°C ⁽⁷⁵⁾, whilst others have demonstrated a yield point at -70°C ⁽⁷⁶⁾.

The issue is complicated by the fact that hydrogen, particularly when introduced by cathodic electrolysis can cause plastic strain in iron and steel, strain which can reduce or completely remove the yield.

As a result, Farrell⁽⁷⁶⁾ wrongly concluded that there was no true yield effect from hydrogen. However, Adair and Hook⁽⁷⁷⁾ showed that hydrogen would give a yield point which could be restored by "annealing" at -70°C , whilst not restoring the yield point due to carbon and nitrogen. This demonstration of classic yield behaviour would

appear to be conclusive proof that hydrogen does behave in a similar manner to carbon and nitrogen but at lower temperatures. Furthermore, laboratory work at Sheffield Hallam suggests that there is a yield point at room temperature but, due to the rapid diffusion of hydrogen out of the specimens, the effect is only noticeable for a short time after hydrogen charging⁽⁷⁸⁾. Lunarska claimed that at normal temperatures and pressures almost all the lattice hydrogen, in a pure iron specimen, will diffuse out within a few minutes after charging⁽⁷⁹⁾. This may be the case but other workers have suggested that in normal steels it will take 24 to 48 hours for the hydrogen levels to drop back to the pre-charged levels⁽⁸⁰⁾.

Additional evidence that hydrogen can show typical interstitial behaviour has come from the work of Gove and Charles⁽⁸¹⁾. Using a specially designed high temperature micro-hardness tester⁽⁸²⁾, that could be operated in a pressurised hydrogen atmosphere, they were able to show that hydrogen, when introduced under pressure as a gas, could cause a reduction in the dynamic strain-ageing peak hardnesses in commercially pure iron and in a mild steel⁽⁸¹⁾, see figures 2.7 and 2.8. The size of the reduction was found to vary with strain rate, increasing with higher strain rates and when the hydrogen was removed the peak reappeared. They looked at the possibility that the hydrogen was reacting with the carbon and nitrogen to form methane and ammonia, however, the highest temperature used in their experiment would have been too low to generate methane and if ammonia had been formed it is highly unlikely that the process would have been reversible (and certainly not reversible for methane formation).

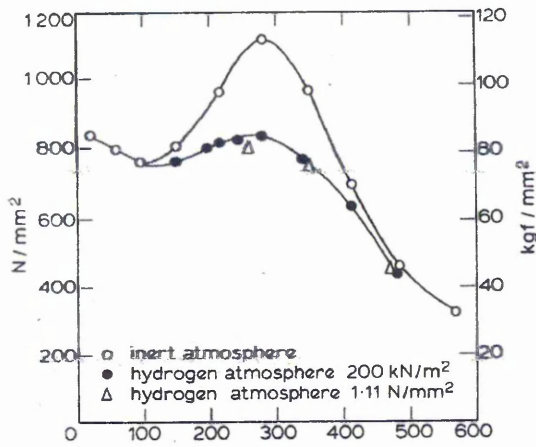


Fig. 2.7 The effect of hydrogen on the hardness of nominally pure iron.
from Gove and Charles⁽⁸¹⁾

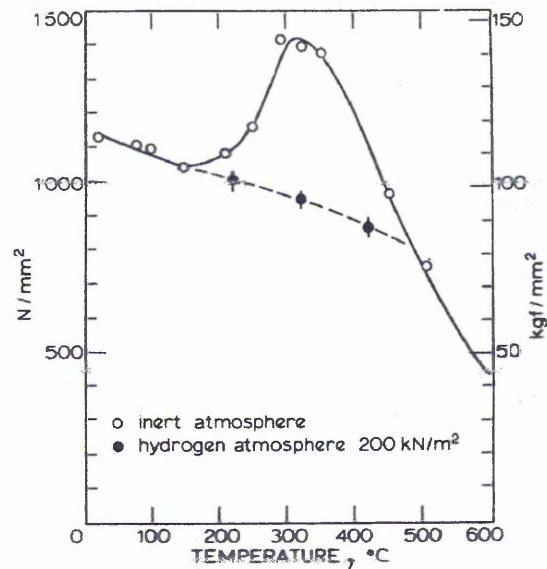


Fig. 2.8 The effect of hydrogen on the hardness of nominally pure iron.
from Gove and Charles⁽⁸¹⁾

This led them to conclude that due to hydrogen's greater mobility it would migrate to preferential sites around dislocations formed during straining and so prevent carbon and nitrogen atoms from occupying these sites and locking the dislocations. (The strain ageing peaks occurred at 250 – 350°C at which temperatures hydrogen has very little locking effect on dislocations.) This effect is only a temporary phenomena as due to hydrogen having a lower interaction energy than carbon and nitrogen (0.28eV compared to 0.55eV) with a dislocation site it is displaced by carbon and nitrogen atoms when the gas pressure is reduced.

This suggests that hydrogen may give rise to strain ageing phenomena similar to that shown by nitrogen but at a lower temperature. This is the case with niobium where Wilcox et al. found that a hydrogen content of 89 ppm. gave serrated yielding, a typical feature of strain ageing behaviour, at 25°C⁽⁸³⁾.

Furthermore, Hardie and McIntyre have shown that hydrogen caused a strain rate dependant ductility minimum in niobium at sub-zero temperatures, see figure 2.9⁽⁸⁴⁾.

The behaviour appears similar to strain ageing due to nitrogen as seen in steels at

elevated temperatures. However, they did not report any corresponding tensile stress peak (a typical feature of strain ageing in steel). This may be due to the poor ductility causing cracking and subsequent failure at loads lower than the true maximum strength. This would appear to be an area where, if hydrogen really does show similar behaviour to nitrogen but at lower temperatures, testing of hydrogen containing steel specimens at sub-zero temperatures may show a dynamic strain ageing effect.

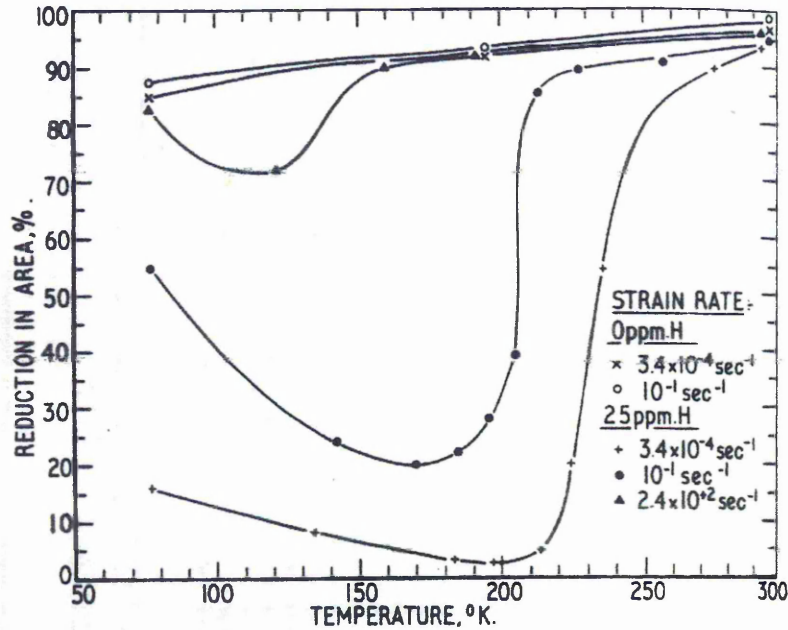


Fig. 2.9 Effect of 25ppm H on the % reduction in area of niobium as a function of temperature at various strain rates⁽⁸⁴⁾.

Hydrogen has been shown to have similar effects to radiation damage which tends to negate any increase in tensile strength due to DSA⁽⁸⁵⁾. (Radiation causes an increase in the number of vacancies.)

Hydrogen is also known to damage fatigue properties of steels both as a gas^(86,87) and when generated during corrosion⁽³⁴⁾. It has been shown that even the most 'resistant' steel shows a sixteen-fold increase in fatigue crack growth rate in hydrogen at 150 bar and above, compared to tests in nitrogen at a similar pressure⁽⁸⁶⁾.

The issue is further complicated, as Cain and Troiano showed that the time to a hydrogen induced fracture at a given stress level varied with the heat treatment of the steel⁽⁸⁷⁾, i.e. varied with the microstructure. This effect was supported by later work by Marsh and Gerberich⁽⁸⁸⁾.

2.3.1 The Movement and Transport of Hydrogen

The mobility of hydrogen in metals is very large, exceeding by many orders of magnitude that of the other interstitials. The cause of this large mobility is not clear because the nature of the interaction of hydrogen with metal lattices is not known well enough.⁽⁸⁹⁾

H₂ has three possible alternatives for the distribution of its valency electrons, since there are two ionic states (H⁺ and H⁻) and one covalent bonding arrangement between any pair of hydrogen atoms⁽⁹⁰⁾. In the gas at room temperature the covalently bonded molecule is the most common. However, when hydrogen is dissolved in a metal it exists as an interstitial atom. The diffusion coefficient (D) of an interstitial atom is given by;

$$D = D_0 e^{(-Q/RT)}$$

Where D₀ is the diffusion constant⁽⁹¹⁾ (or frequency factor⁽⁹²⁾) and Q is the activation energy for diffusion. The respective values for hydrogen, carbon and nitrogen are;

$$\text{Hydrogen } D_0 = 1.14 \times 10^{-4} \text{ m}^2\text{s}^{-1} \quad Q = 35.5 \text{ kJmole}^{-1}$$

$$\text{Carbon } D_0 = 4.88 \times 10^{-7} \text{ m}^2\text{s}^{-1} \quad Q = 76.7 \text{ kJmole}^{-1}$$

$$\text{Nitrogen } D_0 = 3.94 \times 10^{-7} \text{ m}^2\text{s}^{-1} \quad Q = 82.0 \text{ kJmole}^{-1} \text{ (91)}$$

This gives diffusion coefficients at 20°C (293K) of $5.35 \times 10^{-11} \text{ m}^2\text{s}^{-1}$ for hydrogen compared to $1.035 \times 10^{-20} \text{ m}^2\text{s}^{-1}$ for carbon and $9.49 \times 10^{-22} \text{ m}^2\text{s}^{-1}$ for nitrogen, indicating

that with a reasonable concentration gradient significant diffusion of hydrogen will occur at room temperature but not for carbon or nitrogen. The actual rate of diffusion at room temperature for hydrogen will be in the order of 25mm per day⁽⁸⁵⁾. However, workers using tritium have reported that absorption and evolution of the gas during plastic deformation is faster than can be accounted for by standard diffusion theory^(93,94). It has even been suggested that hydrogen diffuses by quantum mechanical tunnelling^(55,72). Heller used the concept of quantum mechanical tunnelling to explain why the hydrogen internal friction peak was at 30K (-243°C) rather than the 50K (-223°C) the temperature predicted by the classical theory. Quantum tunnelling does occur with very small light particles, such as electrons, but this is unlikely to be the case with hydrogen atoms as the probability of tunnelling decreases exponentially with the width of the barrier and the square root of the mass of the particle⁽⁹⁵⁾.

The absorption of hydrogen into SAE 4340 steel has been shown to be independent of the microstructure at low to medium stresses <350 MPA (<50 ksi) but as the tensile stress increases above 350MPa (50 ksi) the absorption increases rapidly in martensite whilst remaining the same for ferrite⁽⁹⁶⁾.

In tests on hydrogen diffusion rates through metals, alloys and oxides Huffine and Williams discovered that diffusion through a continuous oxide film is much lower than through the metal (an FeCrAl alloy)⁽⁹⁷⁾.

However, simple diffusion is not the only mechanism for transport in hydrogen through a metal lattice as lattice distortion, as in internal friction, can effect the diffusion rate.

Based on measurements of incubation times for crack initiation in hydrogen charged metals Johnson et al. concluded that the tri-axial stress field ahead of a crack tip would raise the diffusion gradient for hydrogen causing it to diffuse to the region of the crack

tip as a result of the lattice distortion⁽⁹⁸⁾. This was supported by Troiano based on evidence that the log of the ratio of the incubation time to the absolute temperature varied linearly with the reciprocal of the absolute temperature⁽⁶⁷⁾.

Tien et al. produced a kinetic model for the transport of hydrogen, as Cottrell atmospheres on dislocations. This gives a higher rate of transfer of hydrogen than normal lattice diffusion and appears to fit data for ductile fracture, but would only apply in these and similar high stress plastic flow situations⁽⁹⁹⁾.

As a consequence of Matsumoto et al.'s findings on the effect of hydrogen on dislocations⁽⁷⁰⁾ King and Block devised a mechanism for hydrogen induced dislocation motion⁽¹⁰⁰⁾. They suggested that in addition to the solid solution softening proposed by Matsumoto et al. and others^(37,81) hydrogen induced motion could be a cause rather than a result of the dislocation motion. Starting from the work done to move an edge dislocation and the force exerted by a crack tip stress field on a solute atom (in this case hydrogen) they calculated that at a distance of 0.02mm from the crack tip each hydrogen atom would experience a force of 3.2×10^{-15} N. Therefore based on a force of 6.8×10^{-3} N to move a dislocation of one metre in length, if the dislocation Cottrell atmosphere contained 2×10^{12} atoms per metre ($6.8 \times 10^{-3} / 3.2 \times 10^{-15}$) the dislocation would be drawn towards the crack tip. (This was based on the assumption that the hydrogen atoms are all strongly enough bound to the dislocation to apply the individual force on each atom to the dislocation as a whole.)

This value was higher than the value range suggested by Hirth⁽⁷¹⁾ of 5×10^9 to 1×10^{11} . (These values were based on the Boltzman approximation used by Cottrell and Bilby where;

$$C = C_0 \exp (W/kT)$$

Where C is the atom fraction at the defect field (dislocation), C_0 is the atom fraction remote from the defect (equilibrium concentration) and W is the interaction energy between solute and defect (k is the Boltzman constant – the ratio of universal gas constant R to Avodagro's constant N_A .) Hirth's values correspond to an equilibrium or perfect lattice concentration of 6.13×10^{-7} this converts to a hydrogen content of 2×10^9 atoms per metre, which is additional to the dislocation core solute atmosphere. In order to reach the hydrogen contents needed for dislocation motion the bulk lattice concentration would need to be increased to a high level by electrolytic charging⁽¹⁰¹⁾

Hydrogen can also be trapped within metals. This trapping can occur at lattice defects⁽⁷³⁾, by adsorption at the interfaces of non-metallic inclusions and in microvoids where the hydrogen forms gas molecules^(100,101). Hirth suggested that the strong binding energy between nitrides (and carbides) and hydrogen would draw hydrogen to the interface⁽¹⁰²⁾. Podgurski and Oriani observed trapping of hydrogen in in nitrogen treated Fe-Al alloys⁽¹⁰³⁾. The binding was believed to occur at the aluminium nitride/ferrite interface. It has also been suggested that the apparently very high hydrogen contents in Armco iron, reported by early workers, were due to trapping at oxides which were present in these materials⁽¹⁰⁴⁾.

Several groups have shown that trapping occurs at interfaces and grain boundaries⁽¹⁰⁵⁾.

Trapping at lattice defects has been put forward as an explanation of the anomalously low and variable diffusivity of hydrogen at temperatures below 200°C ⁽¹⁰⁶⁾ and Hargi et al. have shown that at temperatures below 0°C grain boundaries actually reduce the measured diffusivity of hydrogen in iron⁽¹⁰⁷⁾.

2.4 Metallic Hydrogen

One area of uncertainty is the state of hydrogen dissolved in steel. The position of hydrogen in the Periodic Table suggests that solid hydrogen should be metallic. In 1935 Wigner and Huntington published their results of theoretical calculations on the density and heat of vapourisation of a potential metallic hydrogen⁽¹⁰⁸⁾. The paper gave details of the method used for estimating the density and heat of vapourisation of metallic hydrogen based on a calculated energy for the hydrogen electron. The initial approximate figures gave a density of 0.8 (as compared to 0.087 for solid molecular hydrogen) and a heat of vapourisation into atomic hydrogen of 48.7 cal as compared to 52.5 cal, the heat of formation of the molecular form. Both these values show that the molecular form is the more stable but suggest that under high pressure it may be possible to alter the crystal structure to the metallic form. However, the paper went on to refine the calculation and points out that the wave function is more complex than that for sodium, on which the original calculation had been based, due to the electron being restricted to a single shell.

The calculations are reworked using several different methods all of which indicate a slightly lower density (0.59 to 0.62) and a much lower range for the heat of vapourisation (10 to 16 cal) both of which properties would make metallic hydrogen far less stable than the normal molecular form.

The conclusion gives further information on normal solid hydrogen which consists of molecules with an inter atomic distance of 0.075nm held together by Van der Waals forces giving a distance of 0.33 nm between atoms in adjacent molecules. In a metallic structure these two distances would be equal as all the bonds would be metallic, i.e. a sharing of the electrons. Applying pressure to solid hydrogen would move the

molecules together and the atoms within individual molecules apart but Wigner calculated that the pressure to achieve equidistant spacing would be in the order of 250,000 atmospheres. However, later work showed that even when subjected to a pressure of 2.5Mbar solid crystalline hydrogen does not show metallic properties⁽¹⁰⁹⁾.

In 1979 Bell and Mao working at the Carnegie Institute for Science, using a diamond anvil high pressure cell, produced a new form of solid hydrogen which they believed was a step towards solid metallic hydrogen⁽¹¹⁰⁾.

Work at Carnegie has continued and model studies have indicated that metallic hydrogen could exist in the centre of gas giant planets such as Jupiter^(111,112).

In 2002 a French team compressed hydrogen to a pressure of 320 GPa at 100 Kelvin. They noted that at 290 GPa the hydrogen turned white then as the pressure increased went through yellow, orange, red and final became opaque at 320 GPa. Above 300 GPA the team found evidence of a lowered energy band gap – a feature of semiconductors. The band gap narrowed as the pressure increased to 320 GPa (this was the maximum pressure they could achieve with their existing equipment). Extrapolating from these results the team calculated that at 450 GPa the band gap would disappear i.e. the hydrogen would become fully metallic^(113, 114).

In hydrogen at ambient pressure the band gap between the highest filled electron energy level and the next available level is 15eV which would qualify it as an insulator. In 1996 a group from the Lawrence Livermore Laboratory⁽¹¹⁵⁾ using a shock pulse system were able to lower this gap down to 0.3eV in fluid hydrogen, using pressures in the range 1.0 – 1.4 Mbar. This is a level comparable to the thermal energy of the fluid, i.e. conductivity equivalent to a metal. This has been backed up by computer model

calculations for fluid deuterium, from which it was concluded that insulator to metal transition during a shock pulse is driven by molecular dissociation⁽¹¹⁶⁾.

Gibala⁽¹¹⁷⁾ referred to hydrogen in metal as being 'ionized'. However, ionization normally results from either the splitting of a molecule to form positively charged cations and negatively charged anions or as a result of direct high voltage charging of an atom. Neither of these situations occur when hydrogen dissolves in a metal.

However, a possible explanation for hydrogen's rapid diffusion, that this work seeks to clarify, would be that hydrogen when dissolved in a metal exists in a metallic state, that is its electron is part of the metallic electron cloud leaving a single proton with a diameter in the order of 4×10^{-6} nm. As a result of work on metal clusters in large organic molecules, Cavanaugh et al. speculated that hydrogen could exist as 'screened protons' as well as H₂ molecules and as though it were negatively charged ligands⁽¹¹⁸⁾. However, in bulk metal the negatively charged particles would only exist, as they pointed out, if the hydrogen interacted with impurities. Similarly gas molecules will form if there are voids in the metal. However, in the absence of voids and impurities then a possible state of dissolved (interstitial) hydrogen could be as protons i.e. a metallic state. A concept suggested by Farrell⁽⁷⁷⁾ back in 1965.

If hydrogen exists in this metallic state this could account for the very high diffusion rates, reported by Donovan et al.^(93,94), as the proton would diffuse rapidly through the structure. In their work on the structure of the atom Geiger and Marsden had shown that when a thin beam of alpha particles (helium nuclei consisting of two protons and two neutrons) was shone on a thin gold foil ~90% of the particles passed through the foil with very little deviation and only 1 in 8000 was scattered straight back towards the source^(119, 120). This would suggest that a single proton should be able to easily move

through a metallic lattice. The work by Heller in 1961⁽⁵⁵⁾ and later repeated by Gibala and Kumnick⁽⁵⁶⁾ both found an internal friction (Snoek) peak for hydrogen at 30 Kelvin (-243°C) when stressed at ~1 Hz, i.e. behaviour consistent with atomic hydrogen. This would appear to indicate that at very low temperatures a significant proportion of the hydrogen is in an atomic interstitial state rather than a metallic 'proton' state. However, the peak found by Heller was at a lower temperature than predicted by classical theory (this predicted a peak for atomic hydrogen at 50K). Heller suggested quantum tunnelling as an explanation. However, it could be better accounted for if the hydrogen were 'metallic' when it would be a proton that moved to the new site leaving its original electron as part of the electron cloud and collecting a 'new' electron at the new site.

The presence of some of the hydrogen in a metallic state could be expected to show behaviour similar to a solid state ionic solution and could be an explanation for some of the trapping phenomena if the proton (hydrogen ion) was forming metastable ionic compounds as has been suggested by Hirth and Carnahan⁽⁷³⁾.

Theoretical calculations of the effects on the electron structure (the energy bands and electron density) of carbon, nitrogen and hydrogen in iron, by Gravičljuk et al.⁽¹²¹⁾ have shown that nitrogen and hydrogen promote the metallic character by increasing the concentration of free electrons whilst carbon has the opposite effect, enhancing localisation of electrons at the iron atoms promoting the covalent characteristic of the inter-atomic bonds. They also conclude that the increased concentration of free electrons in the dislocation atmospheres due to the effect of hydrogen should decrease the line tension, the distance between the dislocations (as reported by Ferreira et al.⁽³⁷⁾) and the stress for activation of dislocation sources which should increase plasticity.

An increase in plasticity and reduction in dislocation spacing would suggest that a small addition of hydrogen should reduce the work hardening (strain hardening) rate. This will be the case at simple dislocation pile-ups, such as occur at grain boundaries and obstructions such as small incoherent precipitates. However, work hardening is not simply related to dislocation spacing but also to the interaction of dislocations on differing slip planes. Any dislocation moving in a specific slip plane will have to intersect dislocations in other slip planes that cross the specific plane. These intersected dislocations are known as 'forest dislocations'^(122,123). The actual effect on dislocation mobility depends upon the types of dislocation, edge or screw, that intersect and hydrogen will have less effect on these interactions.

Having said this Gourmelon did find that in a single crystal of high purity iron at low strains the strain hardening rate and the flow stress were reduced when hydrogen was present but at higher strains the opposite effects occurred⁽¹²⁴⁾. Lunarska et al related this behaviour to the differing methods of slip that occurred within a single crystal with increasing strain⁽⁷⁹⁾.

At room temperature in pure iron a three stage shear stress – shear strain can be seen in iron crystals. *'In Stage I, dislocations of the primary slip system glide over large distances. With increasing strains, dislocations become jogged as a result of their mutual interactions and cross slip. These jogs restrain dislocation mobility, but act as dislocation sources. At the end of Stage I, dislocations are accumulated in sheets parallel to the primary slip plane. These dislocation sheets (about 2µm wide) are stable throughout Stages II and III, being the main obstacle for dislocation motion. The dislocations can move through the channels between these sheets. The increase in long-*

range stresses produced by dislocation sheets are considered to be the cause of work hardening in Stage III.⁽¹²⁵⁾

These variations in slip that can be observed in a single crystal would not be apparent in a normal polycrystal fine grained steel, therefore any change in the strain hardening rate that could be observed would depend upon the main slip mechanism that was in operation.

This leaves open the following questions:

Does hydrogen when dissolved in steel show metallic behaviour and can the increased micro ductility of a hydrogen treated steel be used to increase the measured ductility of a steel with a high free nitrogen content?

3.0 Experimental Work

3.0.1 Experimental Materials

The following materials have been acquired for these investigations;-

- ◆ Armco iron bar - purchased from Goodfellow Cambridge Ltd.
- ◆ Mild steel plate with medium low nitrogen content.
- ◆ Mild steel plate with high free nitrogen content.

The compositions and cast numbers for these metals are given in table 1.

Table 1. Chemical Analysis (ppm)

Material	Cast	C wt %	Si wt%	Mn wt %	P wt %	S wt %	Cu wt %	Al wt %	N (total) ppm
Armco iron	Fe7970	0.001 *	<0.1	0.05	0.003	0.005	0.007	-	30
Mild Steel	F8104	0.17	0.33	0.83	0.008	0.005	-	0.03	44
Mild Steel	F8105	0.16	0.33	0.84	0.010	0.005	-	<0.004	130

* This result was later found to be wrong the actual carbon content being 0.01wt%.

3.1 Evaluation of the Feasibility of using a Thermistor Bridge to Measure a Small Concentration of Ammonia in a Hydrogen Gas Stream

The determination of free nitrogen in steel can be carried out by passing pure hydrogen over filings of the sample steel at a temperature of 450°C. The principle is that hydrogen reacts with the free nitrogen, but not with that combined as nitrides, to form ammonia. The quantity of ammonia is then measured to give the original free nitrogen content. The ammonia can be measured by various techniques based on either potentiometric titration or the indophenol blue colourmetric method. An improved version of this technique was developed by Long ⁽¹²⁶⁾ who used an ammonium ion selective electrode to measure the amount of ammonia released. However, in order to calibrate the measurement a set of standard strength solutions have to be freshly made up, making a single measurement expensive and time consuming.

The weight of nitrogen in a one gram sample steel containing 100ppm of free nitrogen is 0.0001 g.

Nitrogen has a Gram Atomic weight of 14 g and ammonia has a Gram Molecular Weight of 17 g.



As one atom of nitrogen combines with hydrogen to give one molecule of ammonia,

therefore 1g of steel will give $0.0001 \times 17/14$ grams of ammonia.

$$\text{Which} = \frac{0.0001 \times 17}{14 \times 17} \text{ Gram Molecules of Ammonia}$$

This will give $22.4 \times 1000 \times 0.0001 / 14 = 0.16$ ml of ammonia at STP.

Or 0.17 ml at 20°C

With a hydrogen flow rate of 140ml/min and assuming all the nitrogen is extracted as ammonia in 30 minutes this would give an average concentration of ammonia in the gas stream of $4.08 \times 10^{-3} \%$. However, it is likely that the bulk of the nitrogen will be extracted from fine filings within a few minutes of the metal reaching temperature. Assuming that three quarters of the nitrogen is extracted in the first five minutes then the concentration during that time would be 0.018%.

The aim of this section of the work was to determine if this small quantity of ammonia could be measured by its effect on the heat transfer efficiency of the hydrogen gas stream. Convective heat transfer is governed by the conduction across the boundary layer the thickness of that layer depending on the viscosity of the fluid and the velocity of flow. Hydrogen has the highest thermal conductivity of any gas at $0.167 \text{ W.m}^{-1}.\text{K}^{-1}$ ⁽¹²⁷⁾ compared to ammonia gas which has a thermal conductivity of $0.022 \text{ W.m}^{-1}.\text{K}^{-1}$ ⁽¹²⁸⁾. A simple calculation based on these values would suggest that a concentration of 0.018% ammonia in the gas stream would decrease the thermal conductivity by 0.26%. The thermal conductivity of a pure gas (k) can be modelled by the following equation;

$$k = \frac{1}{3}c_m n l c$$

where c_m is the heat capacity per molecule,

n is the number of molecules

l is the mean free path

c is the mean velocity of the molecules.

Using a simplified estimation for the mean free path l the equation predicts that the thermal conductivity will not vary with pressure except at very high or very low pressures⁽¹²⁹⁾. This has been found to be the case for noble gases such as argon when held at a constant temperature. However, the equation breaks down when used to

predict the effect of changing temperature on thermal conductivity. This is because in the equation the assumption is made that there is an equilibrium distribution of energy between molecules (or atoms) that have just collided but even with monatomic argon this is not the case as work by Kannuluik and Carman has shown⁽¹³⁰⁾.

The problem becomes even more complex for a mixture of molecular gases as the mean free path is affected by interactions between the molecules and the distribution of energy cannot be treated as an equilibrium distribution due to the different masses of the colliding molecules. This makes the calculation of the actual thermal conductivity of a mixture of gases extremely complex^(131,132,133,134). The conductivity is influenced by a range of factors all of which would tend to increase the effect of the higher molecular weight gas (ie. increases the apparent concentration of ammonia).

However, changes in thermal conductivity of a gas mixture have been used as a means of analysing the composition of gas mixtures particularly binary mixtures one component of which is hydrogen^(135,136).

In this work it was hoped that the actual change in the thermal conductivity could be measured to an acceptable degree of accuracy by using a set of thermistors in a Wheatstone bridge network.

The thermistor is a temperature sensitive device where, unlike normal resistance materials, the resistance decreases with increasing temperature⁽¹³⁷⁾. However, the relationship between resistance and temperature is highly nonlinear compared to other temperature sensing devices, see figure 3.1.1.

For a 10,000 ohm base level thermistor (measured at 25°C) over a small range the change in resistance for one degree Celsius can be several ohms⁽¹³⁷⁾. This makes

thermistors very useful for detecting small changes in temperature. If four matched thermistors are used in a Wheatstone bridge network then very small changes in temperature can be detected.

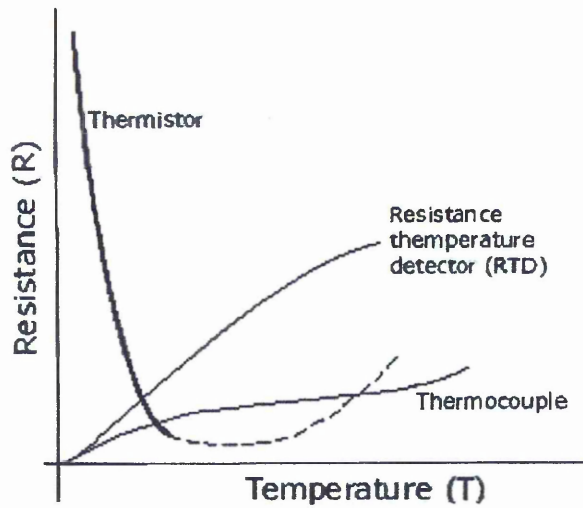


Fig. 3.1.1 Typical Characteristics of three Temperature Transducers⁽¹³⁸⁾

3.1.1 Apparatus

Figure 3.1.2 shows the thermistor bridge network used for this experiment. Figure 3.1.3 is a circuit diagram of the thermistor bridge. The incoming pure hydrogen passes over thermistors AB and CD and the hydrogen containing ammonia passes over thermistors EF and GH. When operating the bridge was protected from drafts by a clear Perspex cover.

The bridge was powered from a 9 volt battery in the black box, which also contained the adjustable potentiometer (P). The output from the bridge was monitored using a modified BBC Master computer running a custom datalogging program. The program records the output from the thermistor bridge taking a reading every second. When the boat is pushed into the furnace

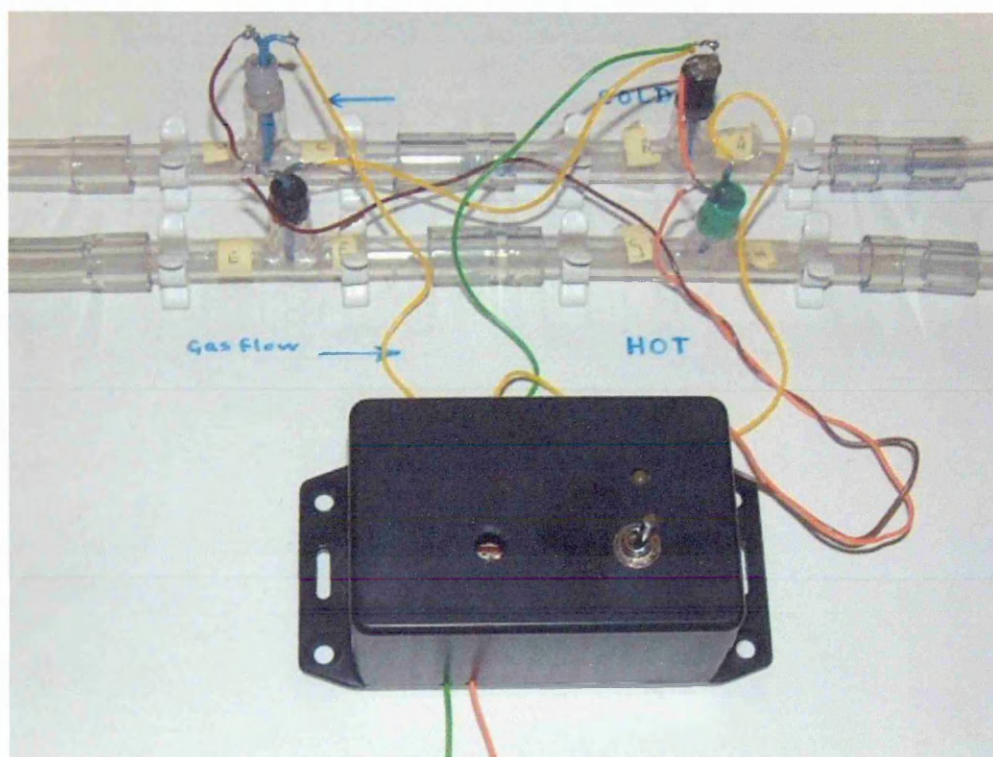


Fig. 3.1.2 Layout of Thermistor Bridge

hot zone the 's' key is pressed and the program then calculates the average of the previous 5 readings. This value is then used as the base level and the difference between this and any subsequent reading is added to a store, which equates to the area under the curve. (The calibration of the datalogging system had been checked annually and found to be $\pm 0.5\text{mv.}$)

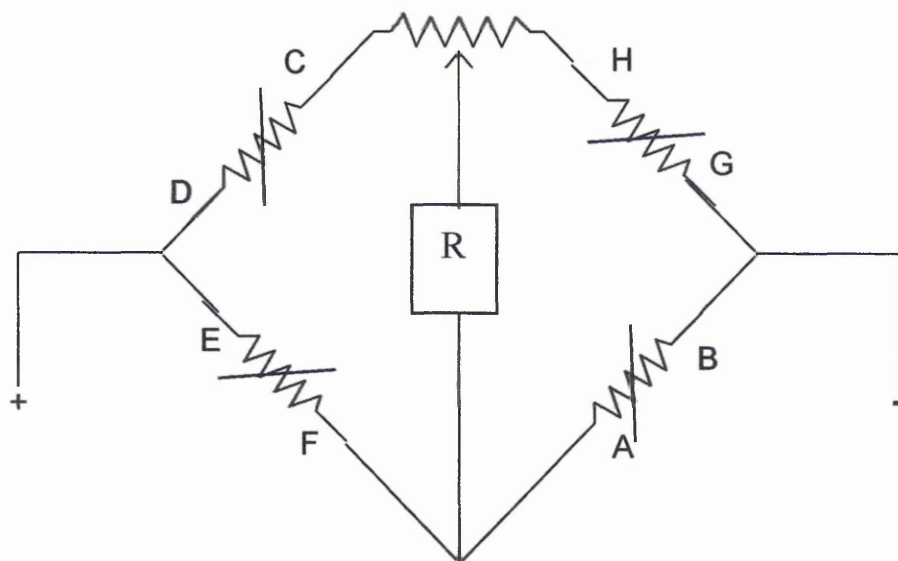


Fig.3.1.3 Schematic of Thermistor Bridge Circuit (R is the recorded output)

3.1.2 Experimental Details

The initial practice, following that described by Long⁽¹²⁶⁾, had been to insert the silica boat containing the sample filings into the furnace whilst running argon through it. The gas supply was then switched over to pure hydrogen and the peak signal generated across the bridge noted. However, trials demonstrated that the change from argon to hydrogen caused a major change in the bridge balance (20-25 mv) which took 10 –15 minutes to settle.

The apparatus was modified by fitting a push rod through the rubber bung that sealed the entry to the furnace tube. The boat containing 1 gram of filings, from a standard sample C3-2, was then placed in the cool entry section of the furnace tube and after

flushing with argon for 10 minutes the gas supply was switched to pure hydrogen. This was allowed to flush the system at a flow rate of 250ml/min for 10 minutes and then reduced to ~140ml/min. The bridge was then switched on and balanced using the potentiometer. (A stable balance, within $\pm 1\text{mv}$, was normally achieved after 5 - 10 minutes.) The boat and sample were then pushed into the hot zone of the furnace which was at $460^{\circ}\text{C} \pm 10^{\circ}\text{C}$.

The initial tests showed a peak rise in the bridge output of ~3 mv, the increased output being sustained over a period of approximately 10 minutes. This gave a total area under the curve of 775mv.sec. However, problems were experienced with the push rod being a very tight fit in the bung once it was inserted in the furnace tube. The push rod was eased backwards and forwards through the bung, to enlarge the hole, and it was noted that small particles of rubber were dragged through with it. These were cleaned off, the hole enlarged, the push rod lubricated with graphite. Repeat tests did not show the 3 mv rise in the signal. The conclusion being that this rise had been due to a reaction with the rubber particles.

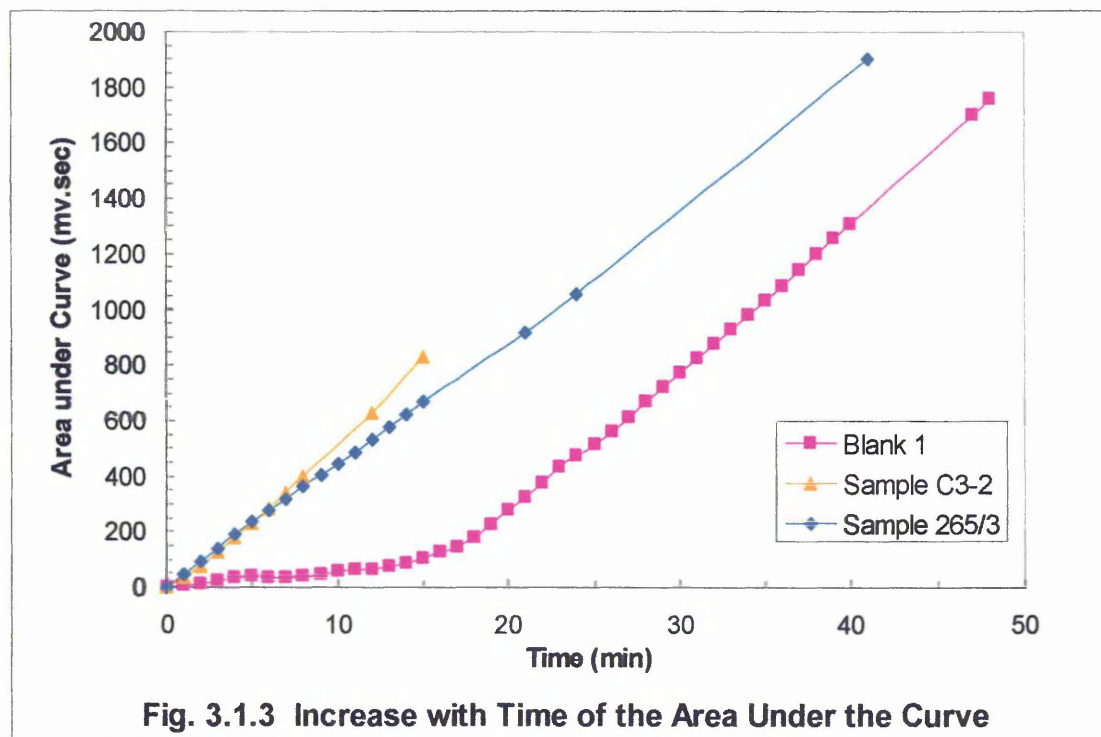
A test was then carried out using a clean empty boat. After purging with argon the hydrogen was turned on and purged for 15 minutes. The bridge was balanced with a 1mv output, the stability ($\pm 1\text{mv}$) was checked over 5 minutes the hydrogen flow rate having been reduced to 100 – 150 ml/min. The empty boat was then pushed into the hot zone and the area under the curve recorded. The curve Blank 1 in figure 3.1.3 shows the increase in the area under the curve during the next 45 minutes.

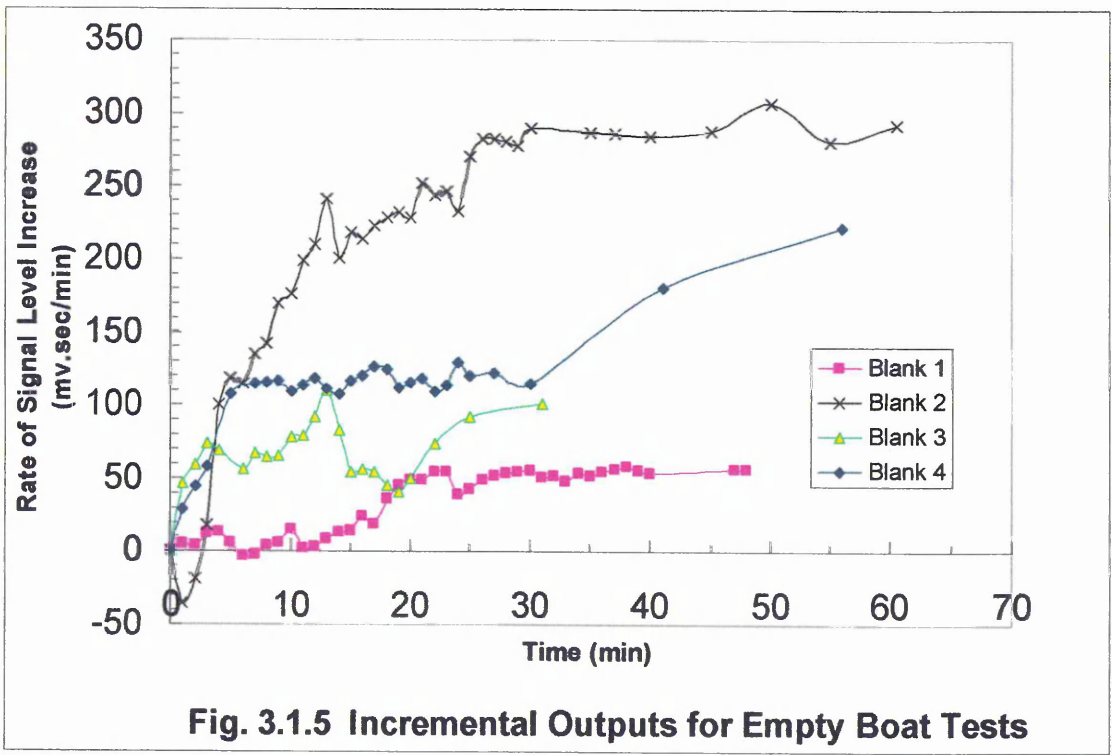
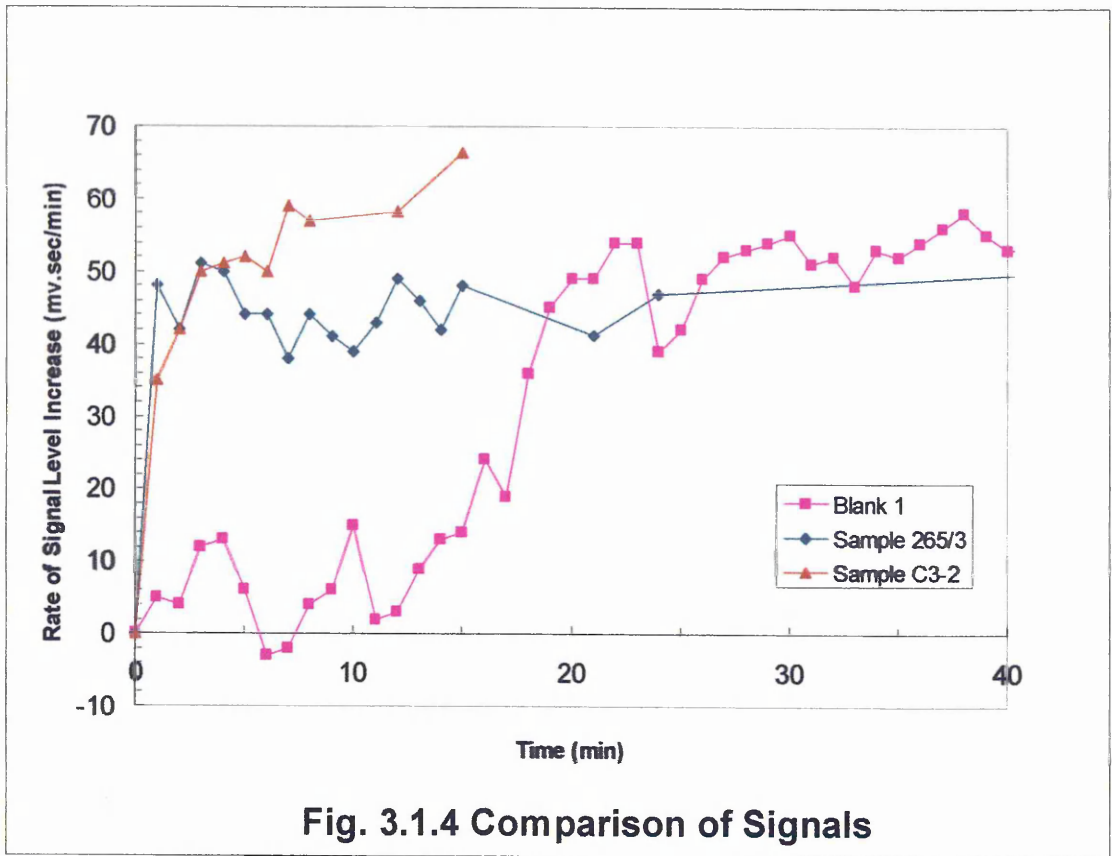
Figure 3.1.3 also shows the results from one gram samples of two steels known to contain free nitrogen. These results appear to show a rapid increase in the signal level

for the two samples and a much slower increase for the empty boat. However, in all three tests the increased output was only of the order of one millivolt.

Figure 3.1.4 shows a plot of the rate of signal increase for each minute after the boat entered the hot zone (measured in millivolt seconds per minute). Both steel samples show a rise to a signal level of 40 – 50 mv.sec/min within the first minute and this level is then sustained over the next 20 minutes, whereas the empty boat did not show any significant change in signal until 15 minutes after entering the hot zone and then stabilised at ~ 50mv.sec/min.

In order to confirm this apparent difference a series of repeat tests using the empty boat were carried out. Figure 3.1.5 shows the signal level for the first empty test run and three subsequent runs. Runs 3 and 4 both show a rapid change within the first minute of the boat entering the hot zone and that further increases occur after 20 – 30 minutes.





As the effects seen appeared to be due to temperature effects it was decided to try to reduce any variations in the temperature of the gas stream leaving the furnace. To do this a condenser was fitted into the gas lines to act as a heat exchanger. The incoming hydrogen was passed through the outer casing cooling the gas from the furnace which passed down the central spiral, the gases moving in counter flow, see figure 3.1.6.

A test run was carried out using an empty boat and this showed an initial signal rise of approximately one millivolt as the boat was moved into the furnace hot zone, however, subsequent tests revealed that this was the result of air being drawn into the furnace by the push rod used to move the boat. A check was carried out by admitting a small amount of argon into the hydrogen and this caused a rise in signal of 40 mv.

In order to prevent any change in the gas entering the furnace two further tests were carried out starting with the furnace cold and the boat in the hot zone and the tube sealed with a solid bung.

Starting with an empty boat in the hot zone, after flushing with argon, the hydrogen was turned on at a flow rate of 150 ml/min and run through for 10 minutes. The hydrogen flow rate was turned down to 100 ml/min and the bridge balanced. The furnace was then turned on and brought up to temperature. The bridge output initially rose slightly but then dropped and continued to run at a level below the initial reference value.

The test was repeated using a one gram sample of a steel known to have a high free nitrogen content. The bridge output again showed a slight initial increase but then dropped to approximately 3mv below the initial reference level and ran at this level for approximately 12 minutes and then dropped to half the initial reference level.

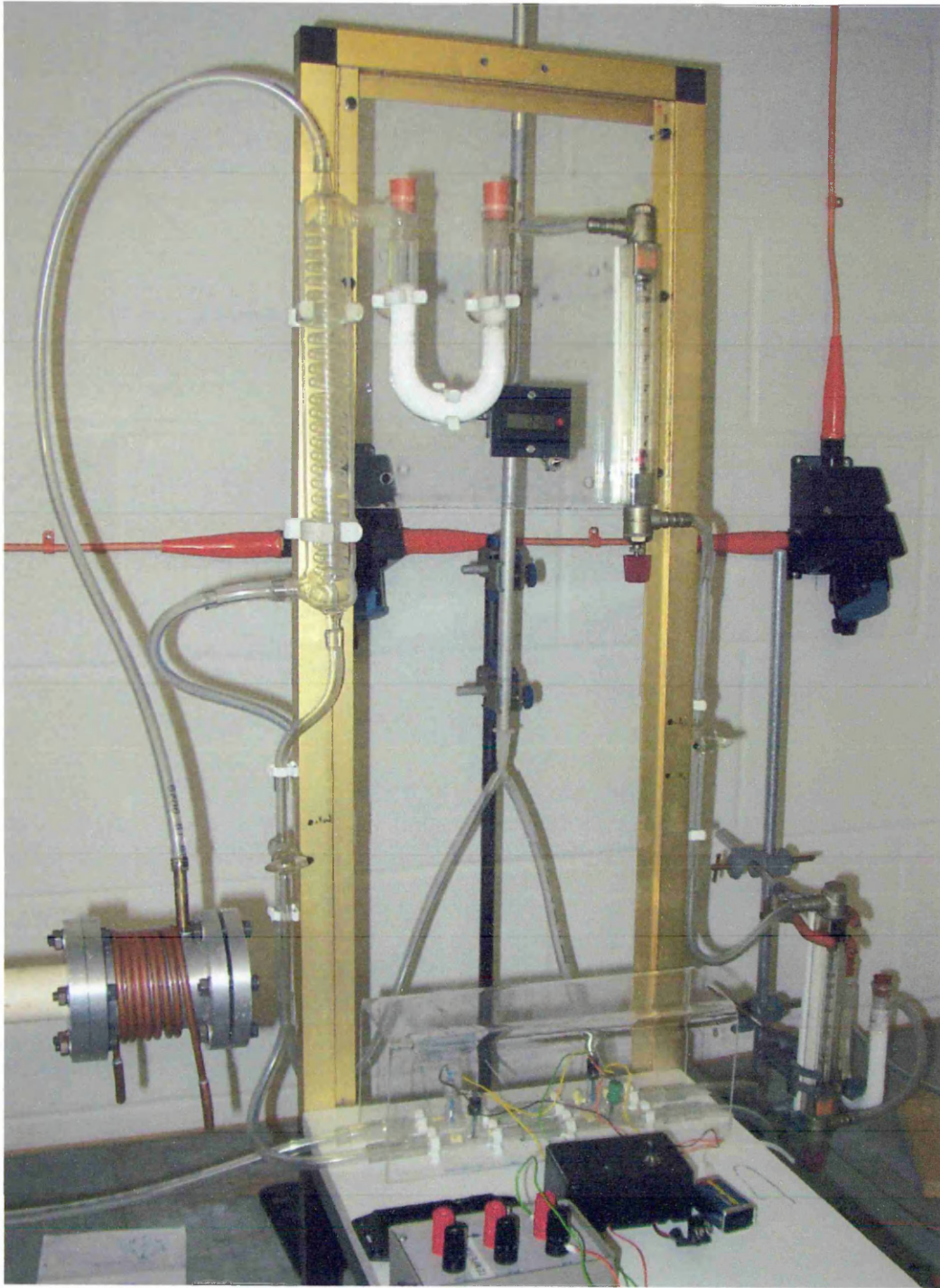


Fig. 3.1.6 Heat Exchanger fitted in the gas streams

3.2 The Measurement of Internal Friction

Work has been done in the past using a thin wire specimen as part of a torsional pendulum with a natural frequency of around 1 cycle per second. As the frequency is fixed, using this system, the damping is normally plotted against temperature and so the peak value for a particular interstitial element is displayed at the temperature where the jump frequency is equal to the natural frequency of the pendulum.

3.2.1 Vibran Interstitial Analyser

The School of Engineering has purchased a modified version of the torsion pendulum, the **Vibran Interstitial Analyser**, which uses forced rotational vibration of the specimen. This allows it to determine the damping over a range of frequencies as well as at differing temperatures.

The analyser uses a coil around a permanent magnet on the pendulum to torsionally oscillate the pendulum / specimen system. The oscillations are measured using a laser reflecting from a mirror on the pendulum on to a solid state optical detector, see figure 3.2.1.

The whole assembly is surrounded by a Perspex windshield and this chamber suspended on bungee cords to suppress the effects of any ambient vibrations on the measurements.

The specimen is in the form of a small flat tensile test piece which is clamped between the fixed base of the pendulum and the suspended top section which contains the actuating magnet. (Details of the specimen are given in appendix I.)

The unit is controlled by a computer running under Microsoft Windows software which drives the oscillator unit over a set series of frequencies and the damping at each frequency is measured and logged by the computer.

For a given interstitial content the damping is proportional to the energy used to produce the oscillation, then within limits variations in the volume of metal stressed do not affect the degree of damping, which means that the specimen size is not a critical factor in the measurements



Fig. 3.2.1. Vibran Pendulum Assembly

3.2.2 Modification of the Vibran Analyser

As delivered the pendulum unit of the Vibran analyser was designed to be operated whilst suspended, on bungee cords, from a modified photographic tripod, see figure 3.2.2. This made changing and setting up the specimen difficult as the assembly was not securely located and only 20 cm from the floor. Initially the unit was lifted and a small trolley placed under it. However, as the cables for the individual units emerge

through the base of the unit this was not well stabilised and the operator still had to get down on hands and knees to align the pendulum.



Fig. 3.2.2 Vibran Analyser Unit as supplied.

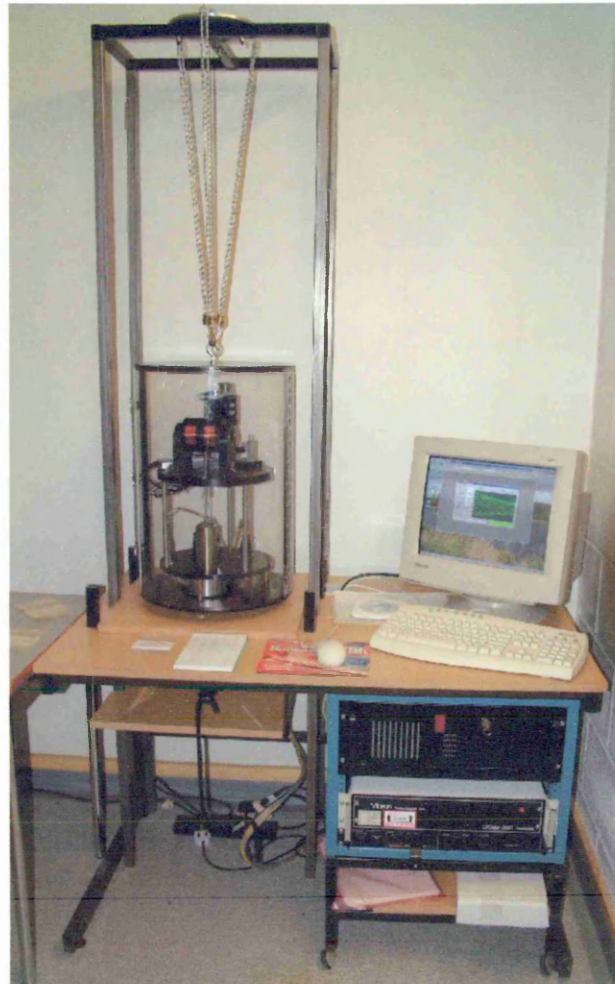
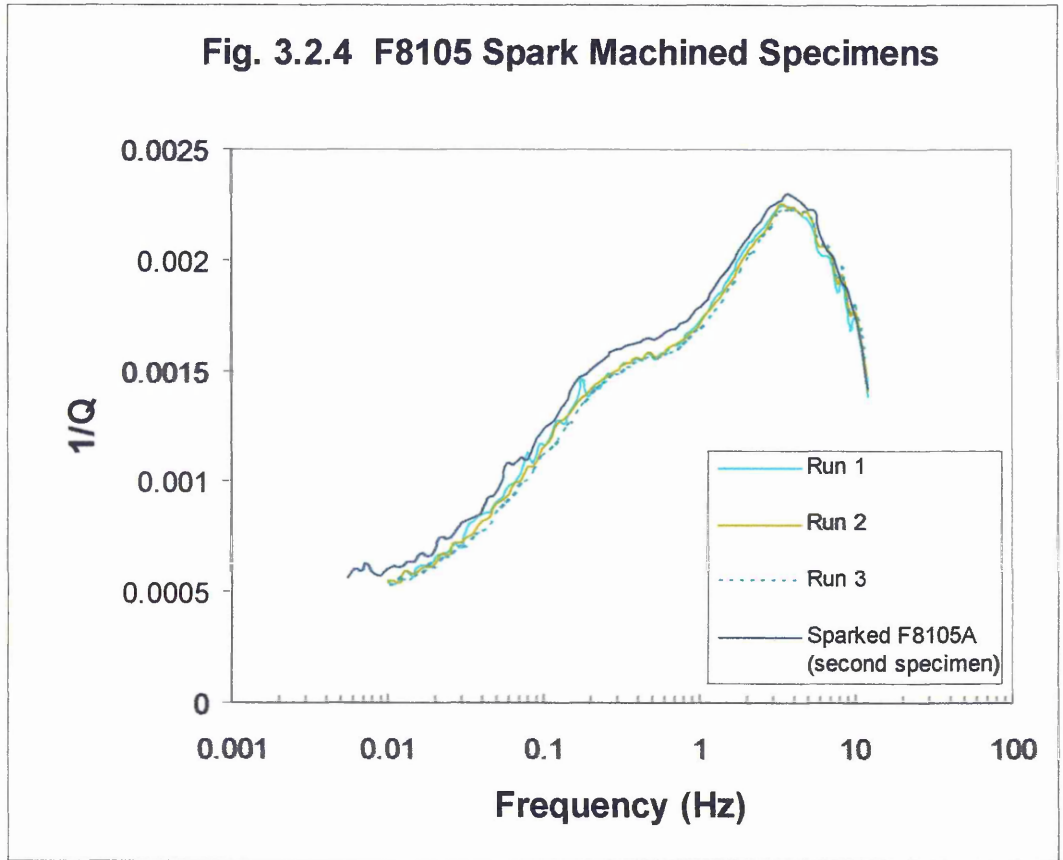


Fig. 3.2.3 SHU modified Vibran Analyser Unit.

The SHU equipment has been modified and is now suspended from a purpose built tower fitted into the control desk, see figure 3.2.3. The desk has a jacking platform that can be raised to support the pendulum chamber during specimen changing and then lowered to allow the chamber to hang free, the electrical cables passing freely through holes in the jacking platform.

The computer system records the damping as a $1/Q$ value over a range of frequencies specified by the operator this can then be displayed as an x-y plot using a data base program such as Microsoft Excel. The reproducibility was checked by running the same specimen several times and by comparing this with a second specimen cut from the same material, see figure 3.2.4. The only significant variation between the two specimens is in the zero level which is easily corrected for by a direct comparison.



3.2.3 Modelling of the Internal Friction Hysteresis Curves

Internal Friction Model

Figure 3.2.5 shows an example of a Snoek peak for carbon in iron. A similar peak is produced by nitrogen in iron.

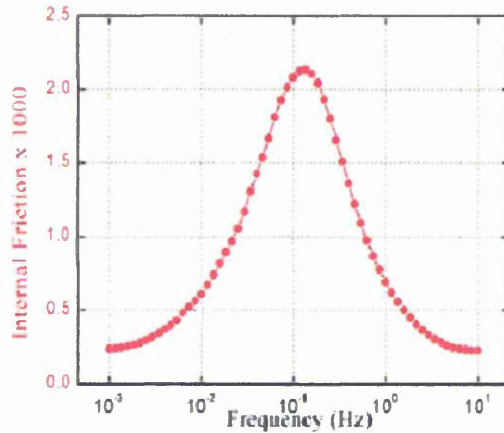


Fig. 3.2.5 Snoek Peak for Carbon in Iron.

A single peak, such as this, can be modelled by the following equation;-

$$y = a \times c / ((\ln(x \times b))^2 + c)$$

where a is the peak height and x is the frequency, c is the factor controlling the width of the peak. The peak position is governed by b where when b=1 the peak occurs at 1 Hz and if b>1 the peak occurs at < 1 Hz and if b<1 the peak occurs at > 1 Hz.

The b factor is made up of effects due to composition.

The initial tests were carried out using two steels with known free nitrogen contents and chemical compositions, see Table 3.2.1.

Table 3.2.1 Chemical Compositions

Cast No.	C %	Si %	Mn %	Cr %	Mo %	Al %	N %	Free N ppm*	Free C Ppm*
F8104	0.17	0.2	0.83	0.01	0.005	0.03	0.0063	8	3.2
F8105	0.16	0.2	0.84	0.01	0.001	<0.004	0.013	55	28

The free nitrogen and carbon values were provided by the steel supplier having been measured using an Automated Piezoelectric Ultrasonic Composite Oscillator Technique (APUCOT) developed by AECL Research, Canada ⁽¹³⁹⁾. This is a resonant bar technique in which the sample is placed on top of quartz crystals that are precisely cut to resonate longitudinally at 40 kHz ⁽¹⁴⁰⁾. This applies a cyclic tensile stress at 40 kHz to the sample.

The original internal friction measuring devices use a pendulum oscillating at a fixed frequency, normally 1Hz. The temperature of the specimen, usually in the form of a wire, was progressively changed to detect the peaks ⁽⁵²⁾. Using this type of apparatus Gladman and McIvor ⁽¹⁴¹⁾ showed that variations in the substitutional elements notably manganese affected the temperature at which the peaks occurred.

In the Vibran apparatus the temperature can be held constant whilst the frequency is varied, in this case the effect of manganese and similar sized substitutional atoms is to vary the frequency at which the peak occurs.

Initial factors for the peak shift in the model were based on extrapolation of Gladman's work, which showed that increasing manganese decreased the temperature at which the peak occurred. Using the Vibran equipment running at a constant temperature an increase in alloy content would give an increase in the frequency of the peak position. On this basis an initial value of b for the nitrogen peak was given by;-

$$b = \frac{1}{(3 \times \%Mn)} .$$

This initial correction factor did not take into account the effect of the other common substitutional alloying elements such as chromium. To take account of this the weight

percentages of silicon, chromium and molybdenum would need to be added to the manganese figure, giving:-

$$b = \frac{1}{(3 \times (\%Mn + \%Si + \%Cr + \%Mo))}$$

As the steel used for the early development work, F8105 had low levels of chromium and molybdenum (0.01 and 0.001% respectively) this did not cause a significant error in the peak position. However, as silicon and chromium do not cause significant lattice distortion compared to manganese and molybdenum the factor has been modified to take this into account:-

$$b = \frac{1}{((3 \times \%Mn + \%Si + \%Cr + 3 \times \%Mo) + 1)}$$

The multiple of three factors for manganese and molybdenum being based on a best fit to a series of measured curves for Armco iron, the high nitrogen steel and the medium nitrogen steel (the +1 value ensures that b defaults to unity for a pure iron).

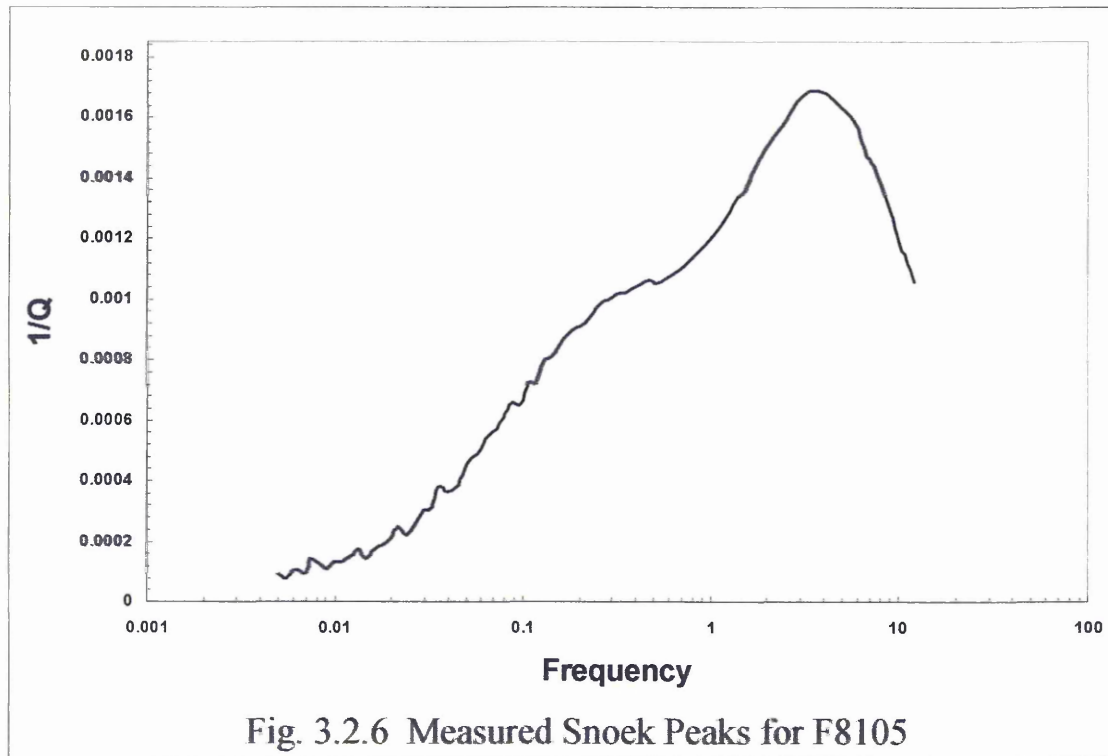
The equation for the internal friction value (1/Q) thus becomes:-

$$\frac{1}{Q} = \frac{a \times c}{(\ln(x / ((3 \times \%Mn + \%Si + \%Cr + 3 \times \%Mo) + 1)))^2 + c}$$

Where **a** is the height of the nitrogen Snoek peak, **c** is a peak width factor and **x** is the frequency.

In order to fit this curve to a measured curve for a steel containing free carbon and free nitrogen it would need to be added to a similar curve for the carbon Snoek peak and a zero correction made for the calculated curves.

Figure 3.2.6 shows the Snoek peaks, measured at 21°C, for a steel (F8105) containing free carbon and nitrogen. The maximum of the nitrogen peak occurs at approximately 3 Hz and overlaps the smaller carbon peak whose maximum occurs around 0.4 Hz



Initially the nitrogen model is fitted to the main peak of the measured data. The model peak is then subtracted from the measured data to give a provisional carbon peak, figure 3.2.7. The carbon peak is then modelled. Addition of the carbon and nitrogen models initially gives an over estimate of the final curve. Using an iterative process the individual model curves are progressively reduced until the additive model gives a good fit with the measured data, figure 3.2.8.

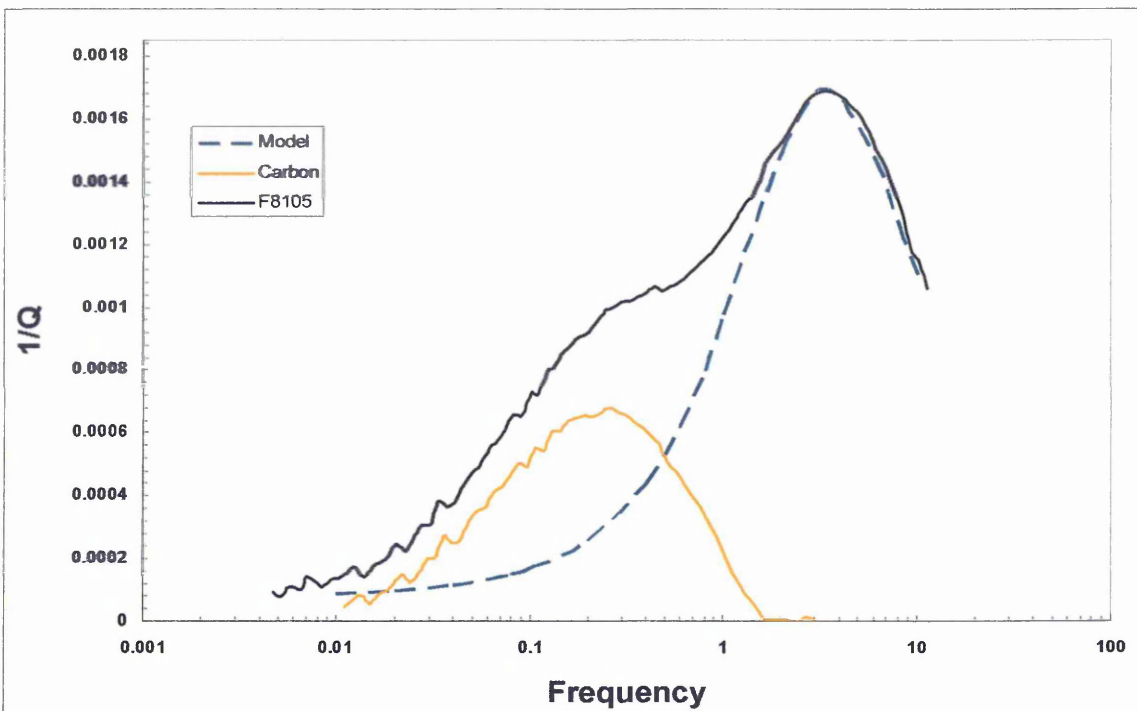


Fig. 3.2.7 Initial separation of Carbon Peak

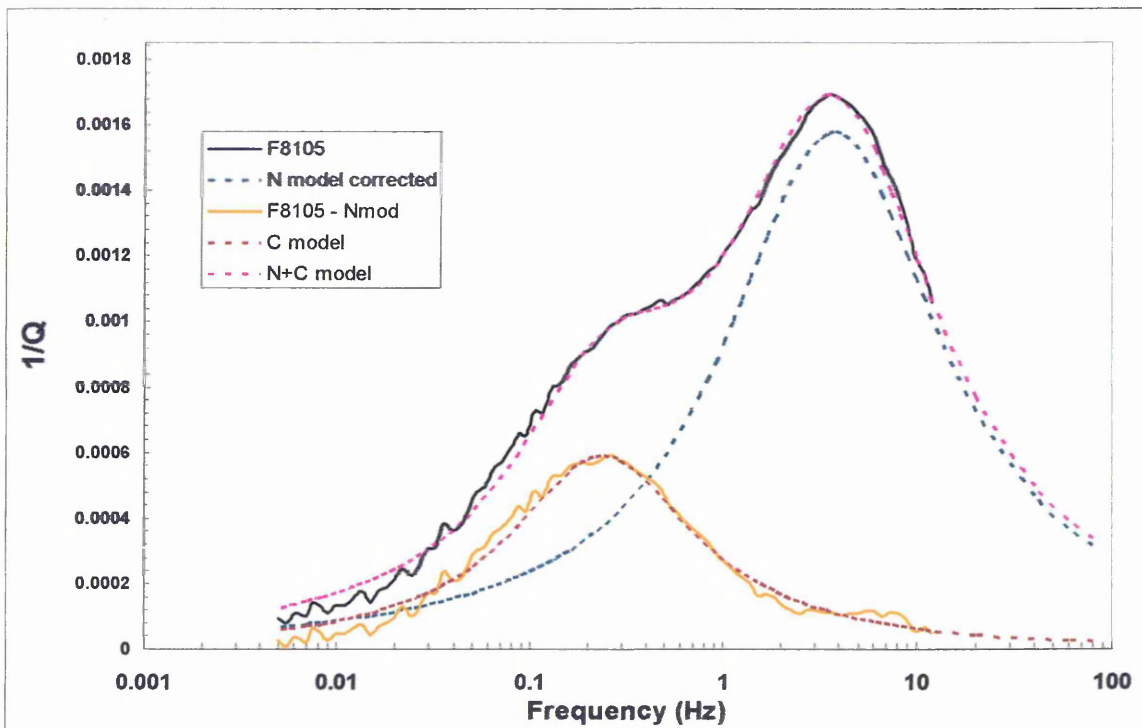


Fig. 3.2.8 Modelled Peaks for F8105

The initial tests were carried out, in the winter, at temperatures close to 21°C and a correction for temperature did not appear to be necessary. However, as the peak positions vary with temperature, and the laboratory would be warmer during the summer months, it was necessary to carry out tests on a standard sample to determine the peak shift per degree Celsius. The apparatus had been supplied with a small oven that could be fitted round the specimen but as the nitrogen peak occurs at around 1 Hertz at room temperature and the maximum frequency the equipment can operate at is only 12 hertz the maximum temperature that the specimen could be tested at before the peak moved out of the measuring range was limited to less than 40° C. Therefore in order to determine the temperature factor over a reasonably wide range a cooling unit was devised to enable testing at temperatures below ambient.

The cooling unit had to meet the following criteria in order to preserve the integrity of the measurements:

- 1) It must not cause any vibration of the specimen or measuring apparatus.
- 2) It must not cause any air currents that might disturb the specimen.
- 3) It should only cool the specimen and the clamping jaws, not the whole of the cabinet.

A venturi cooling system was initially considered but the air flow required would have significantly affected the specimen.

The design that was finally decided upon used a 25mm bore copper tube to surround the specimen. Small bore copper tubing was then wound around this tube and soldered to it. This was then insulated using epoxy foam and encased in a plastic tube.

The unit was cooled by pumping antifreeze through the small bore tubing, the antifreeze in turn being cooled by pumping it through a top tank containing a freezing mixture

(initially ice and antifreeze and then acetone and dry ice for lower temperatures). The header tank, pump and cooling tank were all clamped to the tower used to support the cabinet, see figure 3.2.9. This allowed the cooled 25mm copper tube to surround but not touch the specimen.

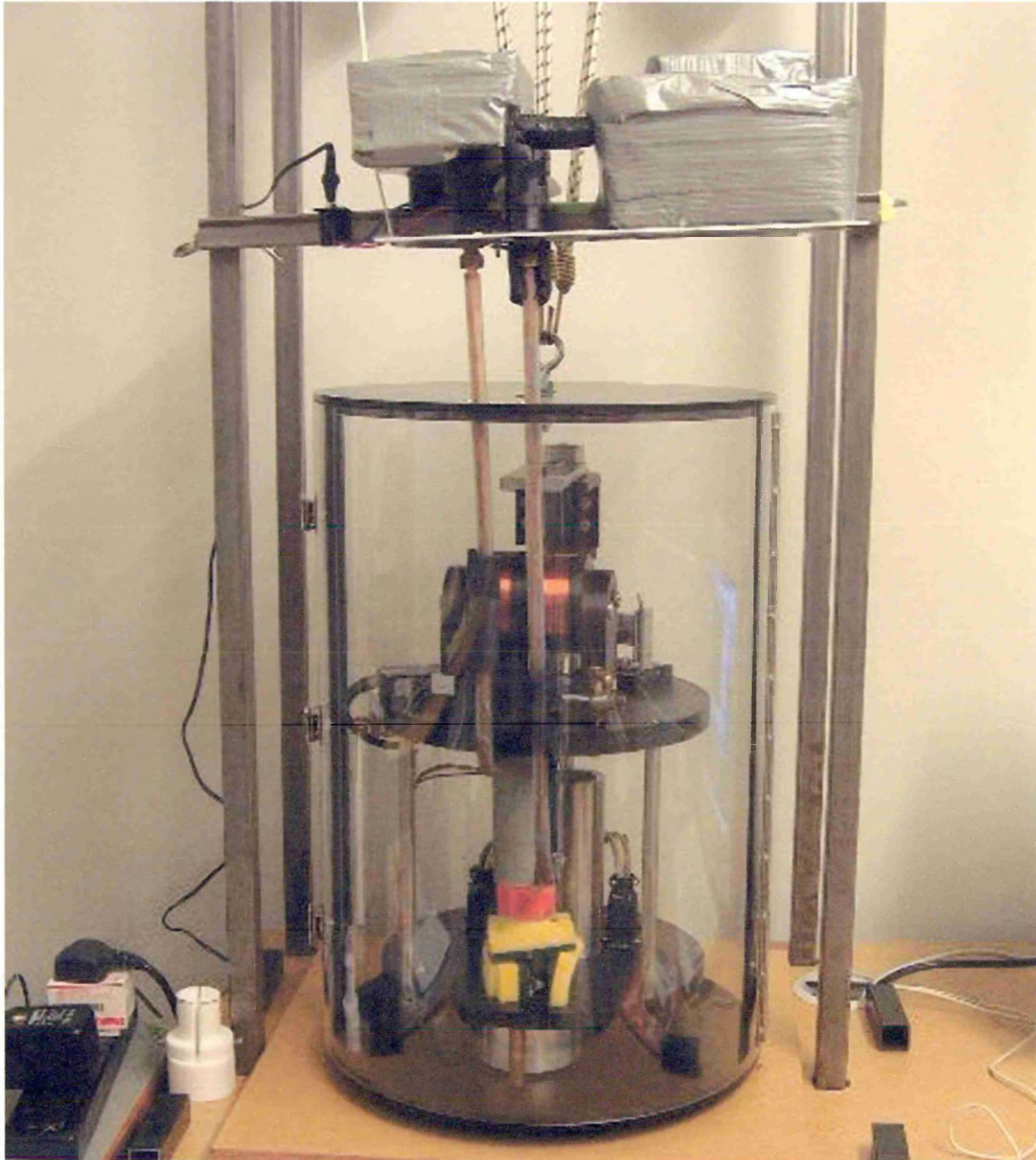


Fig. 3.2.9 Cooling Unit

The base of the cooled tube was sealed, to prevent the cooled air from leaking, with sponge insulation which fitted tightly round the bottom specimen clamp.

The specimen temperature was monitored using a thin sheathed type K thermocouple, placed close to the specimen inside the cooling tube.

Using this system it was possible to take the specimen down to 10°C (15° below the ambient temperature). It was not possible to go to any lower temperature as the antifreeze became too viscous to pump round the system.

Table 3.2.2 gives the peak frequency versus temperature for readings taken between 10.06 to 40.9°C and the results are shown graphically in figure 3.2.10.

Table 3.2.2 Effect of Temperature on the Position of the Nitrogen Peak

Nitrogen Peak Frequency (Hz)	Temperature (°C)
1.846	10.06
1.846	11.27
2.248	14.9
3.334	17.87
3.1	19.64
3.334	21.17
3.679	21.48
3.679	21.56
5.456	25.5
6.644	28.81
7.89	30.15
8.4	36.67
8.5	40.90

However, analysis of the plot at 40.9°C shows that whilst the apparatus gives readings up to 12 Hz the sudden drop off above 10 Hz suggests that these readings are not accurate, i.e. the true position of the peak at 40°C is greater than 8.5 Hz.

A plot of temperature against the log of the peak frequency (ignoring the 40°C data) gave a good approximation to a linear function with an R^2 value of 0.9579. This is shown in figure 3.2.11. (A second order polynomial only gave a slightly better fit with

an R^2 value of 0.9623. However, as the improvement was only minimal and was not significant within the normal operating temperature range of the equipment it was not used for the final model.) The slope of the line (0.0655) shown in figure 3.2.11 gave a temperature correction factor of ;

$$0.0655 \times (21 - T)$$

where T is the average temperature during the test. (The data logging system records the temperature at every reading.)

A similar process was followed to determine the shift of the carbon peak with temperature. In this case it was necessary, in order to determine the peak position, to first remove the modelled nitrogen peak from the measured curve. Table 3.2.3 gives the carbon peak position against temperature and fig. 3.2.12 shows the plot of frequency against temperature and fig.3.2.13 shows the plot of log frequency against temperature. This gave a temperature correction factor for carbon of ;

$$0.0664 \times (21 - T)$$

Table 3.2.3 Effect of Temperature on the Position of the Carbon Peak

Carbon Peak Frequency (Hz)	Temperature (°C)
	10.06
0.106	11.27
0.143	14.9
0.174	17.87
0.1915	19.64
0.2	21.17
0.23	21.48
0.2332	21.56
0.3458	25.5
0.382	28.81
0.465	30.15
0.625	36.67
0.625	40.90

This gave the following final model for the nitrogen internal friction;

$$= \frac{N_p \times w_f}{\{ [\ln(f/b) + 0.0655(21 - T)]^2 + w_f - p_b \}}$$

Where

N_p = Nitrogen peak height

w_f = peak width factor

f = frequency

b = alloy factor

T = ambient temperature

p_b = peak baseline factor

The carbon internal friction was modelled using an equivalent equation.

The final model was generated in a Microsoft Excel spread sheet, the raw data being downloaded from the Vibran computer. To reduce noise on the measured signal three scans of the frequency range were recorded per measurement and averaged, this average was then rolling averaged over five values to produce a smoother curve to fit to. A zero correction was applied to the data to bring the $1/Q$ value close to zero at a frequency of 0.005 Hz, the lower measurement limit.

Figures 3.2.14 to 3.2.17 show the measured data (to which a zero correction has been applied) from a specimen of F8105 high nitrogen steel and the fitted curves generated by the final model for a range of temperatures from 14.9 to 36.67°C.

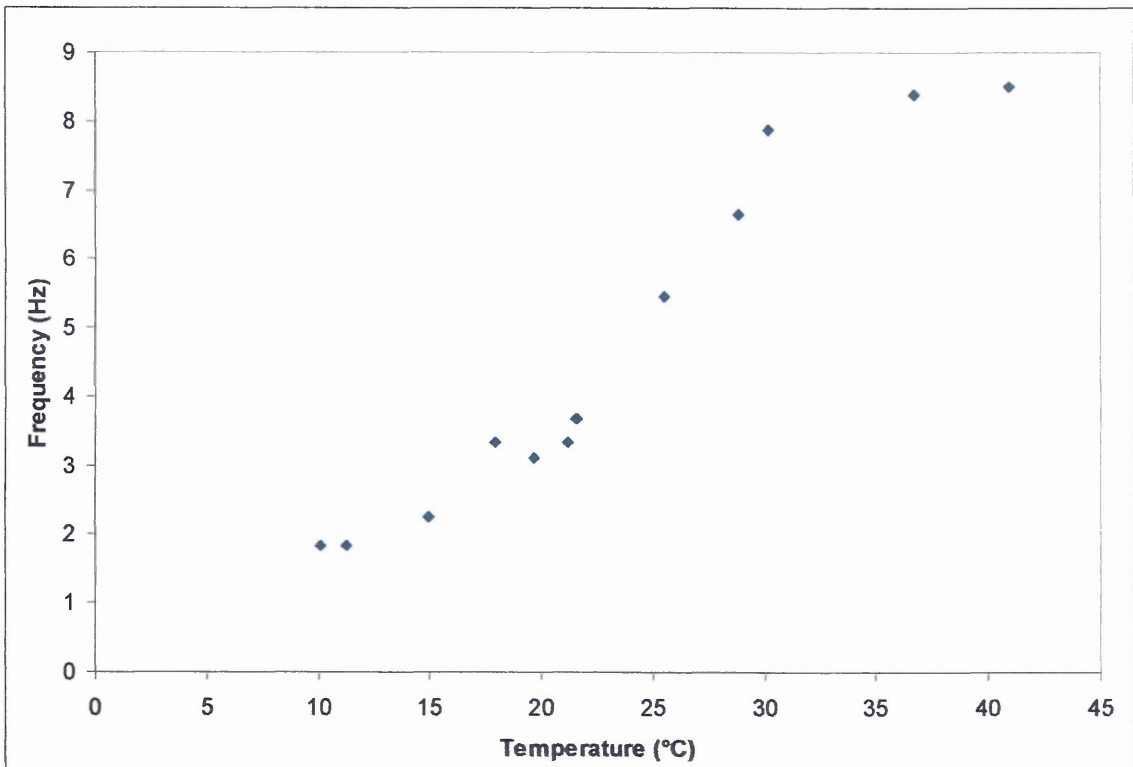


Fig. 3.2.10 Effect of Temperature on Nitrogen Peak Position

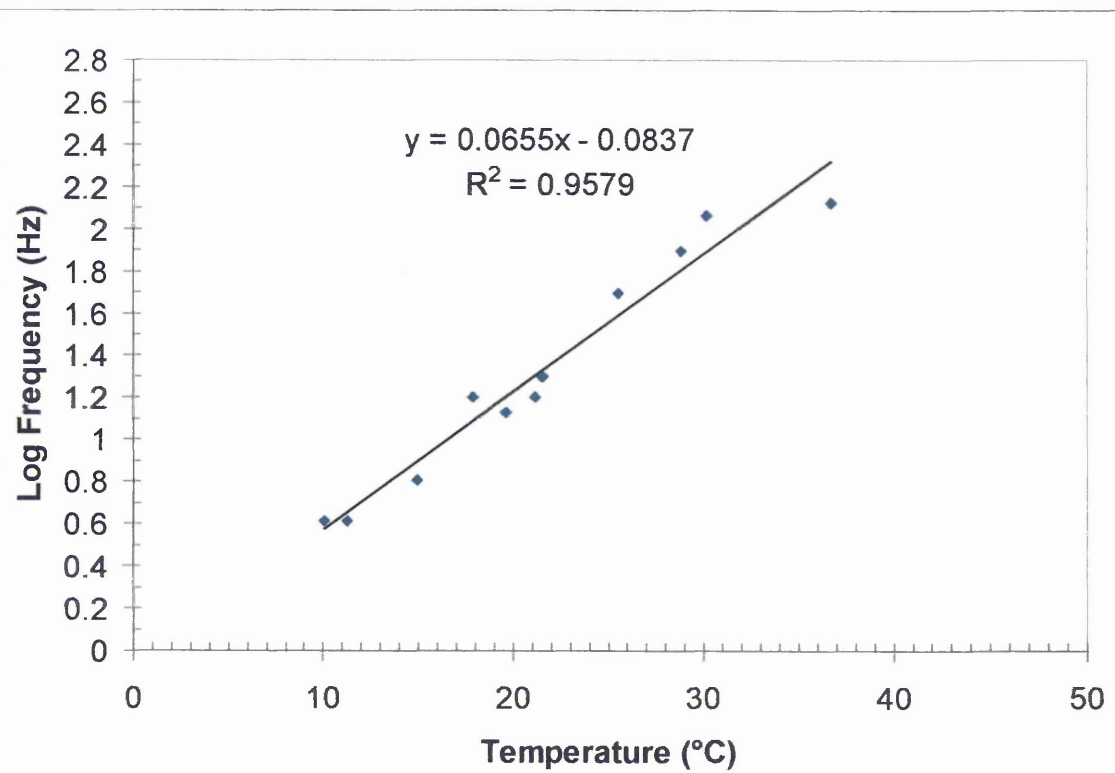


Fig. 3.2.11 Log of Nitrogen Peak Frequency v Temperature

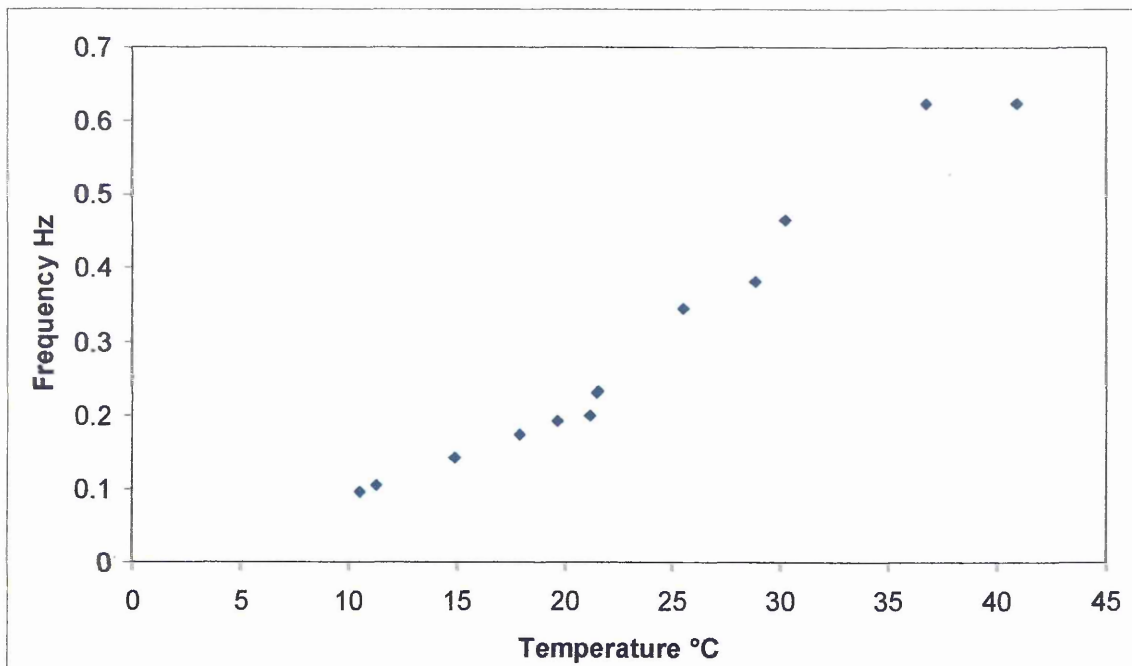


Fig. 3.2.12 Effect of Temperature on Carbon Peak Position

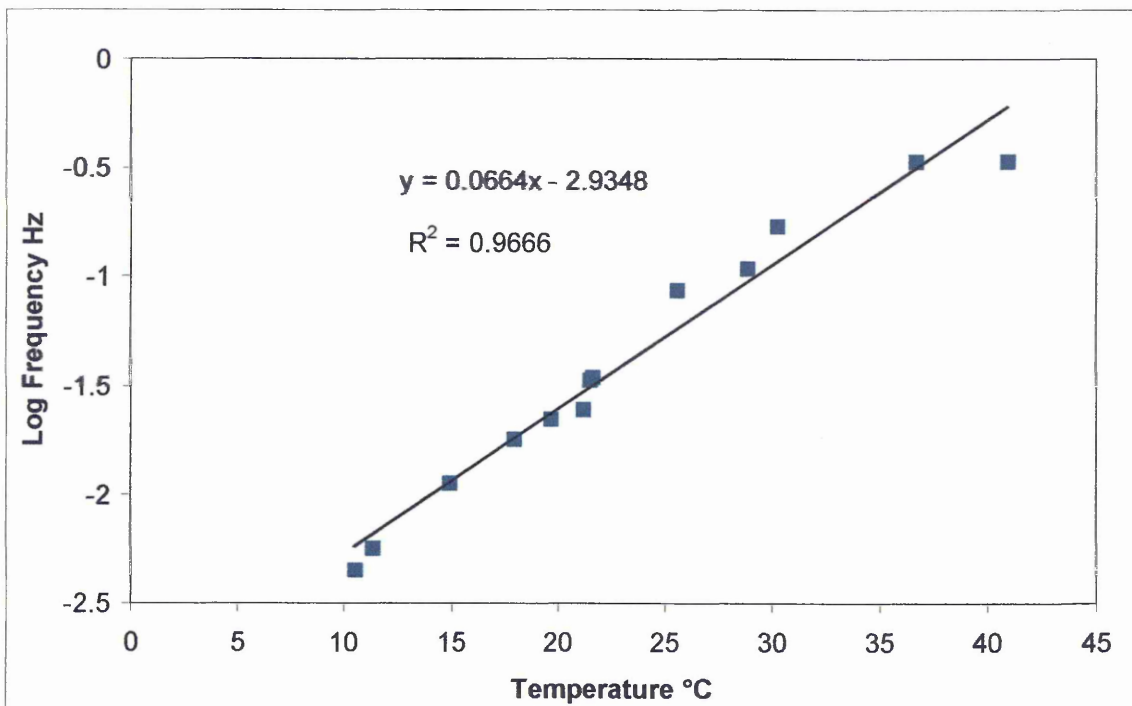
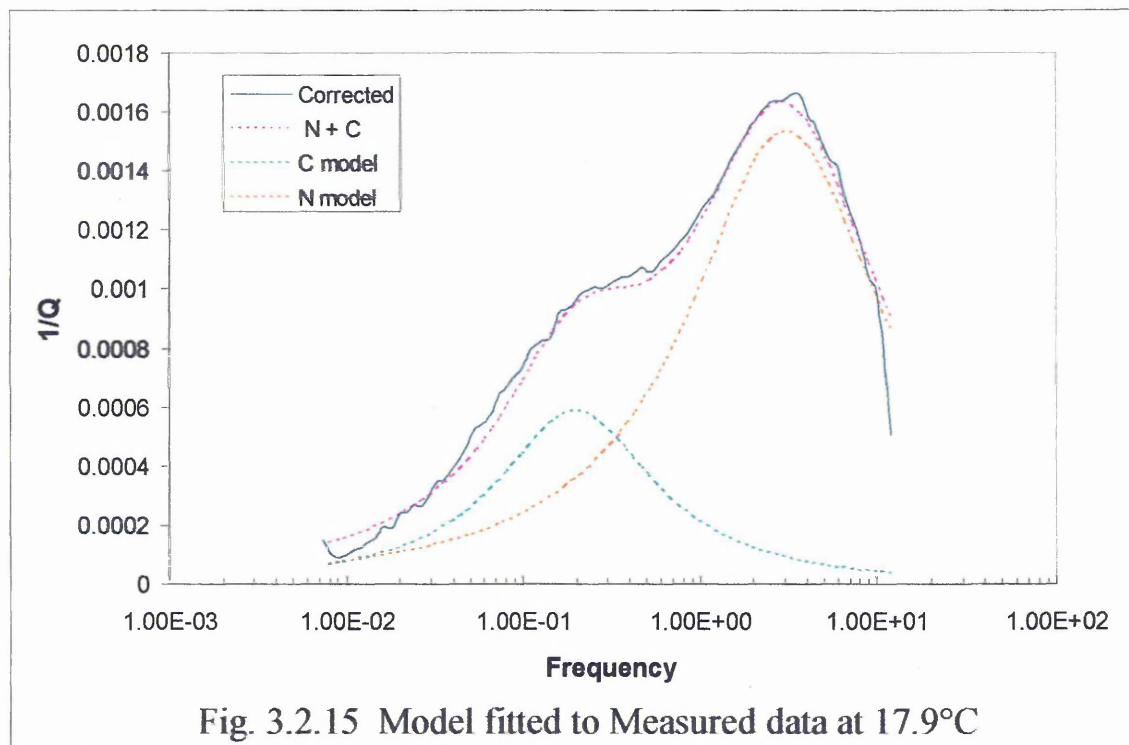
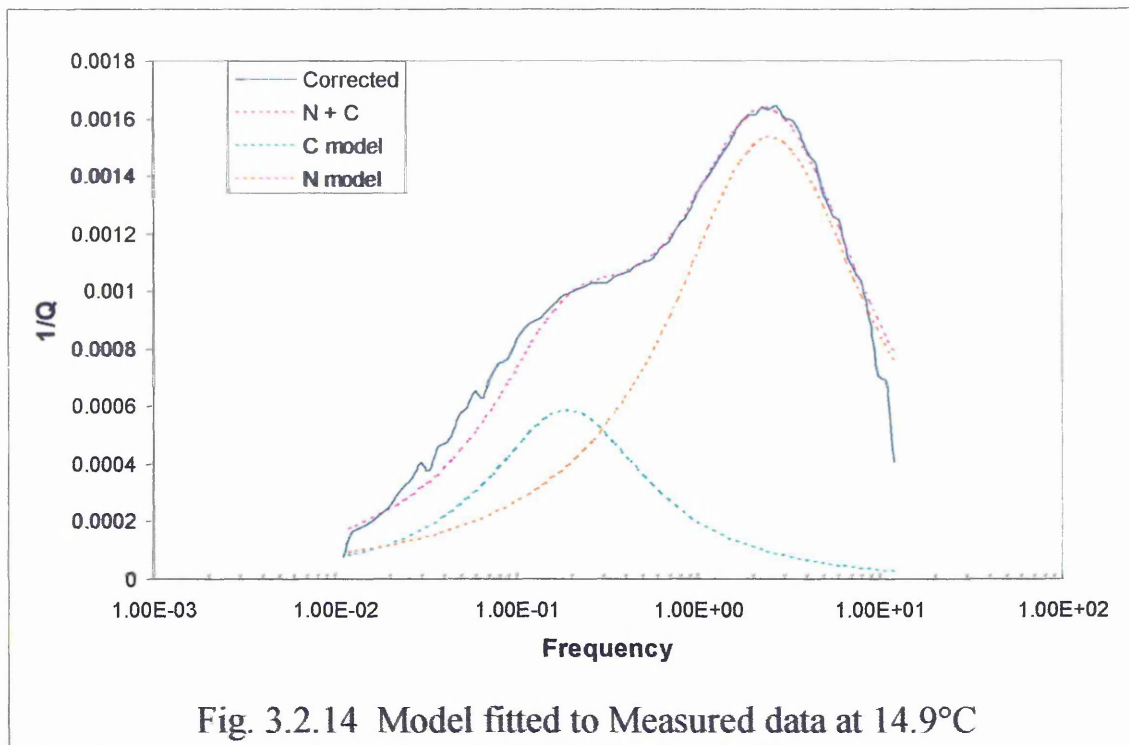


Fig. 3.2.13 Log of Carbon Peak Frequency v Temperature



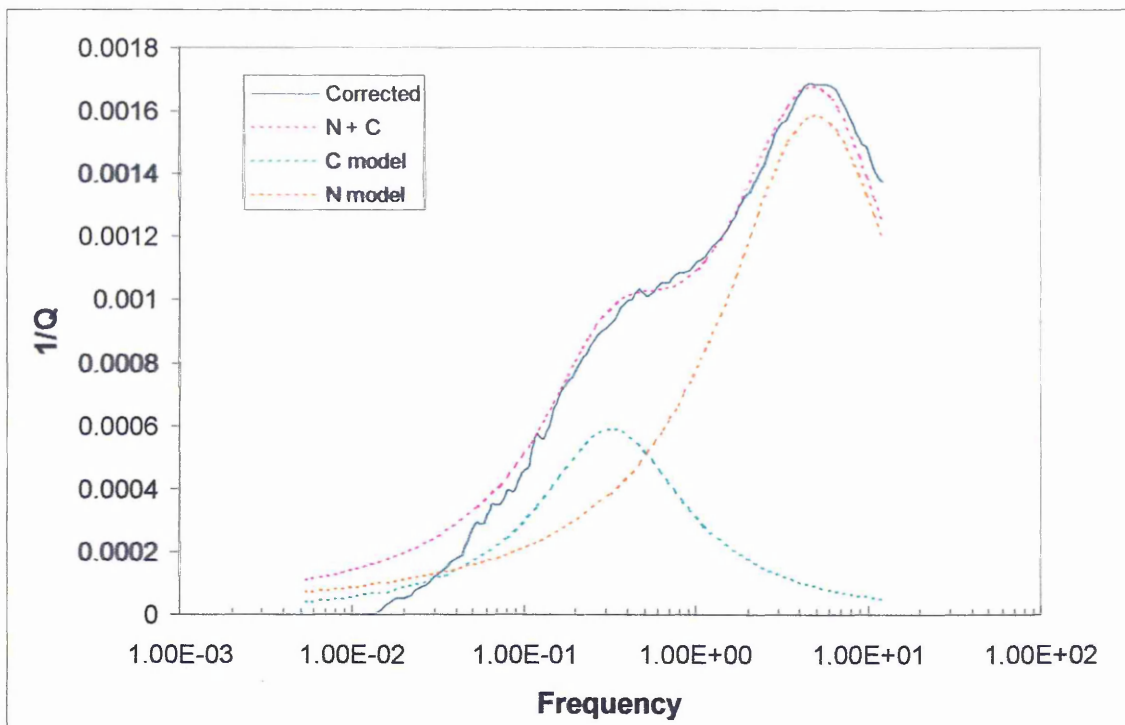


Fig. 3.2.16 Model fitted to Measured data at 25.3°C

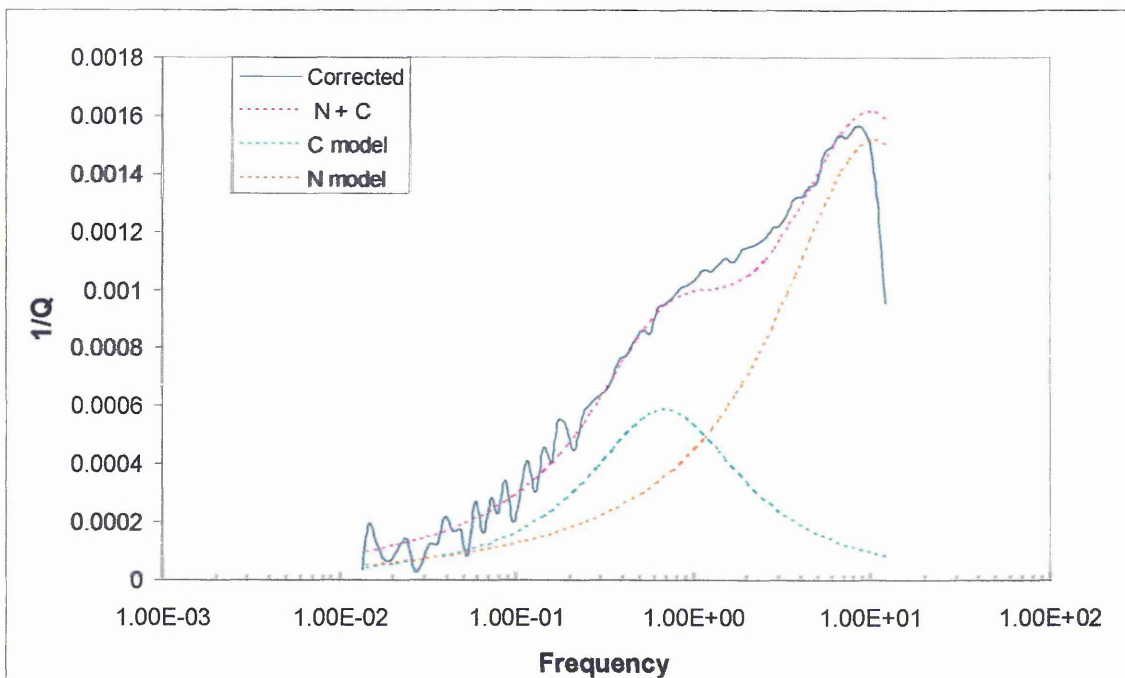


Fig. 3.2.17 Model fitted to Measured data at 36.6°C

The individual peak heights for the carbon and nitrogen were then calibrated using the data from the APUCOT measurements. This gave the following scaling factors for the nitrogen and carbon peak heights;

$$\text{Free Nitrogen (ppm)} = \text{model peak height} \times 34,375$$

$$\text{Free Carbon (ppm)} = \text{model peak height} \times 46,670$$

Using these calibrations the model was fitted to measured data from steel F8104, see figure 3.2.18. This gave free nitrogen and free carbon contents of 8.8 ppm and 2 ppm which fits well with the APUCOT data of 8 ppm for the nitrogen and 3.2 ppm for the carbon.

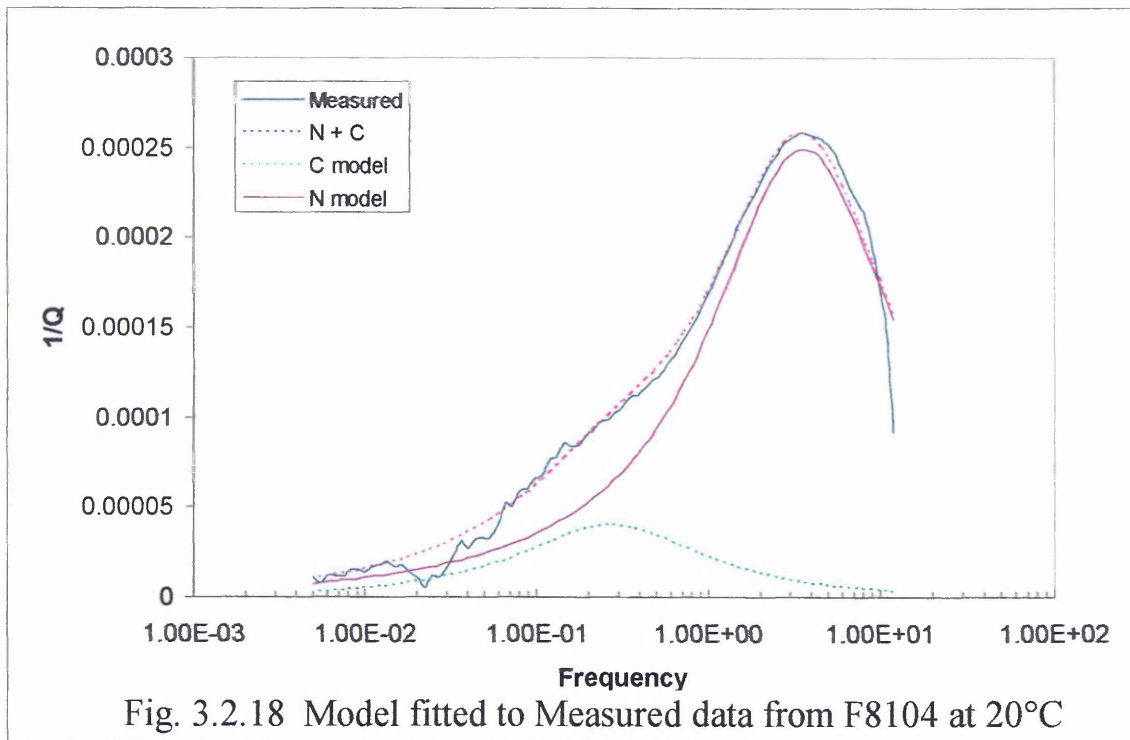


Figure 3.2.19 shows an example of the Excel spread sheet for an aluminium killed mild steel VS3764B which had a total nitrogen content of 0.005 wt%. The peak values shown in red are adjusted until the modelled curve (New N + C) fits the data curve (Corrected).

Specimen file no. 04092902

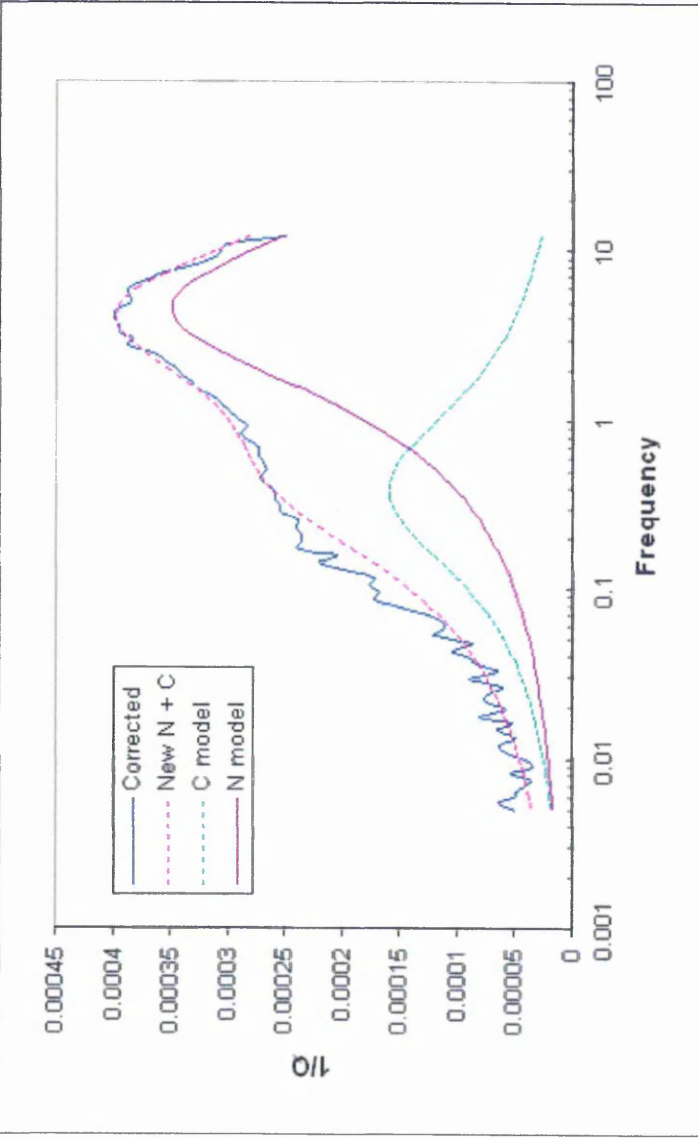
Chemical Analysis		Si	Mn	Cr	Mo	Al	N
C	0.21	0.2	0.7	0.2	0.005	0.032	0.005

Zero correction Test Temperature

Nitrogen Peak 0.00035
baseline 0.000001

Carbon Peak 0.00016
Baseline 0.0000001

Width Nitrogen 2.5
Factors Carbon 2.5



N ppm = 12.0

C ppm = 7.5

Alloy Nitrogen 3.515
Factors Carbon 0.302

Fig.3.2.19a Example of an Excel Results sheet

Put results in these F.Hz	Two columns		Corrected 1/Q	N model	C model	New N + C		
	1/Q	1/Q						
12	0.0007	0.00025	1.227867	0.000224	0.000254	3.683339	2.81069E-05	0.0002817
10.87	0.000752	0.000302	1.128967	0.000238	0.000268	3.584439	2.94974E-05	0.0002973
9.854	0.000757	0.000307	1.030838	0.000252	0.000282	3.48631	3.09729E-05	0.0003128
8.929	0.000766	0.000316	0.932265	0.000266	0.000295	3.387737	3.25591E-05	0.000328
8.092	0.000785	0.000335	0.833836	0.00028	0.000308	3.289309	3.4256E-05	0.0003425
7.332	0.000812	0.000362	0.735209	0.000294	0.00032	3.190681	3.60791E-05	0.0003561
6.644	0.00082	0.00037	0.636675	0.000307	0.00033	3.092147	3.80339E-05	0.0003682
6.021	0.000837	0.000387	0.538214	0.000319	0.000338	2.993686	4.01315E-05	0.0003786
5.456	0.000836	0.000386	0.439676	0.000329	0.000345	2.895149	4.23875E-05	0.0003869
4.944	0.000835	0.000385	0.341135	0.000338	0.000348	2.796607	4.48136E-05	0.0003929
4.48	0.000849	0.000399	0.242584	0.000344	0.000349	2.698056	4.74238E-05	0.0003964
4.06	0.000849	0.000399	0.144143	0.000348	0.000347	2.599616	5.02295E-05	0.0003974
3.679	0.000846	0.000396	0.045601	0.000349	0.000343	2.501074	5.32522E-05	0.0003959
3.334	0.000844	0.000394	-0.05287	0.000347	0.000336	2.402605	5.65028E-05	0.0003923
3.021	0.000833	0.000383	-0.15145	0.000343	0.000327	2.304021	6.00038E-05	0.0003868
2.738	0.000837	0.000387	-0.24981	0.000337	0.000316	2.20566	6.37587E-05	0.0003798
2.481	0.000815	0.000365	-0.34838	0.000328	0.000304	2.107094	6.7799E-05	0.0003717
2.248	0.000806	0.000356	-0.447	0.000317	0.000291	2.008474	7.21334E-05	0.0003628
2.037	0.000796	0.000346	-0.54556	0.000305	0.000277	1.909911	7.67675E-05	0.0003536
1.846	0.000789	0.000339	-0.64402	0.000292	0.000263	1.811454	8.17052E-05	0.0003445
1.673	0.000782	0.000332	-0.74242	0.000278	0.000249	1.713051	8.6949E-05	0.0003356
1.516	0.000776	0.000326	-0.84096	0.000264	0.000235	1.614508	9.25022E-05	0.0003272
1.374	0.000765	0.000315	-0.93931	0.00025	0.000221	1.516159	9.83277E-05	0.0003195
1.245	0.000757	0.000307	-1.0379	0.000236	0.000208	1.417568	0.00010442	0.0003125

Fig.3.2.19b Example of an Excel Results sheet

3.2.4 Internal Friction Measurements

Once the equipment had been calibrated, comparative measurements were carried out on specimens produced by:

- i) Cutting from a machined block using a fine water cooled cutting wheel in an Acutom high speed specimen cutter.
- ii) Spark machining specimens from a machined block and then thinning to the finish size by hand polishing on silicon carbide papers.

No significant differences between the two methods were observed and so all subsequent specimens were produced by the spark machining route as this was available at the university.

Figure 3.2.20 shows the results from the Armco iron material. This was found to have a low free nitrogen content of 8.6 ppm but with a very high free carbon content of 115.7 ppm (0.01157%) much higher than the suppliers analysis of 0.001%!

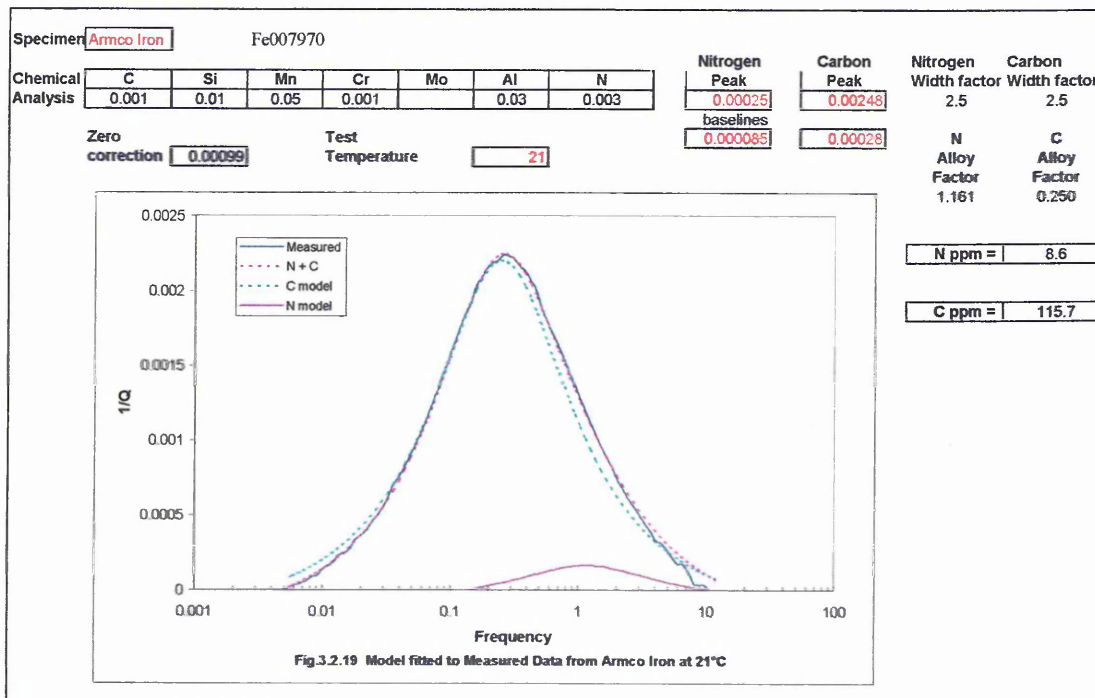


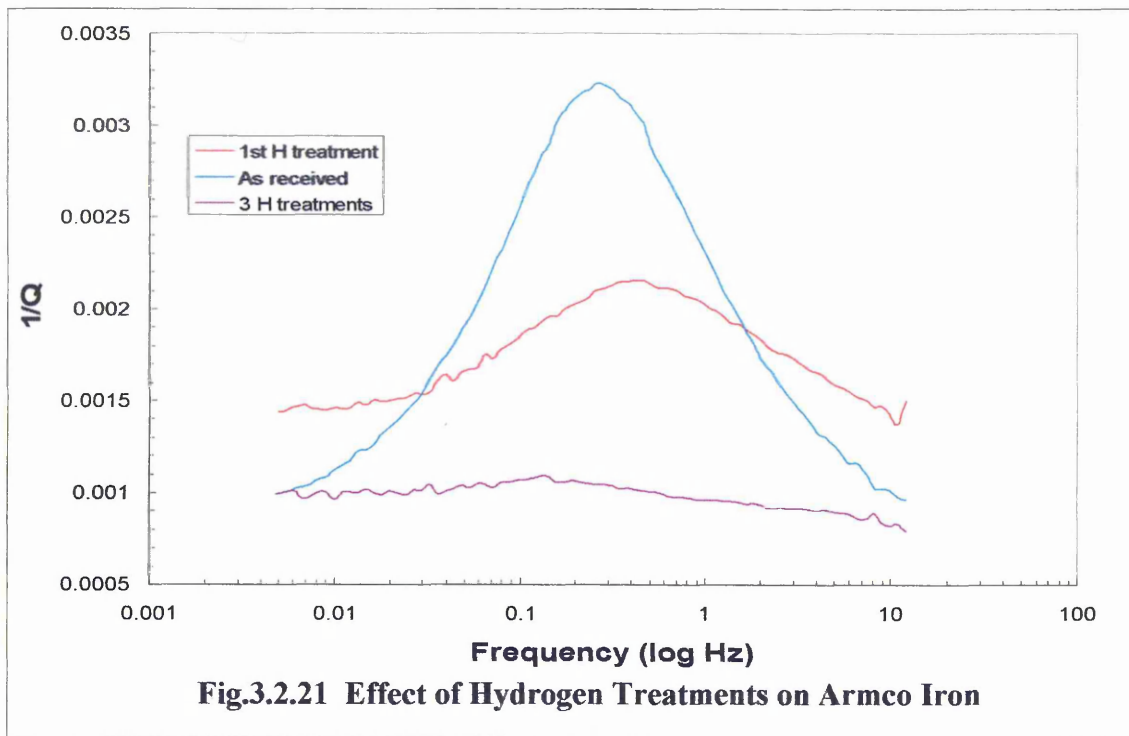
Fig.3.2.20 Model fitted to Measured Data from Armco Iron at 21°C

To check this result a second specimen of the Armco iron was tested and this gave a nitrogen value of 7.9 ppm and a carbon value of 119 ppm (0.0119%).

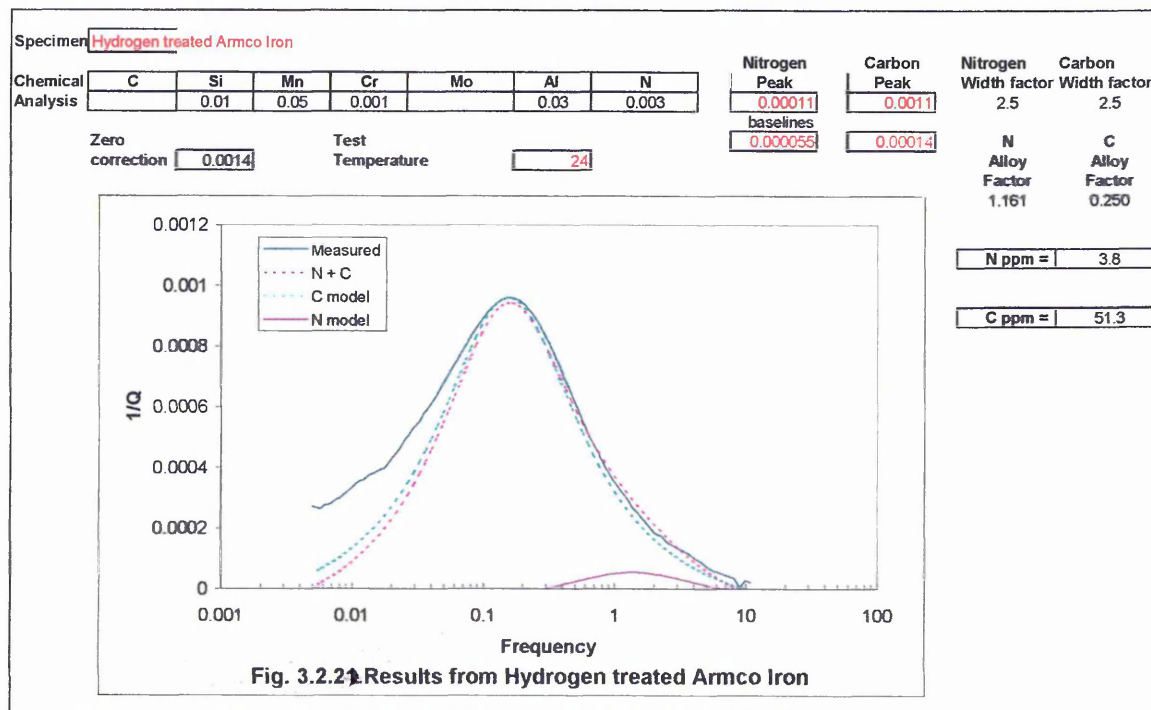
This high carbon level was unlikely to be the result of specimen preparation as it was not seen in F8104, F8105 and the subsequently tested sample VS3764B (or in later tests) all of which were prepared by the same method i.e. spark machined.

In order to determine if the peaks really were due to carbon the second specimen was heated in a stream of hydrogen at 440°C for 4 hours. This was based on the assumption that if the carbon values were real then the treatment would reduce the carbon content by forming methane (and nitrogen as ammonia). (A later chemical analysis of the Armco iron was carried out by Corus Central Laboratory which gave a carbon content of 0.01%.)

Figure 3.2.21 shows the 'as recorded' curves for the as received material, the first hydrogen treatment and after an additional two treatments. In order to allow any dissolved hydrogen to diffuse out of the specimen it was left in air at room temperature for 24 hours before being measured.

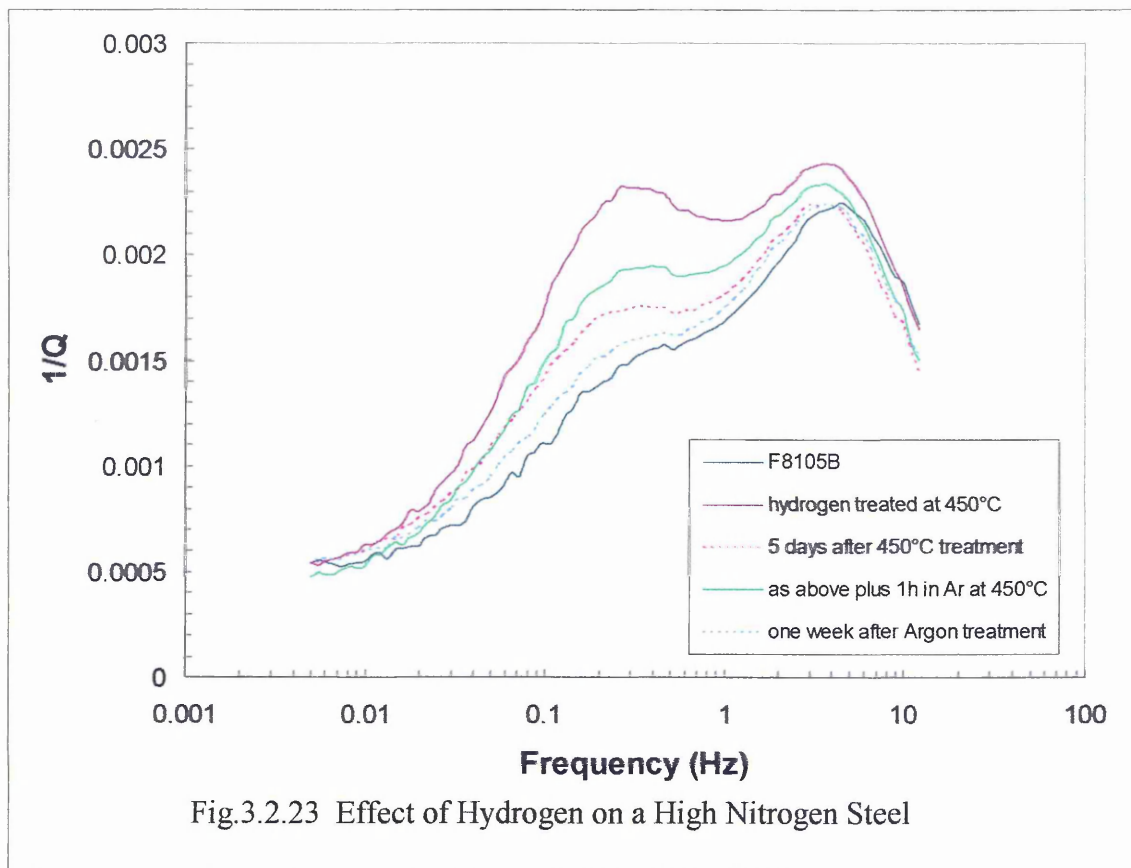


The results clearly show that carbon has been removed by the hydrogen treatment. The final free carbon values being measured at 51.3 ppm and the free nitrogen at 3.8 ppm, see figure 3.2.22.



The equilibrium constant for the reaction between hydrogen and carbon is such that decarburisation by the formation of methane is not significant at temperatures below 650°C. However, as this experiment shows if any methane formed is carried away from the metal surface by a stream of hydrogen then Le Chatelier's Principle would predict that the reaction will occur at a lower temperature. Incidentally this is a further reason why the thermistor bridge detection system (see section 3.1) could never give an accurate nitrogen content as the gas stream will also contain small amounts of methane as well as the ammonia.

The small size and rapid diffusion rate of hydrogen in iron would suggest that any internal friction peak at temperatures near to room temperature would occur at much higher frequencies than the Vibran apparatus could measure. However, to check if there was any detectable effect due to hydrogen further hydrogen treatments were carried on a specimen of the high nitrogen steel F8105. In this case the specimen was hydrogen treated 1 hour and 15 minutes at 450°C. Testing was started within 75 minutes of the specimen leaving the furnace. Figure 3.2.23 shows the effect of the hydrogen treatment, a retest of the specimen after five days at room temperature and for a subsequent treatment in pure argon at 450°C designed to allow the hydrogen to diffuse out of the specimen.



A final measurement was carried out one week after the argon treatment. The increase in the peak heights immediately after treatment in the gases does not appear to be an artefact of the measuring system as the $1/Q$ values in the region 0.005 to 0.01 Hertz are reasonably constant. The fact that the carbon peak shows a significantly greater height increase after the hydrogen treatment than the nitrogen is probably due to the fact that at 450°C nitrogen would be preferentially removed as ammonia rather than the carbon (this effect would be enhanced by the high level of free nitrogen in the steel).

These results raise the question “why do hydrogen and argon apparently raise the peak heights?”

One possible explanation is that rapid cooling of the specimen after the heat treatment has trapped carbon and nitrogen in interstitial locations whereas in steel that has been at room temperature for several days some of the carbon and nitrogen atoms will have

diffused to dislocations and so will not change positions within the body centred cubic cells during a stress cycle. However, quenching tests on an Armco iron sample heated in vacuum and then quenched with argon gas did not show any significant effect on the measured Snoek peak.

As has been shown, if hydrogen reduces the elastic strain around dislocations ⁽³⁷⁾ and generally in metal crystals ⁽⁶⁴⁾ then the maximum energy stored in the sample during an oscillation (W) should be reduced. Then from equation 2 (page 24);

$$\text{Internal friction } \delta = \frac{\Delta W}{2W}$$

The measured internal friction should increase when hydrogen is present in the specimen and then gradually decrease as the hydrogen diffuses out of the specimen.

The effect of the argon treatment appears to be linked to the presence of hydrogen as the argon treatment on its own does not have any effect. Possibly the argon treatment has released hydrogen that was trapped in some way and so not able to reduce elastic strain. Again over time this newly released hydrogen either diffuses out of the specimen or is re-trapped over a period of several days.

3.2.5 Observations on the Effect of Free Nitrogen on the Impact Transition Temperature

As the free nitrogen values were available this gave the opportunity to see how the measured values of the Impact Transition Temperatures for these steels compared to the values predicted by the Pickering Gladman equation;-

$$ITT = -19 + 44*(Si\%) + 700*\sqrt{N_f} + 2.2*(Pearlite\%) - 11.5*d^{-1/2}$$

and the Mintz equation –

$$ITT = 15 + 50*(Si\%) + 2750*N_f\% + 2.2*(Pearlite\%) - 11.5*d^{-1/2} + 70*Al\%$$

Where N_f = free nitrogen content and d = average grain diameter in millimetres.

The chemical analyses of the four steels examined are given in table 3.2.6.1.

Table 3.2.5.1

Steel	C	Si	Mn	S	Cr	Mo	Al	N (Total)
F8104	0.17	0.33	0.84	-	0.01	0.005	0.03	0.0063
F8105	0.16	0.33	0.83	-	0.01	0.001	<0.004	0.013
VS3764A	0.21	0.20	0.70	0.002	0.2	0.005	<0.005	0.008
VS3764B	0.20	0.19	0.71	0.024	0.2	0.005	<0.005	0.007

Sets of standard ‘V’ notch Charpy specimens were machined from each of the steels.

Initial impact tests at 100°C and –196°C were carried out to establish the upper and lower shelf energies. Tests were then carried out at intermediate temperatures to establish the Impact Transition Temperature. A total of six tests were carried out on F8104, seven on F8105 and nine on VS3764B. The Charpy data and grain size measurements for VS3764A were provided by M.R. Corrigan⁽¹⁴²⁾.

Sections were cut, from each steel, for grain size and percentage pearlite determinations.

Internal friction specimens were also cut from each of the steels for measurements of the free nitrogen contents using the Vibran Interstitial Analyser.

3.2.6.2 Results

The impact values at the various test temperatures, for the Charpy tests, are given in table 3.2.6.2 and shown graphically in figure 1. The ITT values were calculated as the temperature where the curve passed through the mid-point between the upper and lower shelf energies.

Table 3.2.6.2

F8104		F8105		VS3764B	
Temp (°C)	Joules	Temp (°C)	Joules	Temp (°C)	Joules
100	153	100	140	100	133
22	156	22	104	50	140
0	142	10	72	20	116
-20	114	0	30	0	104
-56	19	-20	13	-10	86
-196	4	-53	4	-20	80
		-196	4	-30	28
				-50	7.5
				-100	4

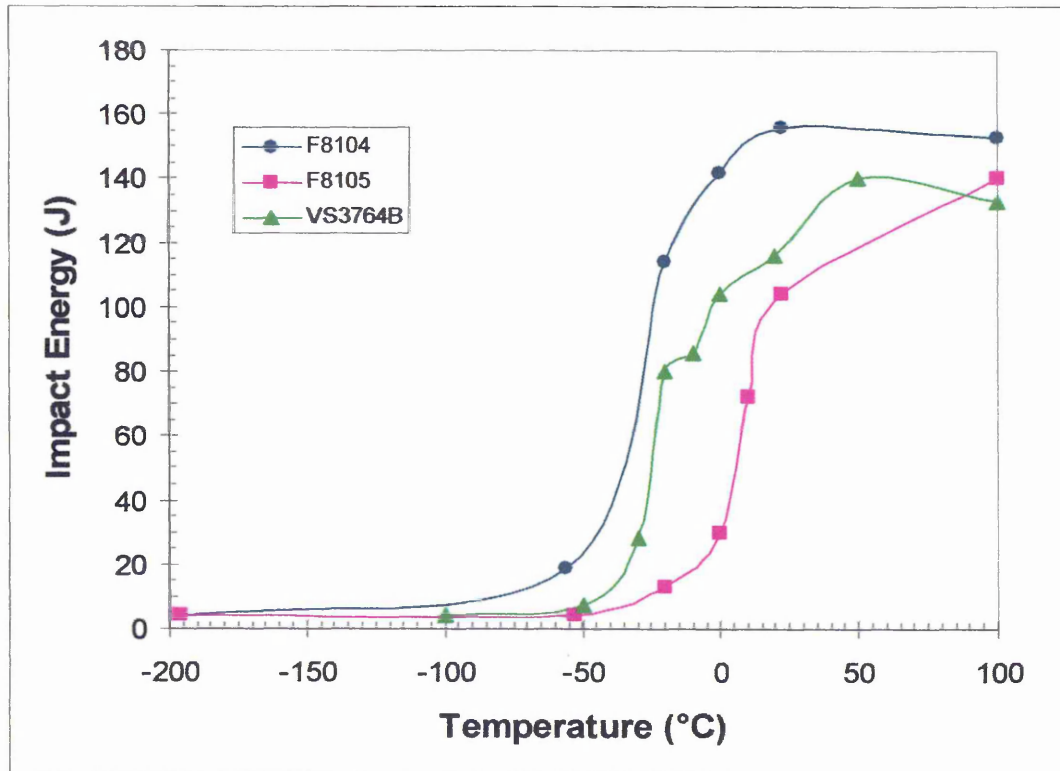


Fig. 3.2.6.1 Charpy Curves

Based on the curves shown in figure 3.2.6.1 the Ductile–Brittle Impact Transition

Temperatures were;-

F8104 = -29°C, F8105 = 9°C, VS3764B = -23°C

VS3764A = -23°C ⁽¹⁴²⁾

In view of the higher sulphur content of VS3764B compared to VS3764A it was expected that this steel would have a higher ITT, however, this did not prove to be the case. (The presence of a sulphide in the specimen tested at -10°C may be the cause of what appears to be an anomalous result.)

The grain sizes were measured using the linear intercept method both in the longitudinal direction and transverse direction (200 grains in each direction). As there was no evidence of any significant elongation of the grains in any of the samples, average grain diameters were calculated, these were;-

F8104 av. diameter = 7.5 µm (0.0075 mm) with a range of 7 – 8 µm.

F8105 av. diameter = 13 µm (0.013 mm) with a range of 12 – 14 µm.

VS3764B av. diameter = 12 µm (0.012 mm) with a range of 11 – 14 µm.

An attempt was made to use an image analysis program to determine the percentage of pearlite in the samples. However, this gave very high levels of pearlite, 32% for F8104 and 41% for F8105! These values were highly unlikely in view of the carbon contents of the steels (0.17% for F8104 and 0.16% for F8105).

In view of this a visual assessment was carried out. This revealed that F8104 had a typical ferrite / pearlite structure but showed significant variations in the proportion of

pearlite across the section, from 15 to 20%. The highest carbon levels occurred in the centre of the plate. There was also definite evidence of decarburisation in the surface layers. (Based on the carbon content the pearlite content should be ~ 21%). F8105 had a more acicular structure and the ferrite grains had a rippled surface texture (this probably was counted as pearlite by the image analysis system). The pearlite content appeared to be approximately 25%. (Based on the carbon content the pearlite content should be ~ 20%).

The internal friction measurements gave the following values for the free nitrogen contents;-

F8104 8ppm (0.0008wt%)

F8105 55ppm (0.0055wt%)

VS3764A 12ppm (0.0012wt%)

VS3764B 12ppm (0.0012wt%)

An SEM examination was carried out on the fracture faces of the specimens of two F series steels that were closest to the Impact Transition Temperature. Neither sample showed any obvious nucleation site though both contained a few alumina (Al_2O_3) inclusions (only one was identified in F8105). There was no evidence of nitrides on the fracture surface of the F8105 specimen.

3.2.6.3 Discussion of Impact Temperature Prediction

As a result of the limited number of slip systems body centred cubic and close packed hexagonal metals all show a transition from ductile behaviour to brittle fracture as temperature decreases. This is due to fact that the yield stress increases as temperature decreases whilst the fracture stress remains relatively unchanged. Figure 3.2.6.2 shows the effect of temperature on the yield strength and true fracture strength for a hot rolled 0.2% carbon steel ⁽¹⁴³⁾.

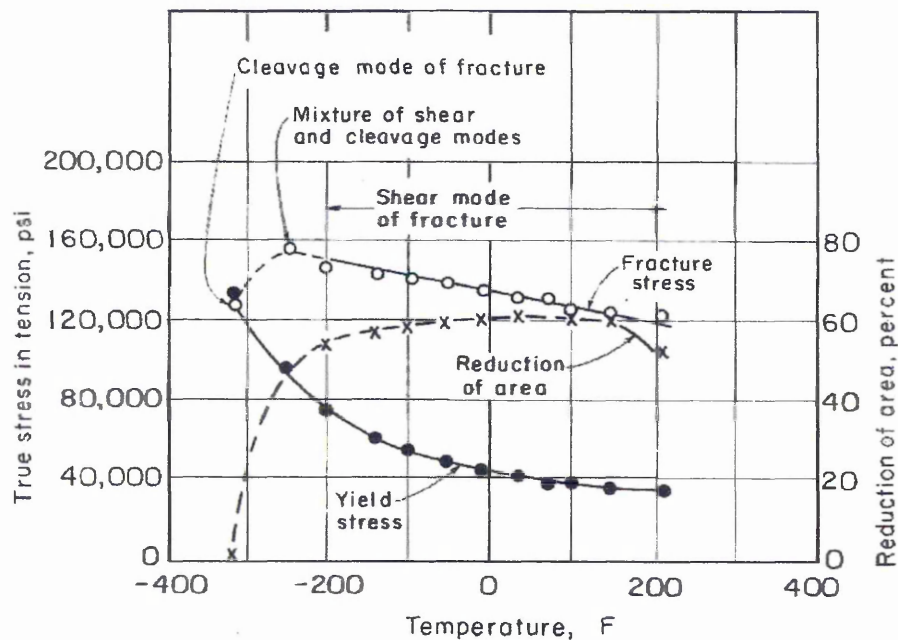


Fig. 3.2.6.2 The effect of testing temperature on the tensile yield strength, true fracture stress and reduction of area for a hot-rolled semikilled 0.2% carbon steel.

from Fracture, H. Liebowitz, ed. vol.1, Academic Press, 1968, p. 397.

This data is from tensile tests where the strain rate is relatively low allowing time for slip. In an impact test the strain rate is much higher, and along with the presence of a notch which causes a tri-axial stress system, results in a much greater restriction on slip ie. a greater tendency to brittle fracture. This effect has also been related to the Ductile Brittle Transition by Knott⁽¹⁴⁴⁾. It is clear from the above that any alloying addition that

increases the yield stress without significantly increasing the fracture stress will raise the Impact Transition Temperature.

The yield strength is made up of two main factors the friction stress (σ_0) and an effect due to grain size and is expressed in the Hall – Petch equation;

$$\text{Yield Stress } \sigma_y = \sigma_0 + k_y d^{-1/2}$$

Various workers have shown that σ_0 the friction stress varies significantly with temperature whilst k_y (sometimes referred to as ‘the unpinning parameter’) does not show any significant change with temperature, table 3.2.6.3 below list the changes for a range of mild steels⁽¹⁴⁵⁾.

Table 3.2.6.3 Variation of Friction Stress with Temperature

Temperature K	σ_0 MPa	k_y MNm ^{-3/2}	Steel
291	7.1	0.71	0.15%C
77	43.3	1.7	" "
291	6.8	0.74	0.04%C, 0.02%Mn
77	40.9	1.6	" "
291	7.7	0.68	0.04%C, 0.47%Mn
77	41.3	1.5	" "
291	14	0.59	0.05%C, 1.9%Mn
77	53.1	0.93	" "
293	32.5	0.84	0.04%C, 3.25%Si
95	42.5	0.9	" "
77	51.5	1.5	" "
293	11.9	0.78	0.2%C
173	24.6	0.74	" "
123	42.2	0.68	" "
98	53.4	0.81	" "
293	5.6	0.68	0.03%C
173	21.1	0.9	" "
77	52	1.2	" "
293	14.4	0.53	0.002%C, 3.28%Ni
77	48.2	0.68	" "

In view of the variation in friction stress with both temperature and composition Heslop and Petch⁽¹⁴⁶⁾ suggested that it could be treated as two components;

$$\sigma_0 = \sigma_0' + \sigma_0''$$

where σ_0' is dependant on temperature only and σ_0'' is dependant on composition only.

The following two figures show the variations in σ_0' and σ_0'' .

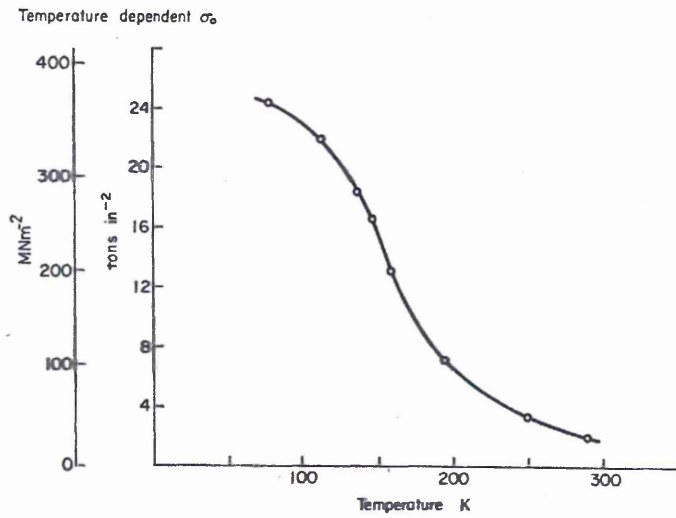


FIG. 3.2.6.3 Variation of σ_0' for mild steel on temperature (Heslop and Petch, 1956)⁽¹⁴⁷⁾

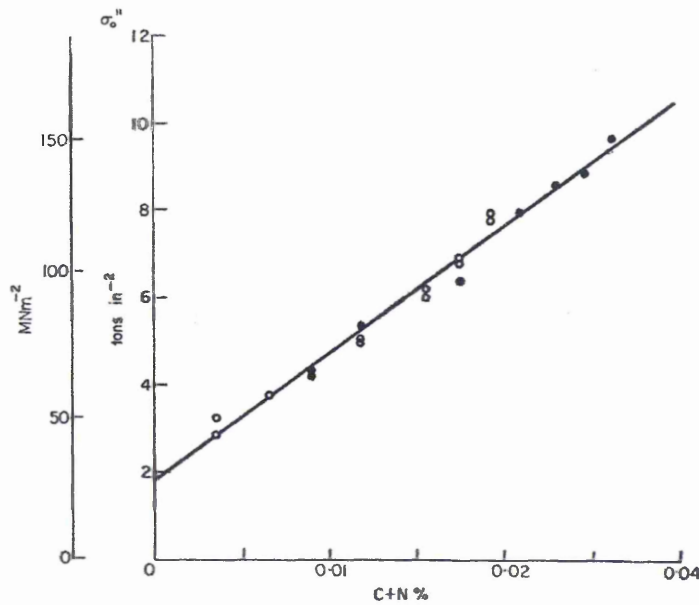


FIG. 3.2.6.4 Variation of σ_0'' for mild steel on composition (Cracknell and Petch, 1955a)⁽¹⁴³⁾

It can be seen from figure 3.2.6.4 that increasing nitrogen gives a linear increase in the friction stress, i.e. a linear increase in the yield stress.

However, Pickering's equations for both the yield stress and the ITT have a factor for free nitrogen to the power 0.5⁽⁴³⁾ but the equation given in the same paper for flow stress uses a linear free nitrogen factor as does the yield stress equation for high carbon steels. It is understood that the yield and ITT equations resulted from a 'blind' mathematical analysis of a large database of measured results rather than a theoretically based model of the mechanisms involved⁽¹⁴⁸⁾. This would suggest that the square root value may simply be a querk of the regression analysis program and the equations produced by Mintz and others⁽¹⁶⁾ would support this.

The original Mintz paper⁽¹⁶⁾ from which the equation is taken does not give any details on the method of determining the free nitrogen content, however the JISI paper⁽¹⁹⁾ published the following year gives the following information; *'For steels without aluminium, the free nitrogen was taken as the chemically analysed acid-soluble nitrogen values, and for steels with aluminium the free nitrogen was taken as the difference between the acid-soluble nitrogen content and the nitrogen combined as aluminium nitride.'* Mention is made of eight steels, four low-silicon and four silicon-killed, which were checked using a torsion pendulum system but these results do not appear to have been used in any of the calculations. This chemical determination, like the hydrogen extraction methods, is liable to give an over estimate compared to the internal friction measurements carried at room temperature.

Table 3.2.6.1 gives a comparison of the ITT values calculated using the Pickering Gladman equation and the Mintz equation using weight percentage values of silicon, free nitrogen and aluminium, as the quoted values for the aluminium contents were

<0.005% for all but F8104 a standard value of 0.002% has been used in the calculations (pearlite percentages are based on the carbon contents). As a means of comparing the different formulas a root mean square value was calculated for the total errors between the calculated and measured values. (It should be noted that Mintz used the 50% ductile / brittle fracture appearance as the criteria for assessing the ITT whereas Pickering and Gladman appear to have used a mid point on the energy temperature plot.)

Table 3.2.6.4 Calculated ITT values using the Standard Formulae

ITT calculated using Pickering Gladman equation

Steel	Free N%	Grain Size	% Pearlite	Si%	ITT(calc)	ITT(meas)	Error
F8104	0.0008	0.0075	21	0.2	-77	-29	-48
F8105	0.0055	0.013	20	0.2	-15	9	-24
VS3764A	0.0012	0.012	25.6	0.2	-35	-23	-12
VS3764B	0.0013	0.012	23	0.2	-39	-23	-16
rms error							28.7

ITT calculated using Mintz equation

Steel	Free N%	Grain Size	% Pearlite	Si%	ITT(calc)	ITT(meas)	Error
F8104	0.0008	0.0075	21	0.2	-57	-29	-28
F8105	0.0055	0.013	20	0.2	-17	9	-26
VS3764A	0.0012	0.012	25.6	0.2	-20	-23	3
VS3764B	0.0013	0.012	23	0.2	-26	-23	-3
rms error							19.2

The calculated values for F8104, F8105 and VS3764B are all lower than the measured value and well outside the acceptable error range. The r.m.s. values for the errors indicate that the Mintz equation gives a better fit to the data but the individual errors on the two 'F' series steels are still well outside any acceptable range..

These two equations both use weight percentage values for the nitrogen and silicon values. The change from ductile to brittle behaviour is a result of lattice strain and locking of dislocations both of which effects are related to the number of atoms not the weight.

In order to determine the factor for the atomic percentage of free nitrogen the data from figure 1.4 was replotted using atomic percent values. This gave a factor of 740 which gives the following version of the equation;-

$$ITT = 15 + 50*(Si\%) + 740*N_f\% + 2.2*(Pearlite \%) - 11.5*d^{-1/2} + 70*Al\%$$

As the levels of silicon and aluminium were very low the factors for silicon and aluminium were left unchanged and as the table below shows using atomic percentages in the Mintz equation gives a significant improvement with an r.m.s. error value of 13.1.

Table 3.2.6.4. Calculated ITT values using Atomic %

ITT calculated using Mintz equation with At%

Steel	Free N At%	Grain Size	% Pearlite	Si At%	ITT(calc)	ITT(meas)	Error
F8104	0.0032	0.0075	21	0.4	-45	-29	-16
F8105	0.022	0.013	20	0.4	-5	9	-14
VS3764A	0.0048	0.012	25.6	0.4	-10	-23	13
VS3764B	0.0052	0.012	23	0.4	-15	-23	8
rms error							13.1

As the method used by Mintz for determining the free nitrogen contents would probably give an over estimate on the value the calculations were rerun using modified nitrogen factors until an optimum fit for the four results was obtained. This was then improved by adjusting the factor for aluminium. This gave the following equation;

$$ITT = 15 + 50*(Si \text{ at}\%) + 1150*(N_f \text{ at}\%) + 2.2*(Pearlite\%) - 11.5*d^{-1/2} + 125*(Al \text{ at}\%)$$

Using this equation the following results were obtained;

Table 3.2.6.5. Calculated ITT values using the Modified Formula

ITT calculated using revised constants and At%

Steel	Free N At%	Grain Size	% Pearlite	Si At%	ITT(calc)	ITT(meas)	Error
F8104	0.0032	0.0075	21	0.4	-40	-29	-11
F8105	0.022	0.013	20	0.4	4	9	-5
VS3764A	0.0048	0.012	25.6	0.4	-8	-23	15
VS3764B	0.0052	0.012	23	0.4	-13	-23	10
rms error							11.0

This gave a r.m.s. error value of 11.0 with each individual error within the standard error band for a Charpy determination.

Examination of the Charpy plot for steel VS3764B (figure 3.2.6.1) shows a kink in the curve for the result at -20°C . Removal of this result would give a higher value for the ITT of $\sim -15^{\circ}\text{C}$ which is well inline with the calculated value.

Whilst the modified equation using atomic percentages gives a good fit to the measured ITT values for these four steels, in order to demonstrate its validity further testing of a much larger range of similar steels would be required.

The Effects of Hydrogen Dissolved in Iron

This work was divided into two sections;

3.3) A series of experiments to determine if interstitial hydrogen was metallic in nature carried out using Armco iron.

3.4) A second series of experiments to see if dissolved hydrogen had an effect on the work hardening rate and to ascertain if it produced a dynamic strain ageing effect at low temperatures. This work was carried out using Armco iron and two mild steels one with a low free nitrogen content (F8104) and one with a high free nitrogen content (F8105).

3.3 Experiment to Examine the Nature of Hydrogen in Iron

3.3.1 Introduction

In 1935 Eugene Wigner predicted that hydrogen, based on its electron configuration, should show metallic behaviour at a sufficiently high pressure⁽¹⁰⁸⁾. However, even when subjected to a pressure of 2.5Mbar solid crystalline hydrogen does not show metallic properties. In hydrogen at ambient pressure the gap between the highest filled electron energy level and the next available level is 15eV which would qualify it as an insulator. In a shock-compression experiment on fluid hydrogen, carried out at the Lawrence Livermore Laboratory, William Nellis was able to lower this gap down to 0.3eV, at pressures in the range 1.0 - 1.4 Mbar. This energy level is comparable to the thermal energy of the fluid, i.e. conductivity equivalent to a metal⁽¹⁰⁹⁾.

The conclusion that can be drawn from this is that whilst hydrogen does not normally show metallic characteristics it can behave as a metal under certain circumstances.

The aim of this experiment was to determine if the interstitial hydrogen behaves in a metallic manner. If so it should release its electron into the electron 'sea' in the metal and it should then be possible to move the nucleus, a single proton, by applying an electrical potential to the test piece.

The speed at which a proton might move under the influence of an electrical potential was estimated based on the speed at which electrons move in a conductor. Beaty⁽¹⁴⁹⁾ gives a simple calculation based on each atom in a conductor releasing a single valency electron into the electron cloud. For an iron conductor 10 mm in diameter carrying a current of 10 amps the electron would move at around 4.2 mm/h. Assuming that a proton having ~2000 times the mass of an electron moves 2000 times slower than an electron (but in the opposite direction) then if the iron contained 0.5at% hydrogen (0.009wt%) the protons could move up to 70 mm per week just as a result of the applied potential.

In order to suppress normal diffusion and so ensure that any movement of the hydrogen was due to the electrical potential along the specimen, the test specimens were to be held in liquid nitrogen at which temperature (77K) it would have a diffusion coefficient of $9.45 \times 10^{-29} \text{ m}^2\text{s}^{-1}$ i.e. negligible thermal diffusion even with a high concentration gradient.

3.3.2 Experimental Method

A set of four notched tensile specimens were machined from Armco iron bar with the notch 25mm from the middle of the test section, see figure 3.3.1. (The analysis of the iron is given in table 1.)

Three of the specimens (identified as 2A, 3B and 4C) were electrolytically charged, with hydrogen, by submerging the non-notched half of the specimens in the electrolyte, see appendix II. As it is known that electrolytic hydrogen charging does not give consistent levels of hydrogen in separate test pieces⁽¹⁰⁴⁾ all three specimens were wrapped together in the platinum foil electrode in order to minimise any variation in the hydrogen contents. The top half of the specimens having been protected with polyurethane varnish to prevent any pick up due to splashing. The aim being to ensure fracture occurred at the notch i.e. at a standard distance from the area originally charged with hydrogen.

The specimens were initially hydrogen charged for 4 hours from 12:30pm to 4:30pm however, due to the failure of a liquid nitrogen delivery they had to be left over night at room temperature and recharged the following morning for a further 4 hours.

Thick copper wires were then attached to each end of two of the specimens (2A and 3B) and all three charged specimens, along with a standard uncharged specimen (1R), immersed in a bath of liquid nitrogen.

A direct current, from a constant current unit, was run through the specimens 2A and 3B. In specimen 2A the current flow was from un-notched end to notched end and in specimen 3B the current flow was in the opposite direction, see figure 3.3.2.

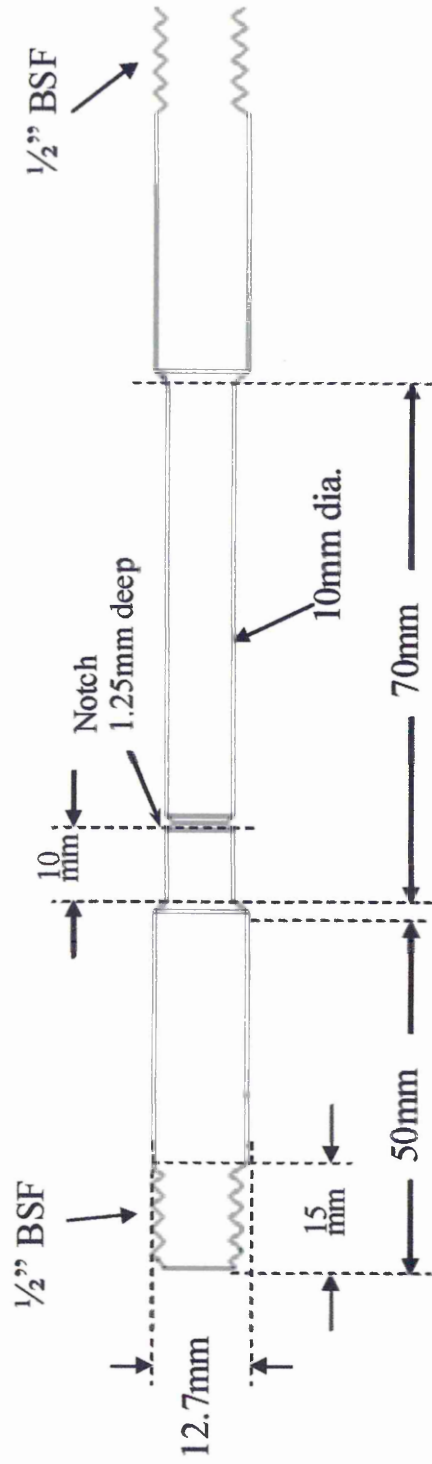


Fig. 3.3.1 Notched Tensile Specimen

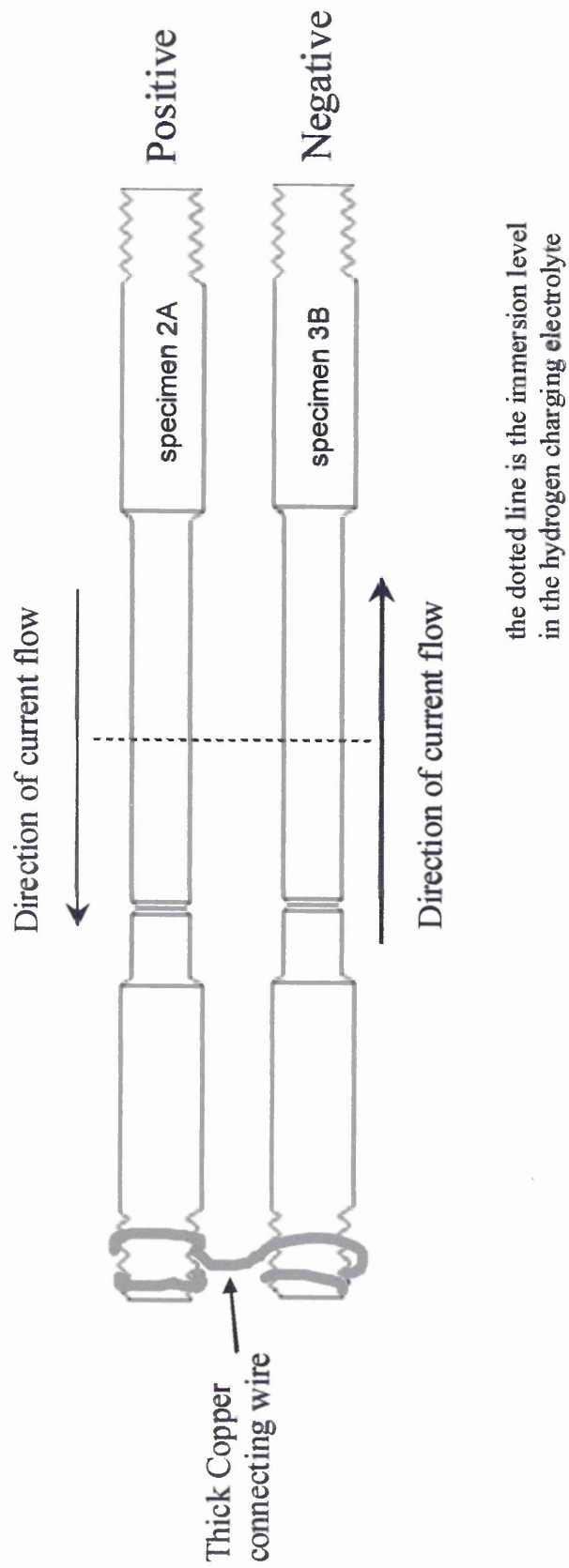


Fig. 3.3.2 Current flow in the Hydrogen Charged Specimens

As the heating effect of the current and subsequent boil off of the liquid nitrogen was uncertain a current of 20 amps was used during the working day, when the bath could be supervised. Initially the current was reduced to 10 amps over the first night and to 5 amps over the weekend, later on the current was left at 20 amps over night. The voltage drop across the specimens was monitored during the treatment using separate signal cables to the power cables.

Problems were encountered due to the copper connecting leads contracting more than the specimens resulting in loose connections which had to be re-tightened several times during the course of the treatment. This was detected by the change in the potential across the specimens. After this had been corrected it was noted that there was a consistent difference between the voltage drop across the first specimen (current flowing towards the notched end) and the voltage drop across the second specimen (current flow away from the notched end). The average voltages, with a current of 20 amps, for the rest of the experiment were 0.116 volts across the first specimen and 0.169 volts across the second.

The total charge passed through the two specimens was 2,466 ampere.hours (an average current of 11 amps.).

The tensile tests using strain control were carried out on all four specimens. The strain speed was measured and controlled using an LVDT reading the cross-head movement. The tests were started with the uncharged specimen and initially a very slow straining speed of $0.2\mu\text{m}/\text{sec}$ was used, the aim being that this would allow hydrogen to diffuse to the strained area of the notch. However, due to the high level of plastic deformation shown by the specimen the slow straining speed resulted in an excessively long test

time. As a result for the three hydrogen charged specimens the tensile tests were run at a straining speed of $0.8\mu\text{m}/\text{sec}$ for the first 4 mm of movement (covering the elastic and yielding zones) and then increased to $1.2\mu\text{m}/\text{sec}$ until failure.

Whilst specimen 2A was being tested specimens 3B and 4C were retained in the nitrogen bath.

The experiment was repeated with a second set of two specimens (5/04 and 6/04) which were placed in the liquid nitrogen bath immediately after hydrogen charging for 4 hours and then subjected to a current of 20 amps for 186.5 hours (5/04 current flowing towards the notch) and 188.5 hours (6/04 current flowing away from the notch). The notch diameters were measured on these specimens so that the yield stresses could be calculated. (A previous repeat test was lost due to problems with the data logging program used to record the tensile results.) It was noted in these tests, and the previous ones where the tensile results were lost, that the voltage drop across the second specimen, where the current was flowing from the notched end to the un-notched end was always greater than that across the first specimen. However, in these later tests the difference was not as marked as in the first experiment.

3.3.3 Results

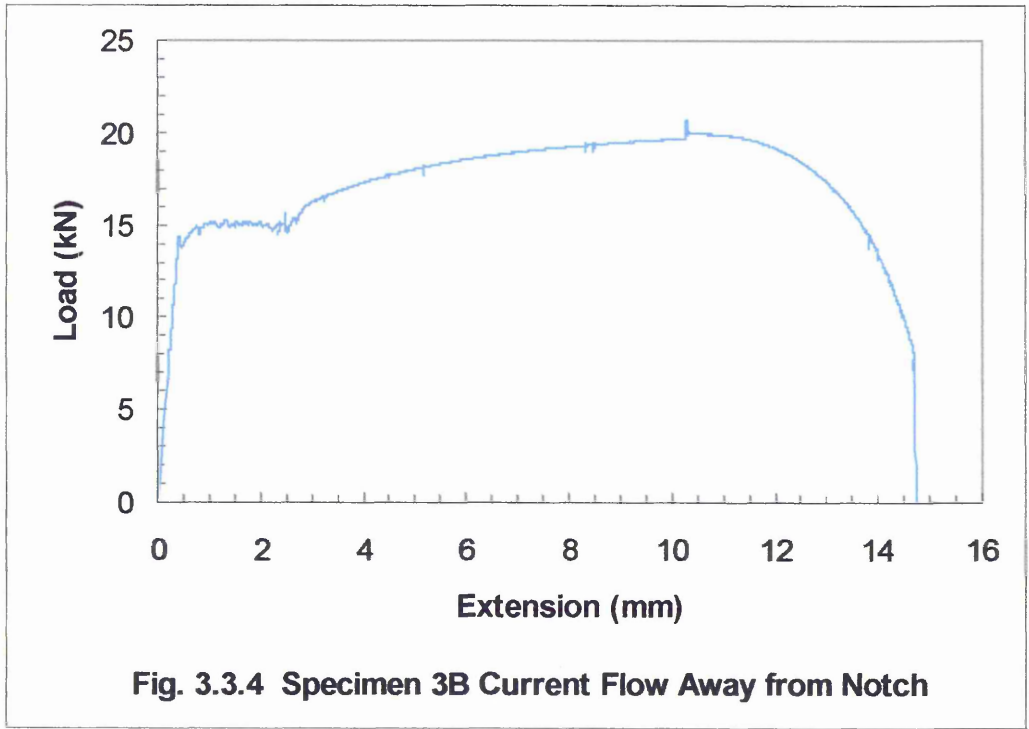
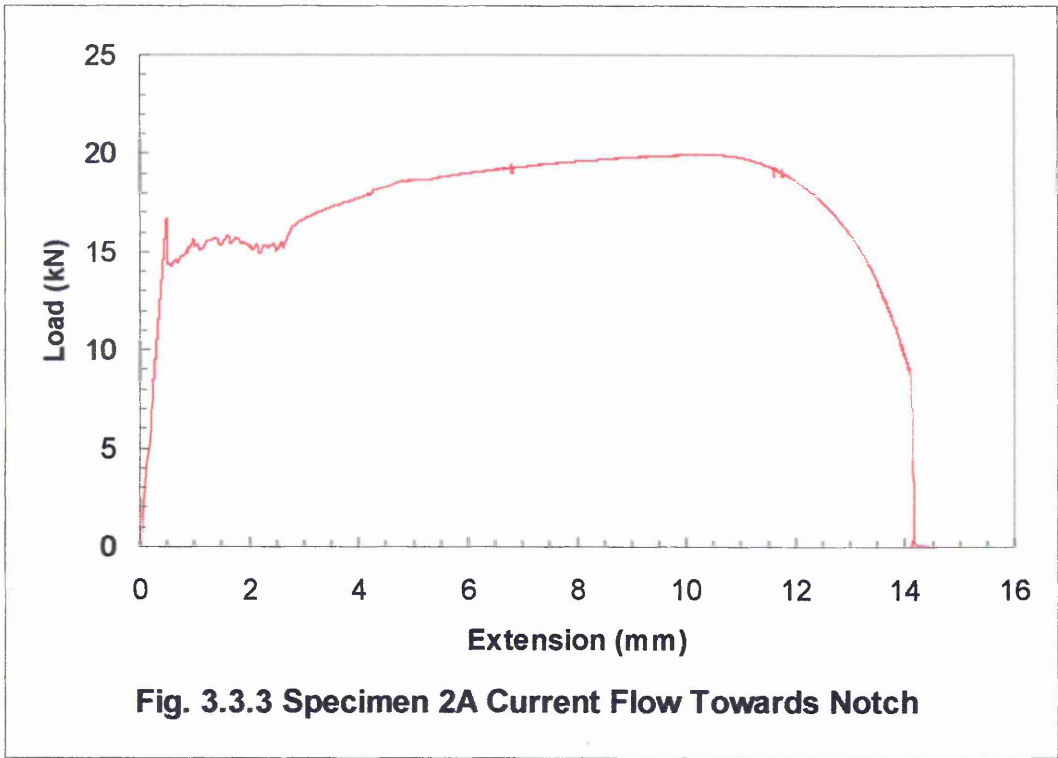
3.3.3.1 Tensile Results

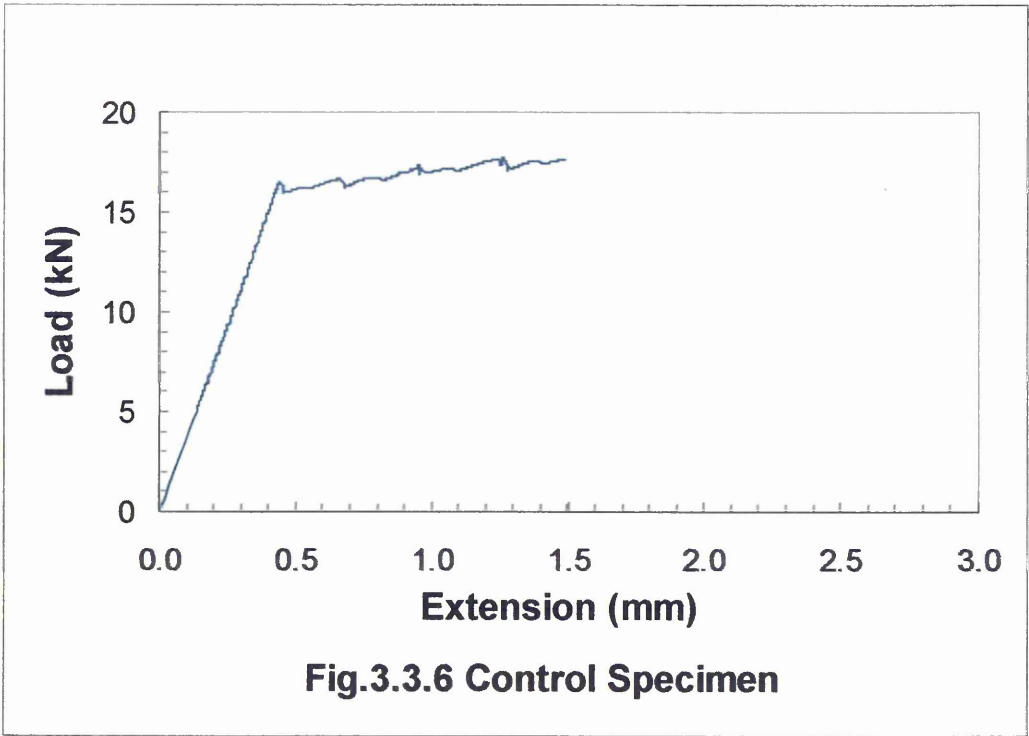
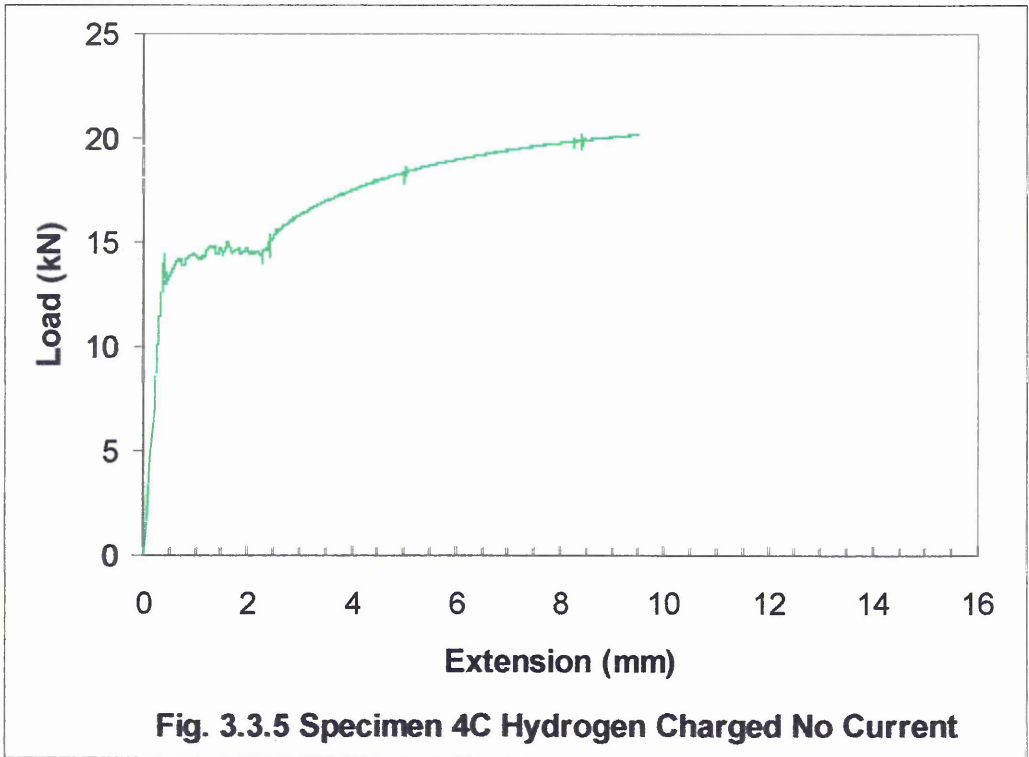
All four initial specimens showed a clear yield point and significant plastic deformation in the material at either side of the notch. The overall extension on the 70mm test sections were 23 -24 % for both charged and electrified specimens and for the control specimen 1R (the non-electrified hydrogen charged specimen, 4C, was damaged during removal from the test machine so it was not possible to get an elongation). Figures 3.3.3 – 6 show the load against ram displacement for the three hydrogen charged specimens and the control specimen. All three charged specimens reached similar maximum loads of around 20kN, however, it was noted that the upper yield point for specimen 2A was significantly higher, at 16.65 kN, than for the other specimens and that this load was not exceeded until the specimen had undergone approximately 2.5 mm of plastic extension (the upper yield loads of the other specimens were all exceeded within 1 mm of plastic extension). Table 3.3.1 gives the upper and lower yield loads for all four specimens and the ratios of upper to lower yields along with the total current flow (charge) in ampere.hours.

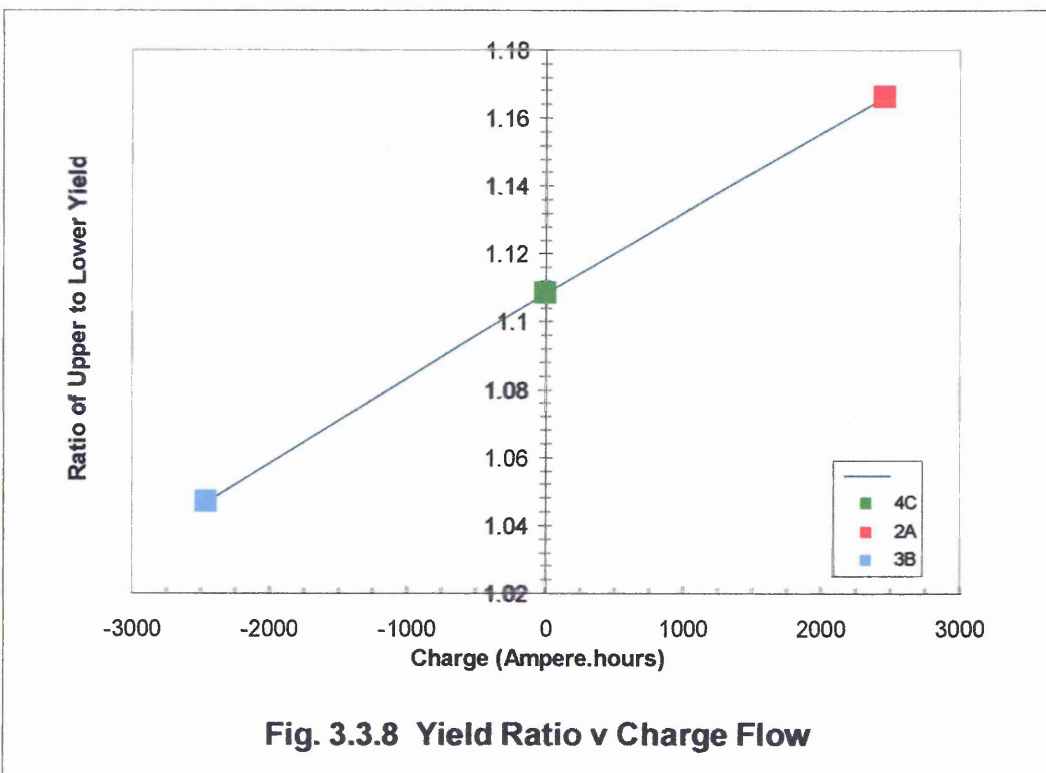
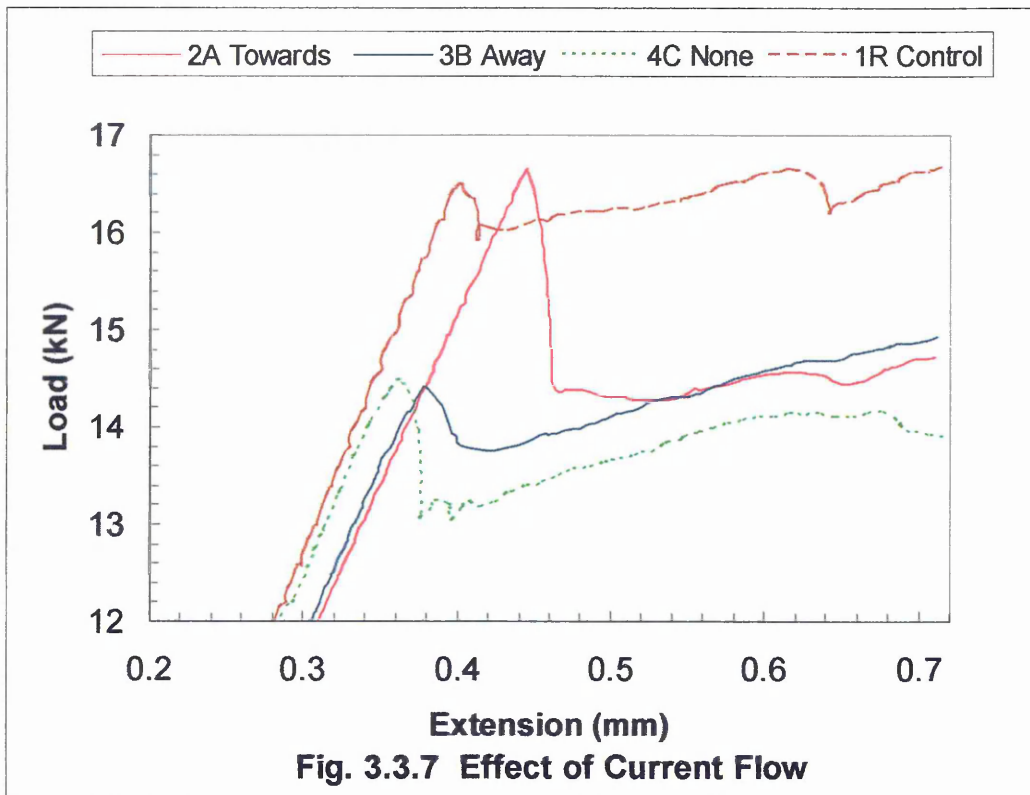
Table 3.3.1. Yield Loads

Specimen No.	Current Flow	Upper Yield (kN)	Lower Yield (kN)	Ratio Upper : Lower	Charge (A.h)
1R	None	16.525	15.912	1.0385	-
2A	Towards notch	16.657	14.27	1.1673	2465
3B	Away from notch	14.407	13.763	1.0468	-2465
4C	None	14.458	13.045	1.1083	0

Figure 3.3.7 is a comparison of the yields of the three hydrogen charged specimens and figure 3.3.8 is a plot of the yield ratios against the charge in ampere hours.





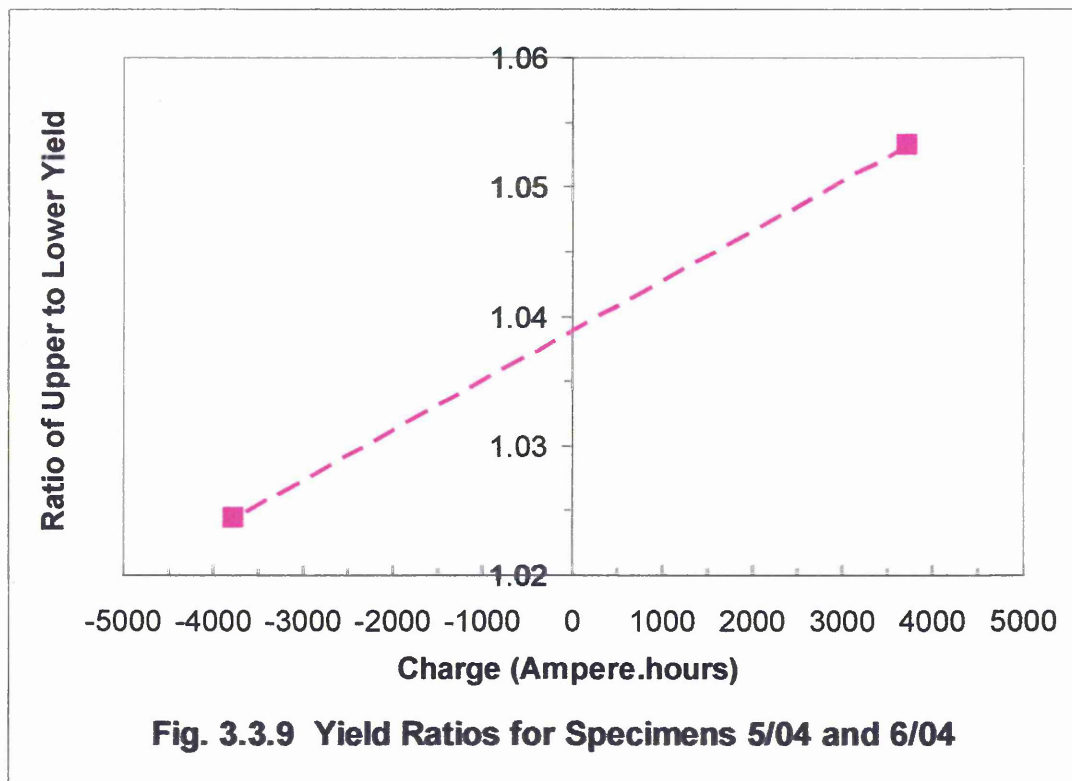


The tensile results from the second set of specimens is given in table 3.3.2 and a plot of upper to lower yield ratio against charge is shown in figure 3.3.9.

Table 3.3.2. Second Set Tensile Results

Specimen No.	Av. Notch dia. (mm)	Current Flow	Upper Yield Stress (MPa)	Lower Yield Stress (MPa)	Upper: Lower Ratio	Charge (A.h)
5/04	7.0655	Toward notch	325.1	308.6	1.0533	3730
6/04	7.2835	Away from notch	274.9	268.4	1.0244	-3770

An attempt was made to measure the hydrogen content close to the fracture of these two specimens but the results were inconclusive.



3.3.3.2 Fracture Examinations

Fracture surfaces from specimens 1R, 2A and 3B were examined optically and then using a Scanning Electron Microscope (SEM). SEM micrographs from the specimens are shown in figures 3.3.10 and 12. All the fractures were very similar with typical ductile failure resulting from microvoid coalescence in the centre of the specimen surrounded by a shear lip. There were no significant differences in the appearance or size of the microvoids in the three specimens. Those in sample 2A had an average diameter of $36\mu\text{m}$ and 3B an average diameter of $38\mu\text{m}$.

Scanning Electron Micrographs

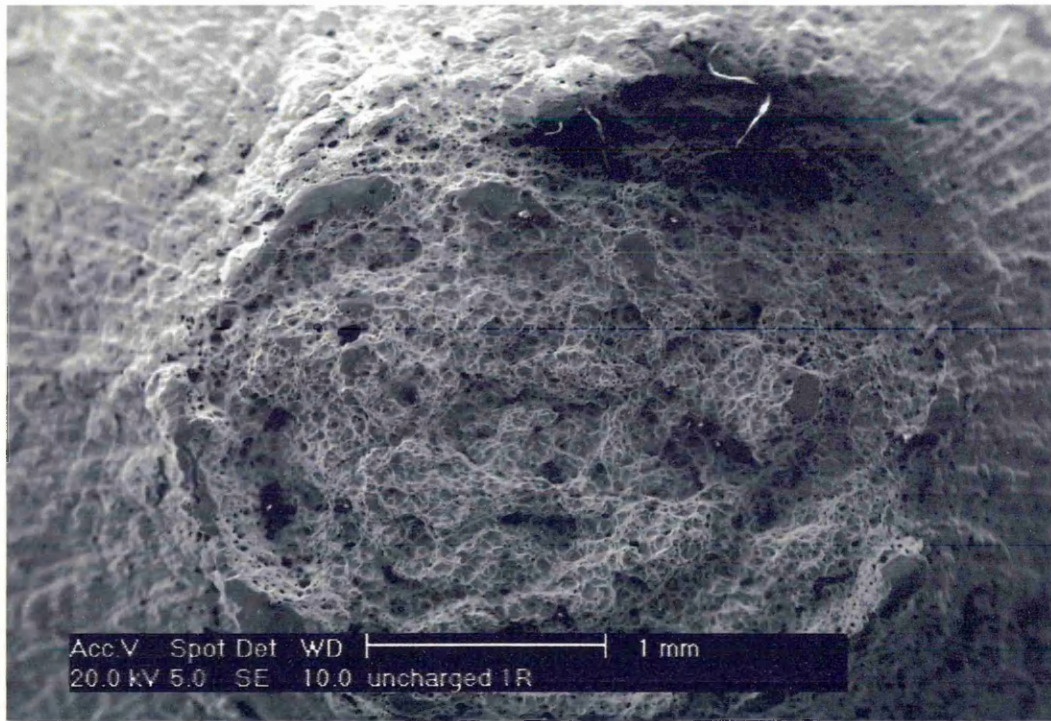


Fig. 3.3.10 Fracture Surface of Specimen 1R

Scanning Electron Micrographs

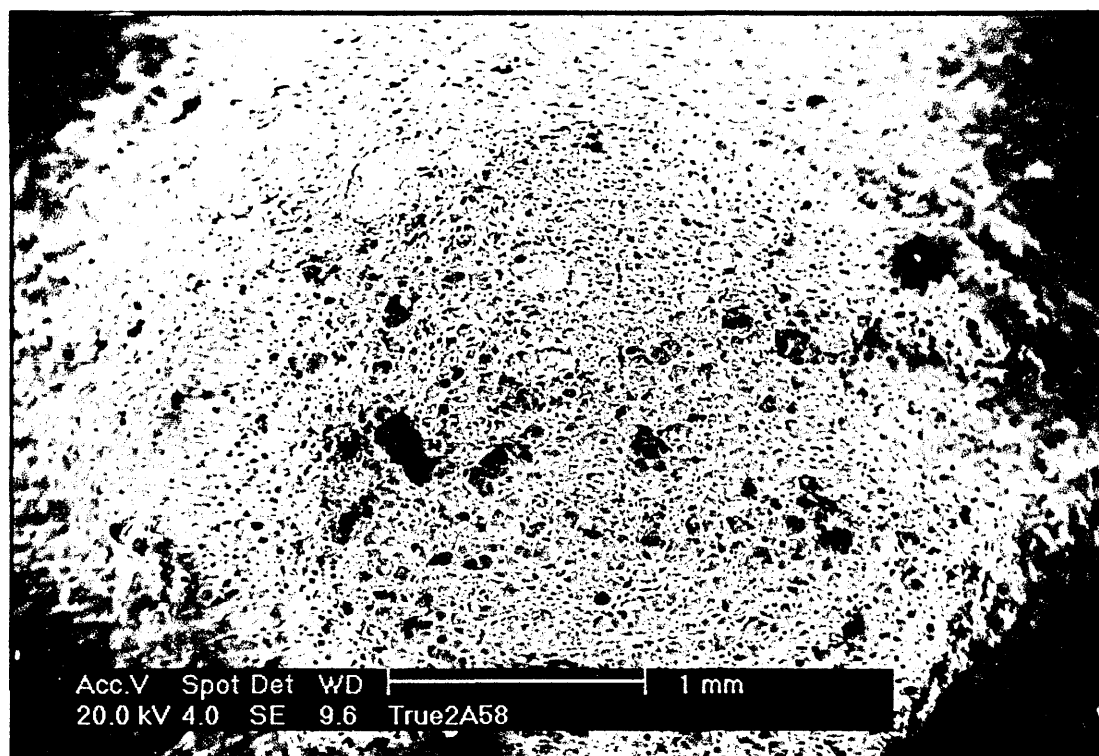


Fig. 3.3.11 Fracture Surface of Specimen 2A

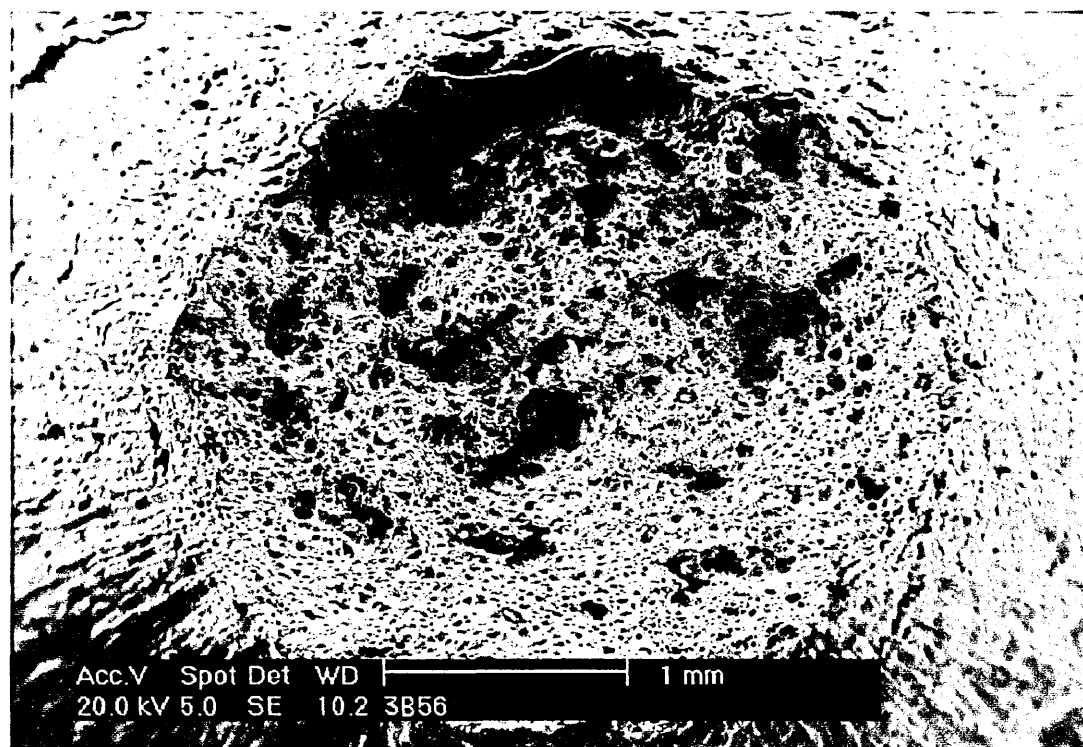


Fig. 3.3.12 Fracture Surface of Specimen 3B

3.3.4 Discussion

The initial expectation was that if the hydrogen was moved to the notch this would result in a more brittle failure. As a result, except for specimen 1R, the actual depth of the notches of the original four specimens was not measured as it was expected that the increased brittleness would result in significant variations in the maximum load.

However, in the event all three hydrogen charged specimens gave very ductile failures with significant necking in the metal at either side of the notches, i.e. there was no significant decrease in ductility and very similar maximum loads. What did show a significant change was the yield behaviour. Figure 3.3.7 shows a comparison of the yield regions for all four specimens.

The third charged specimen was a further reference showing the effect of hydrogen that has diffused naturally to the notch both during charging, the overnight stand at room temperature (these tests were carried out in January when over night temperatures in the laboratory were around 10°C) and during testing (the diffusion will have been virtually zero when the specimens were in the liquid nitrogen). However, if hydrogen exists as a proton with the electron in the 'sea' then it should, under the influence of an electric current, diffuse to the negative end of the specimen. Alternatively if it is present as a weak hydride (H⁻) then it should diffuse much more slowly to the positive end of the specimen.

Hydrogen has been shown to give a yield point effect in iron at sub-zero temperatures but there is some question as to the actual temperature at which this occurs. Early work by Rogers suggested that it only occurs below -120°C⁽⁷⁵⁾ whilst others have demonstrated a yield point at -70°C⁽⁷⁶⁾ and later work by Rogers found a yield point at -12°C in Armco iron⁽³⁶⁾. Laboratory work at Sheffield Hallam suggests that there is a

yield point at room temperature but due to the rapid diffusion of hydrogen out of the specimens the effect is only noticeable for a short time after hydrogen charging⁽⁷⁸⁾.

The previous charging experiments, at Hallam had also indicated that hydrogen caused an increase in the upper to lower yield ratio⁽⁷⁸⁾ and this effect is clearly seen in the comparison of the standard specimen and the non-electrified hydrogen charged specimen, where some hydrogen from the first charging would have diffused along the specimen overnight, see figure 3.3.7.

A comparison of the upper to lower yield ratios of the three original hydrogen charged specimens clearly shows the effect of the electric current. Specimen 2A, where the current would have moved protons ('metallic hydrogen') towards the notch shows the highest ratio, whilst specimen 3B has the lowest ratio of the charged specimens and is only slightly higher than the uncharged reference specimen (1R).

The second pair of specimens show the same trend as the original set but in these specimens as no diffusion at room temperature occurred prior to immersion in the liquid nitrogen the difference between the two specimens is less pronounced than between 2A and 3B as there was virtually no hydrogen to be moved away from the notch in specimen 6/04. Moreover these two specimens having only been charged for 4 hours in total would have had a lower hydrogen content.

Comparison of the ratios of 3B and 4C, the standard charged specimen, is clear evidence that hydrogen, from the first charging, that would have diffused naturally toward the notch when the specimens were at room temperature overnight, has been moved back away from the notch by the influence of an electrical potential. The only way these effects could occur is if the majority of the hydrogen is in a metallic state, i.e. existing as protons having released their electrons into the metallic electron cloud.

This is consistent with Graviljuk's findings that hydrogen (and nitrogen) increase the concentration of free electrons⁽¹²¹⁾.

The actual charge used, in the first experiment, to move the hydrogen from its initial position towards the notch was 2465 amp.h. (887,400 coulombs). As the charge on the electron is 1.6×10^{-19} coulombs, this equates to a movement of 5.5×10^{24} electrons.

If the hydrogen is metallic and therefore exists as protons a small proportion of this charge will be due to the movement of these protons (in the opposite direction).

If the following assumptions are made;

1. The average hydrogen content was 10ppm (0.0001wt%) equivalent to an atomic percentage of 0.0056 at%.
2. Each iron atom gives a single electron to the electron cloud and each hydrogen atom gives up its single electron to the cloud.

Then for every million iron atoms there will be 56 hydrogen atoms and if these exist in a metallic state then the charge would include the movement of 3×10^{20} protons.

3.4 Experiment to ascertain the Effect of Hydrogen on Work Hardening

3.4.1 Introduction

Dynamic Strain Ageing is a well documented effect of free nitrogen (and to a lesser extent free carbon) in steels^(20, 23-27,42). The effect gives rise to an increase in tensile strength, and corresponding decrease in ductility in the temperature range from 200 to 450°C. The aim of this series of experiments was to ascertain if hydrogen produced a similar effect but at lower temperatures.

Measurements were also planned to investigate the effect of hydrogen on the work hardening behaviour of the test steels. Ferreira's work⁽³⁷⁾ has shown that hydrogen reduces the elastic interactions between dislocations and it is reasonable to assume that this should result in a reduction of the work hardening exponent. However, a reduction in the work hardening exponent should result in a reduction in the tensile stress or an increase in the plastic deformation prior to the maximum strength being reached, i.e. an opposite effect to that resulting from dynamic strain ageing.

In order to suppress any effects due to nitrogen and carbon it was planned to carry out all the tests in the temperature range 0 to -75°C. The tests being carried out on specimens of Armco iron (free nitrogen 2-3 ppm, free carbon 114-117 ppm), high nitrogen steel F8105 (free nitrogen 54 ppm, free carbon 29 ppm) and medium nitrogen steel F8104 (free nitrogen 9 ppm, free carbon 2 ppm). This would allow an additional check that, at these test temperatures, nitrogen and carbon were not having a significant effect (work by Karimi Taheri et al. has shown that for steels containing 32ppm of nitrogen strain ageing does not occur below 315°C⁽¹⁵⁰⁾). (The free nitrogen and carbon

measurements were carried out using the Vibran Internal Friction Apparatus, see section 3.3.).

3.4.2 Experimental Details

The specimens were treated as pairs with one specimen being strained in the ‘as received’ condition whilst the other one was given a standard hydrogen charging treatment where a platinum foil electrode was wrapped around the gauge length and the specimen then immersed in an electrolyte containing a second platinum electrode and a constant potential applied for 4 hours, see appendix II. After charging the specimens were packed in dry ice until they were fitted into the testing frame, at which point they were brought up to the test temperature. It was hoped that by having a standard procedure all the treated specimens would have similar hydrogen contents.

It was originally intended to carry out low temperature slow strain rate tests in a temperature controlled chamber. However, due to the closure of a research budget the order for the chamber was cancelled. This meant that the testing had to be carried out

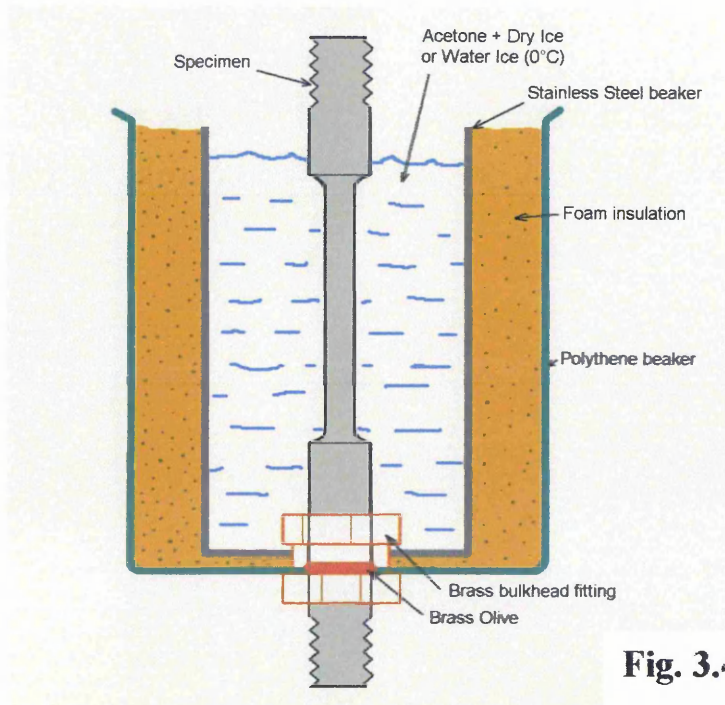


Fig. 3.4.1 Cooling Unit

using a 'home-made' cooling unit. This consisted of a stainless steel beaker fitted with a brass bulkhead unit, with brass nut and olive sealing system, fitted in the centre of the base, see figure 3.4.1.

The specimen had an extended shoulder section on the lower half (see figure 3.4.2) on to which the olive was clamped to seal the specimen into the beaker. This whole assembly was surrounded by foam insulation in a polyethylene beaker.

The stainless steel beaker was filled with acetone to which was added dry ice to cool the specimen (tests at 0°C used a water – water ice cooling mixture) the temperature being monitored using a thermocouple fitted in the beaker. The output from the thermocouple was recorded, using a lineariser unit to give 1mv per degree Celsius, either on a chart recorder or in later tests by a specially written program running on a calibrated BBC Master computer.

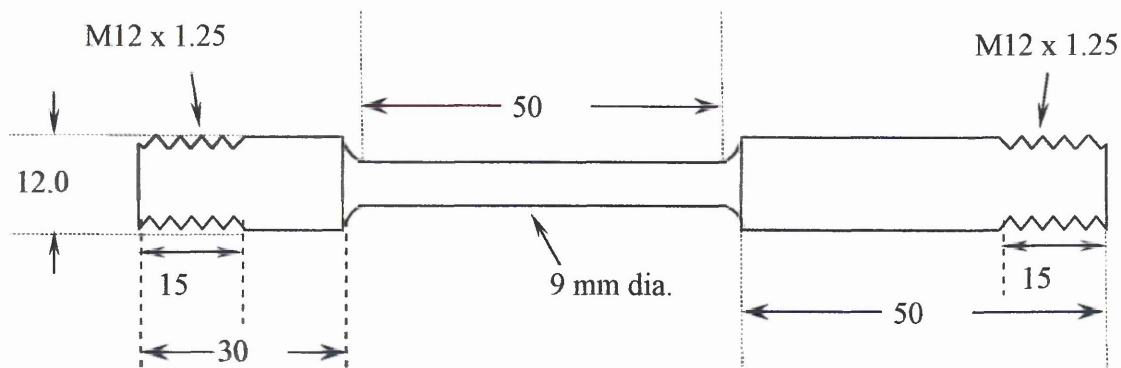


Fig. 3.4.2 Hydrogen Dynamic Strain Ageing Specimen

The program gave a temperature readout for the last four readings which was updated every three seconds, as well as a plot of temperature against time to show any long term trends. Temperature control was achieved by adding small amounts of dry ice at regular

intervals (usually around every minute) whilst monitoring the temperature. The amount of dry ice added and the frequency of the additions was based on assessing the trend in the temperature change. In most cases this resulted in temperature variations about the set point of better than $\pm 5^{\circ}\text{C}$. As this variation was the temperature seen by the very low thermal mass thermocouple the actual variation in the specimen temperature, which had a much higher thermal mass would have been even less than $\pm 5^{\circ}\text{C}$.

All the tensile tests were run under Strain Control running at a strain rate of 5×10^{-5} (a speed of $2.5\mu\text{m}$ per second). This rate was chosen as a compromise as being sufficiently fast to prevent the diffusion of carbon and nitrogen from having any significant effect, yet sufficiently slow to allow for hydrogen to diffuse through the strained section of the specimen.

The initial set of tests using Armco iron specimens were carried out on an old test frame running throughout the test under strain control governed by the internal displacement transducer. The frame was controlled using onboard electronics as opposed to the more modern system of control via a PC based system. This system did not have any built in data logging and so the data was logged using the BBC Master computer running a data logging program in extended BASIC128. The program logged time, load (as a voltage signal from the test frame) and displacement, measured using a linear potentiometer with a stroke of 125mm i.e. sufficient to cover the total extension during the test.

Unfortunately after the completion of the Armco tests the test frame developed a fault in the control system and could not be used for further strain rate controlled tests.

Tests on the two nitrogen containing steels F8104 and F8105 were carried out on a test frame using the Rubicon PC based control system. This system incorporates data logging of time, load, displacement measured by an external Linear Voltage

Displacement Transducer (LVDT), displacement measured by the internal sensor and an indication of which sensor is controlling during strain rate control.

The only LVDT units calibrated for use with the system only had a maximum stroke of 10 mm, therefore the strain rate was controlled for the first 7.5 mm of stroke from the external LVDT and thereafter by the internal displacement sensor of the tensile test frame. This gave rise to problems both in setting up the data logging and due to the fact that running at a slow speed with a relatively short logging interval the internal displacement sensor was running at the limit of its resolution. This meant that when strain control was switched to the internal sensor the recorded data had a high noise level.

3.4.2 Experimental Results

Tests were carried out at a range of temperatures on both standard specimens and on specimens charged with hydrogen. The initial test results showed inconsistent scatter, this was found to be due to the specimens having been cut from two different casts of Armco iron. A second set of tests was carried out on specimens all from the same cast and the results from these tests are given in table 3.4.1. The load results for the test of untreated iron at 0°C were lost due to problems with the data logging system. Problems were also encountered with the test of the untreated specimen at -70°C which led to the loss of data during the plastic extension phase of the test.

The results of the tests on Steel F8105 are given in table 3.4.2. and those for F8104 in table 3.4.3. Copies of the load extension curves are in appendix III. (The data file for the F8105 high nitrogen steel in the untreated condition was lost due to a computer error, however, the yield and maximum loads were recorded manually during the test.)

None of the specimens showed any indication of the multiple yielding that can be a feature of DSA.

True stresses and true strains were calculated for each completed test and plots of log true stress against true strain on a log scale constructed. The work hardening exponents were determined by matching a straight line plot to the plastic portion of these curves.

Figure 3.4.3 shows an example of this.

Table 3.4.1 Tensile Test Results for Armco Iron

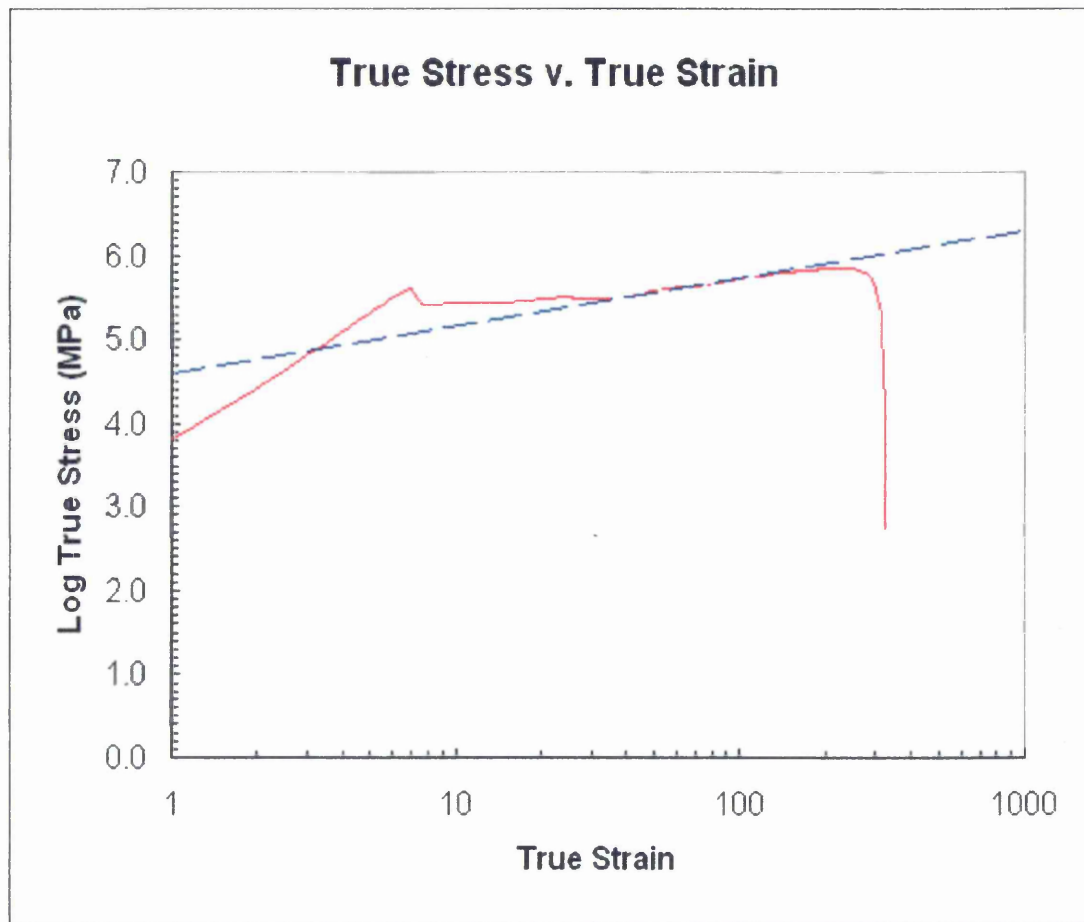
	Temperature °C	TS Mpa	YS MPa	%EI	%R of A	n	K	Upper/Lower Yield ratio
Untreated	-70	333	259.2	20	91.64			1.00
	-45	343.4	247.2	38	88.86	0.31	680	1.01
	-20	320.4	179.1	39.6	90.75	0.3	630	1.08
	0			31	87.31			
Hydrogen treated	-70	362.5	274.9	26	70.36	0.16	520	1.00
	-45	345.2	221.3	36	71.56	0.25	550	1.21
	-20	331.5	196.8	40.4	72.5	0.29	620	1.19
	-10	323	183.9	40	75.06	0.32	680	1.16

Table 3.4.2 Tensile Test Results for F8105 Steel

	Temperature °C	TS Mpa	YS MPa	%EI	%R of A	n	K	Upper/Lower Yield ratio
Untreated	-26	553.6	323.3	25.2	66.68	0.295	1155	1.043
	-56	590.4	351.1	25.6	56.88			1.048
	-75	518.9	313.8	27	70.82			1.067
Hydrogen treated	-26	545.6	332.8	25.4	56.39	0.285	1095	1.087
	-56	584.8	356.6	25.4	50.11	0.283	1150	1.084
	-75	553.2	339.3	23	50.68	0.295	1140	1.024

Table 3.4.3 Tensile Test Results for F8104 Steel

	Temperature °C	TS Mpa	YS MPa	%EI	%R of A	n	K	Upper/Lower Yield ratio
Untreated	-50	560.3	385.5	30.4	60.4	0.375	1400	1.08685
Hydrogen Treated	-50	558.4	384	22.6	34.99	0.31	1175	1.11389



	n =	E	Kεⁿ	Calc		
	0.25	0.001	97.805	4.583	1	
	K =		1	550	6.3099	1000

Fig. 3.4.3 True Stress – True Strain Plot of the Hydrogen treated Armco Iron tested at -45°C , showing the calculation of the work hardening coefficient.

3.4.3 Discussion of Results

All the specimens, with the exception of the Armco iron tested at -70°C and the high nitrogen (F8105) tested at -75°C showed that hydrogen increased the Upper to Lower Yield ratio. This is further confirmation of the previous findings, both in this work and earlier work at Sheffield Hallam ⁽⁷⁸⁾, that hydrogen does affect the yield point. The fact that the effect is not seen at -70°C , and below, is a result of the slow rate of diffusion at these temperatures (and the strain rate of these tests).

The increase in the tensile strength of approximately 200MPa of the untreated steels F8104 and F8105 compared to the untreated Armco iron is typical of the expected effect of the increased carbon, and in the case of F8105, increased nitrogen levels.

However, the results from the Armco iron, the F8105 (high nitrogen) and the F8104 specimens all show an unusual feature, whilst the percentage elongations for comparable temperatures are similar, the hydrogen treated specimens show significantly lower percentage reductions in area. In the Armco iron specimen the hydrogen treated samples, on average, actually show a higher percentage elongation than the untreated samples. These results are shown in figures 3.4.4 and 3.4.5. This effect appears to be the result of small cracks or cavities that have occurred in the hydrogen treated samples, see figures 3.4.6. For instance, in this specimen, measurements of the crack widths show that for the linear portion of the test length, on average, the cracks constitute 2.5% of the overall length. Figures 3.4.7 and 3.4.8 show comparable hydrogen treated and plain Armco iron specimens after testing. These cracks have caused the steel structure to behave like a trelliswork allowing it to increase in length by opening up the trellis rather than true plastic deformation. This is consistent with the fractographic evidence for plastic flow seen by other workers⁽⁶⁴⁾

As Ferreira has shown hydrogen reduces the strain fields around dislocations allowing them to move closer together under the action of a stress⁽³⁷⁾ and Hänninen et al.⁽⁶⁹⁾ have observed dislocation movement in strained specimens treated with hydrogen. This movement and closing up of dislocations should encourage the formation of micro-cracks. These voids thus created will allow hydrogen atoms to form hydrogen molecules within them, if sufficient hydrogen is already dissolved in the metal. The overall effect will be a reduction in the ductility measured at the macro level but an increase at the micro or atomic level. This increased ductility at the micro level would aid the opening of the trellis structure whilst the macro effect reduces the reduction in area due to a reduction in the true plastic deformation in the necked area.

However, whilst the hydrogen treated specimens all showed this cracking to some degree it did not have any major effect on the tensile strengths. The untreated samples of Armco and the high nitrogen steel both show a peak in the tensile strength around -50°C, with the hydrogen treated samples having very similar strengths at that temperature. However, in both the Armco and the high nitrogen steel (F8105) the tensile strengths at -70°C were significantly higher than the untreated specimens. Figures 3.4.9 and 10 show the plots of tensile strength against temperature for these two materials. The single temperature results for the low free nitrogen steel F8104 are very similar and well within the expected repeatability range for tests on identical specimens, (see table 3.4.3). Again these are at -50°C where the other two materials showed similar strengths in the treated and untreated conditions.

Similarly the Lower Yield Stresses at -70°C are slightly higher for the hydrogen treated samples.

An examination of the work hardening coefficients in tables 3.4.1 to 3.4.3 shows that at every temperature where it is possible to make a direct comparison the presence of hydrogen reduces the work hardening coefficient. The effect being particularly noticeable in the Armco iron tested at -45°C and the low free nitrogen steel (F8104) tested at -50°C .

These results are consistent with hydrogen reducing the strain fields around dislocations⁽³⁸⁾ allowing them to move closer together under a given stress, i.e. for a given strain the stress should be lower. It would also suggest that the main mechanism of slip is dislocation glide.

However, all the results where comparisons can be made of the work hardening coefficients are in the temperature range -56 to -20°C and in this temperature range there are no significant differences between the tensile strengths of the hydrogen treated and the untreated specimens. This is in marked contrast to the -70 and -75°C specimens where both the hydrogen treated Armco and high nitrogen steel have significantly higher tensile strengths.

A possible explanation for this is that at around -75°C , where hydrogen diffusion is very slow the hydrogen acts as a metallic interstitial giving a strengthening effect and a corresponding loss in ductility, measured as reduction in area. (Adair and Cook's work⁽⁷⁶⁾ showed that whilst hydrogen diffusion does occur at -70°C it is very slow.) This is consistent with Hardie and McIntyre's findings that hydrogen at sub-zero temperatures causes a ductility minimum in niobium a Body Centred Cubic (BCC) metal⁽⁸⁴⁾. Whereas at the higher temperatures the diffusion rate of the hydrogen is high enough for it to diffuse into microcracks and form hydrogen gas molecules (H_2) which do not give a significant strength increase and only marginally affects the reduction in

area. The damaging effects of a high pressure build up of hydrogen gas in internal cracks and cavities is unlikely to have occurred in these specimens which have only had a relatively short electrolytic charging treatment.

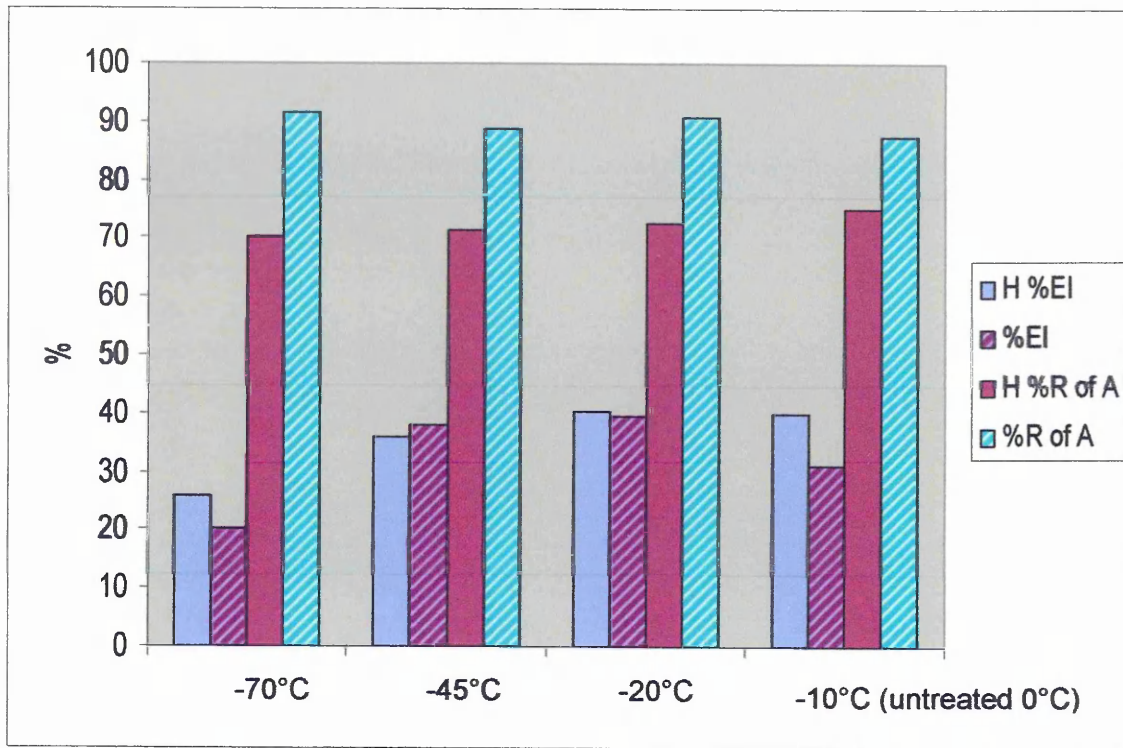


Fig. 3.4.4 Comparison of Elongation and Reduction of Area Values for Hydrogen treated and Untreated Armco Iron Specimens.

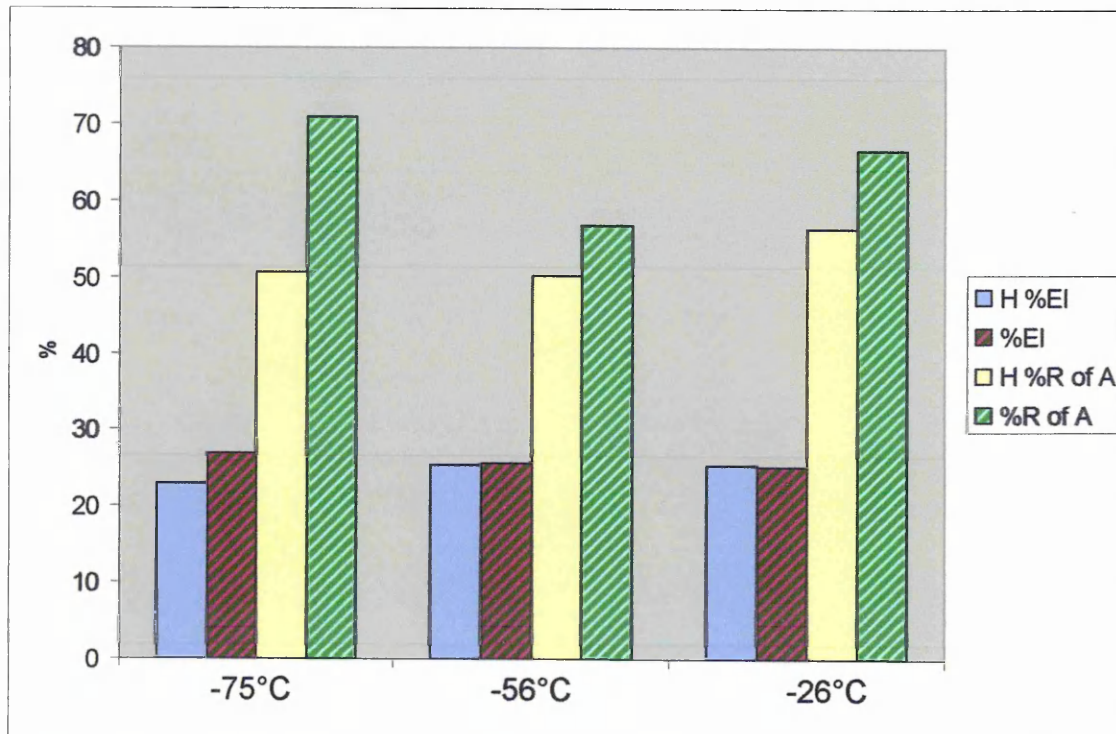


Fig. 3.4.5 Comparison of Elongation and Reduction of Area Values for Hydrogen treated and Untreated F8105 Specimens.

Fig.3.4.6 Hydrogen treated Armco Iron Specimen tested at -10°C

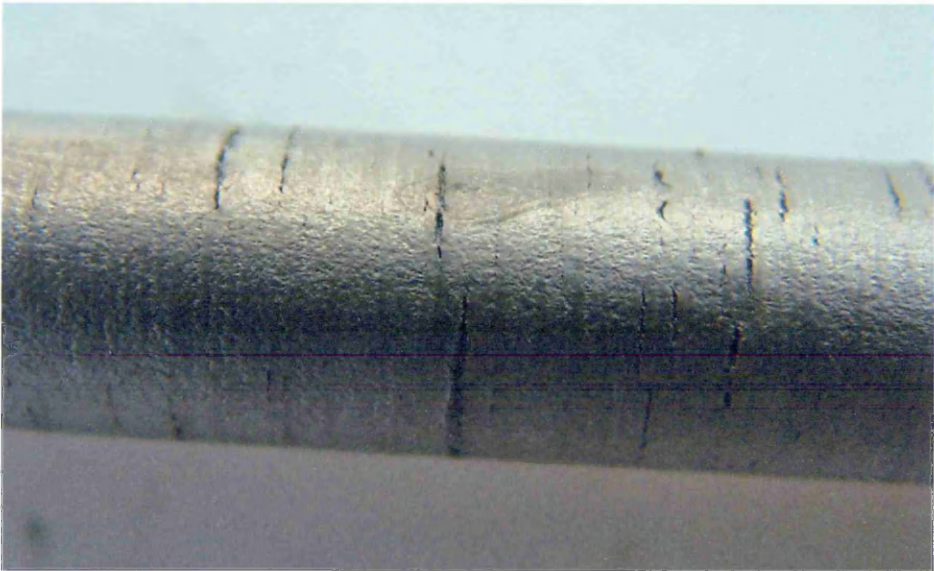
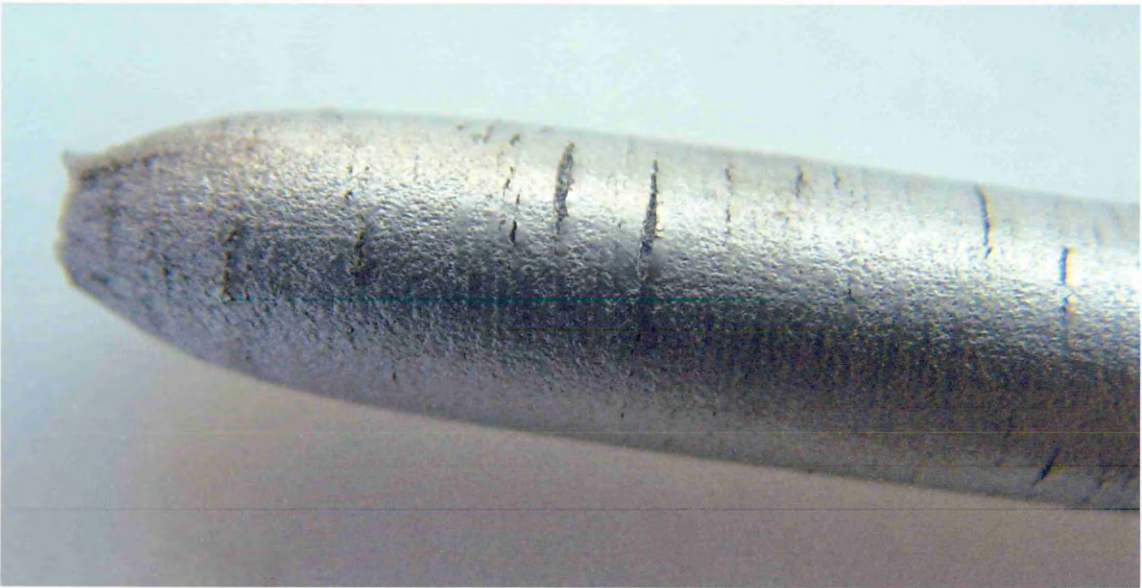


Fig.3.4.7 Hydrogen treated Armco Iron Tensile Specimens

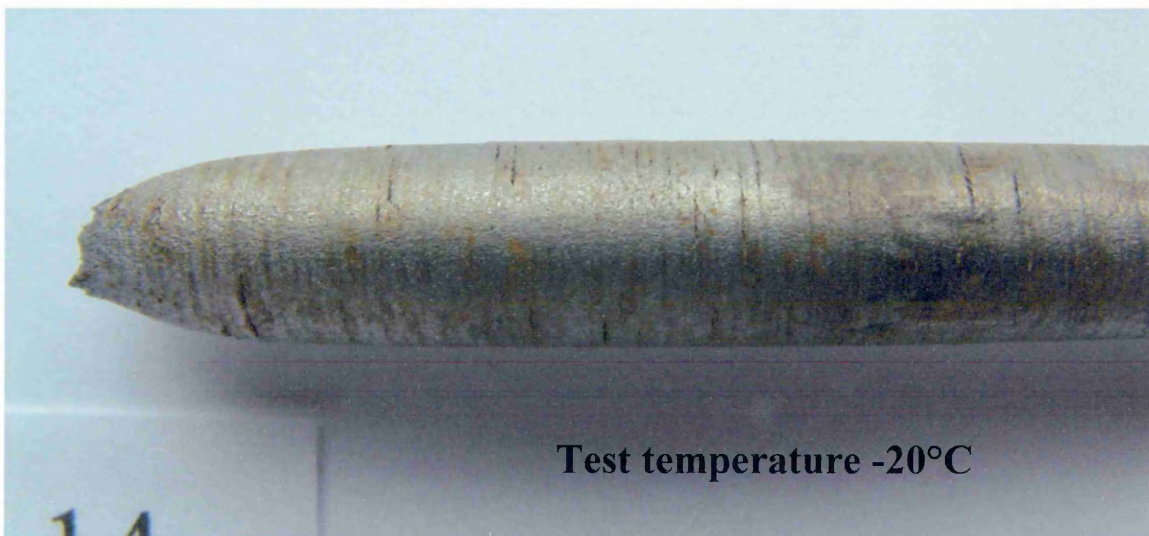
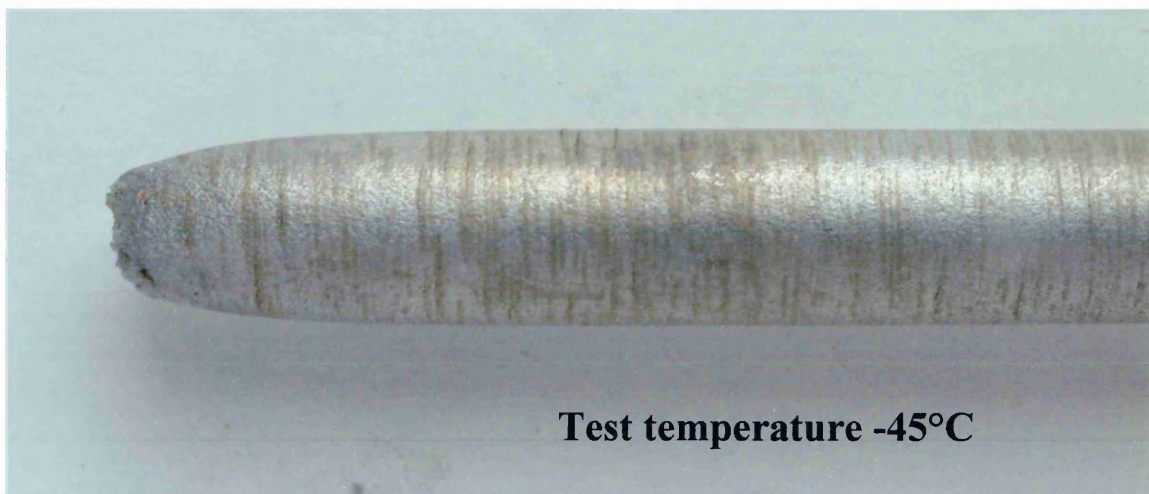
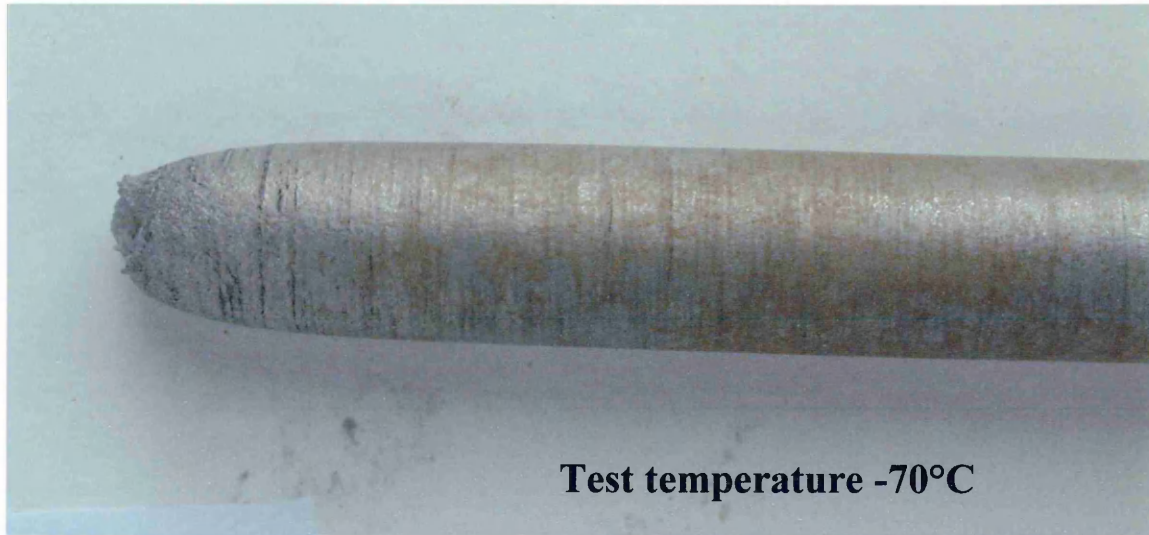
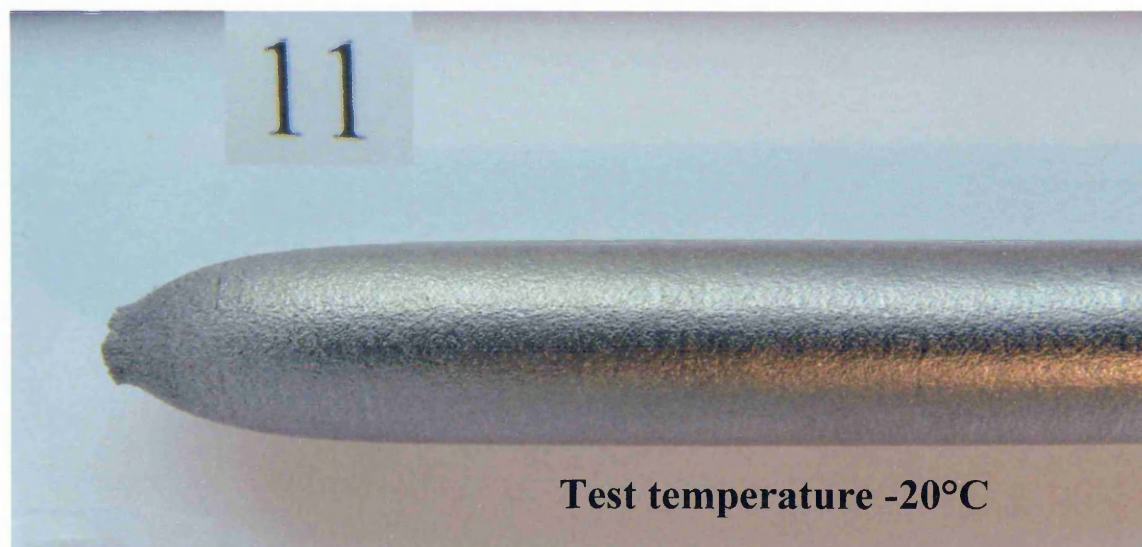
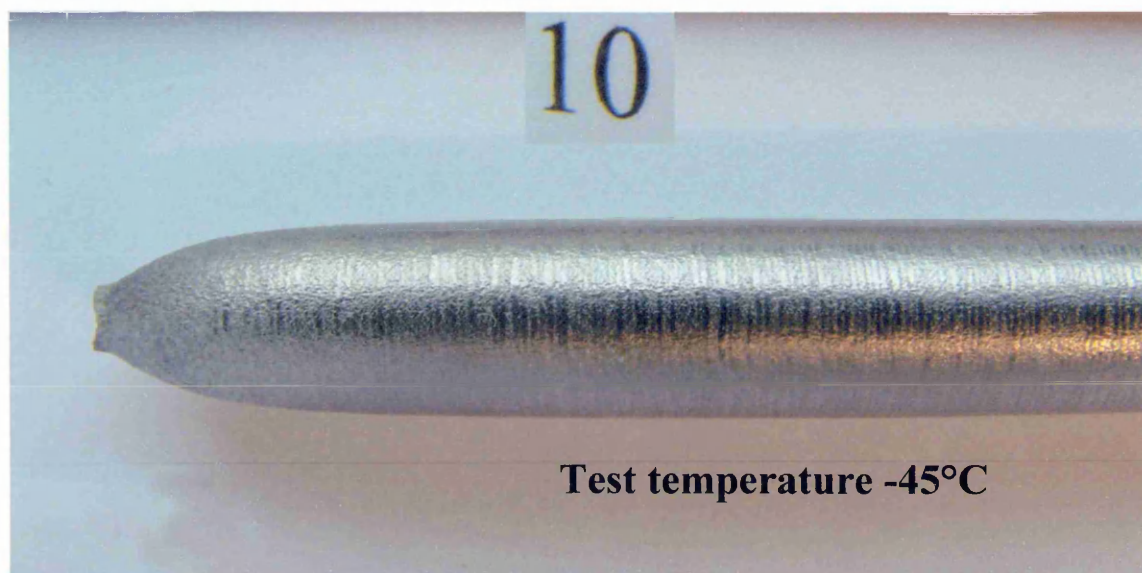
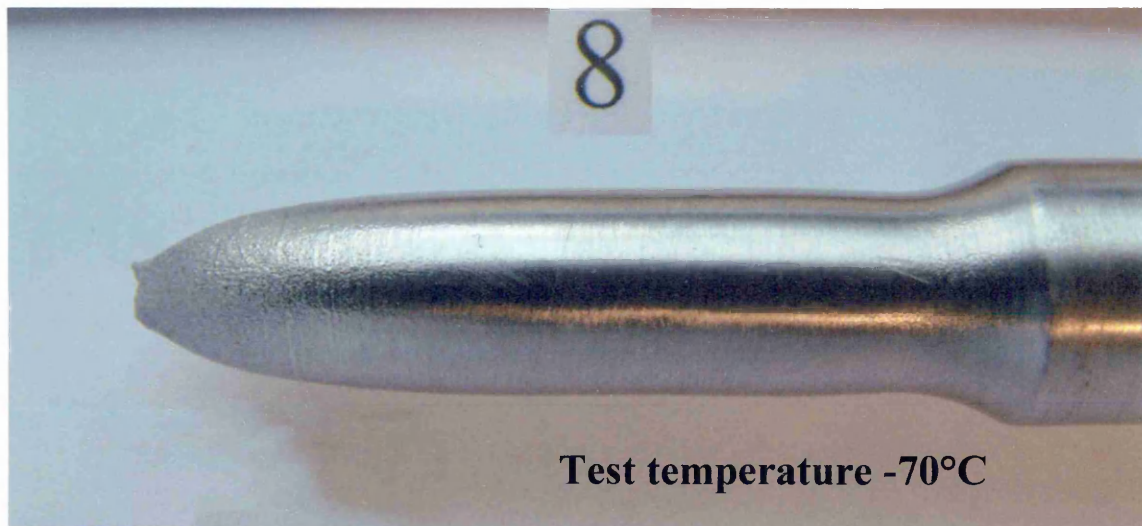


Fig.3.4.8 Untreated Armco Iron Tensile Specimens



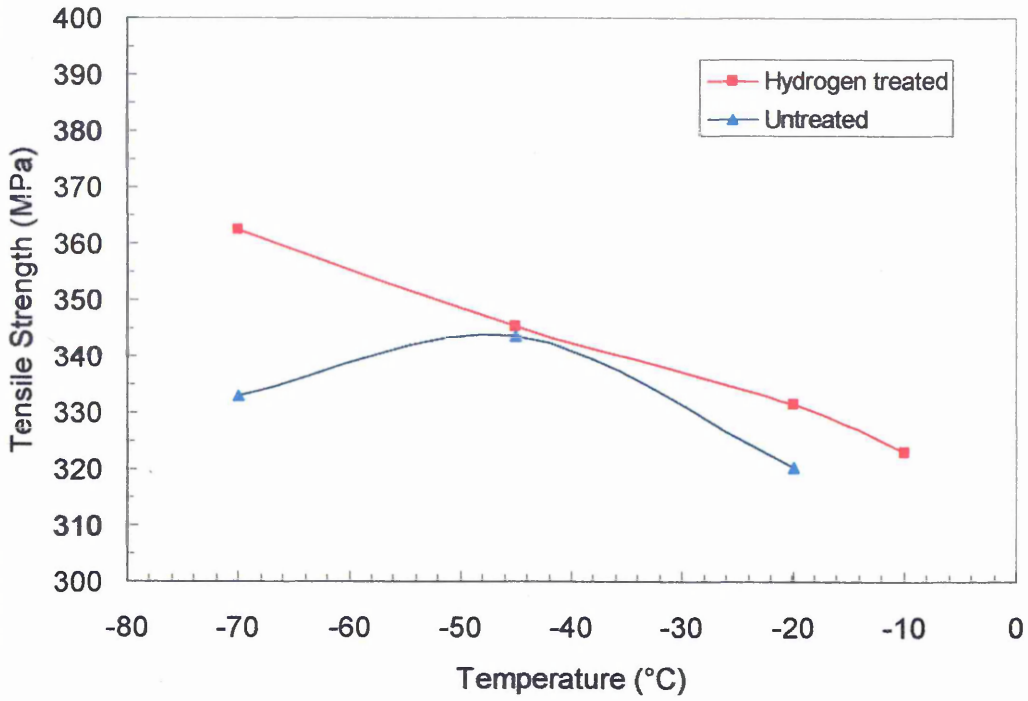


Fig. 3.4.9 Tensile Strengths of treated and untreated Armco Iron

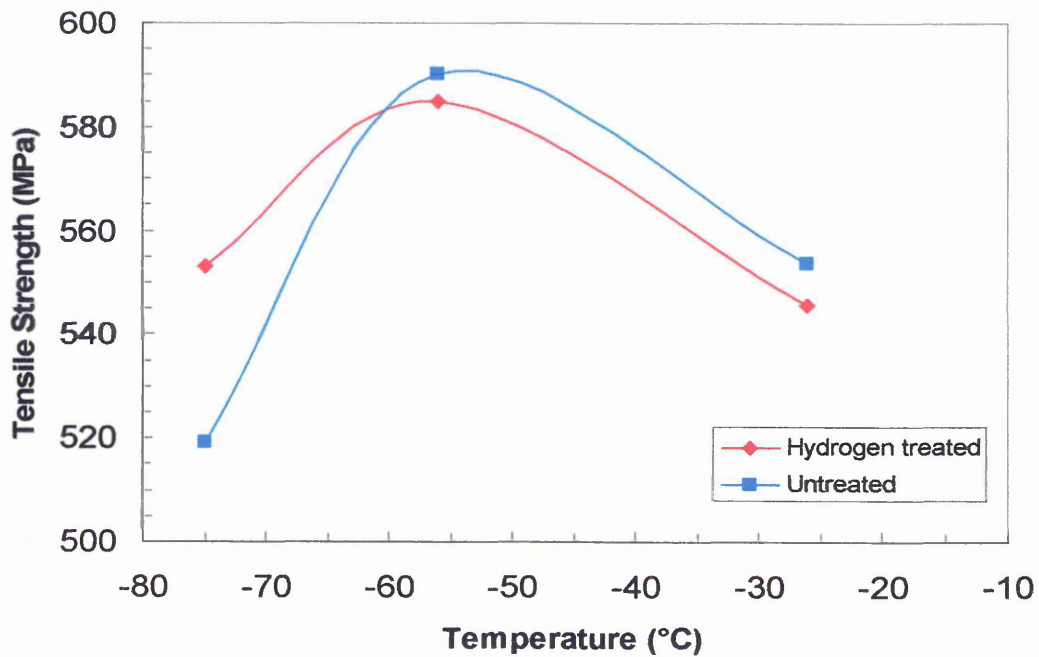
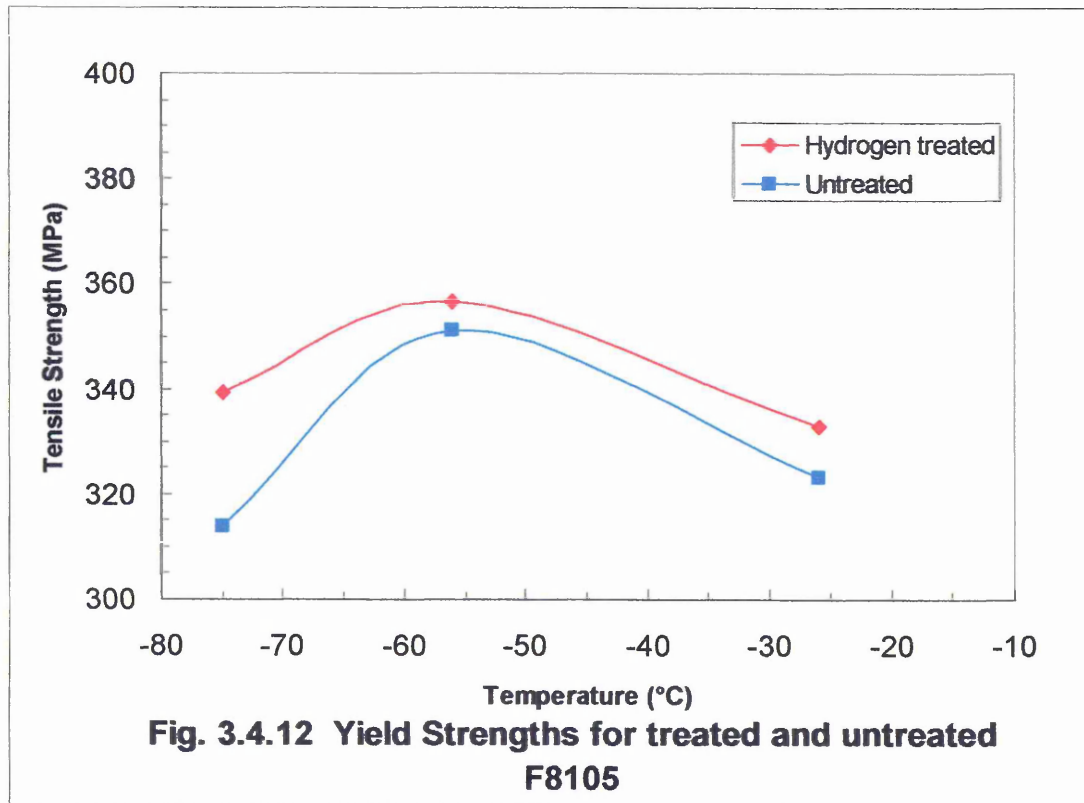
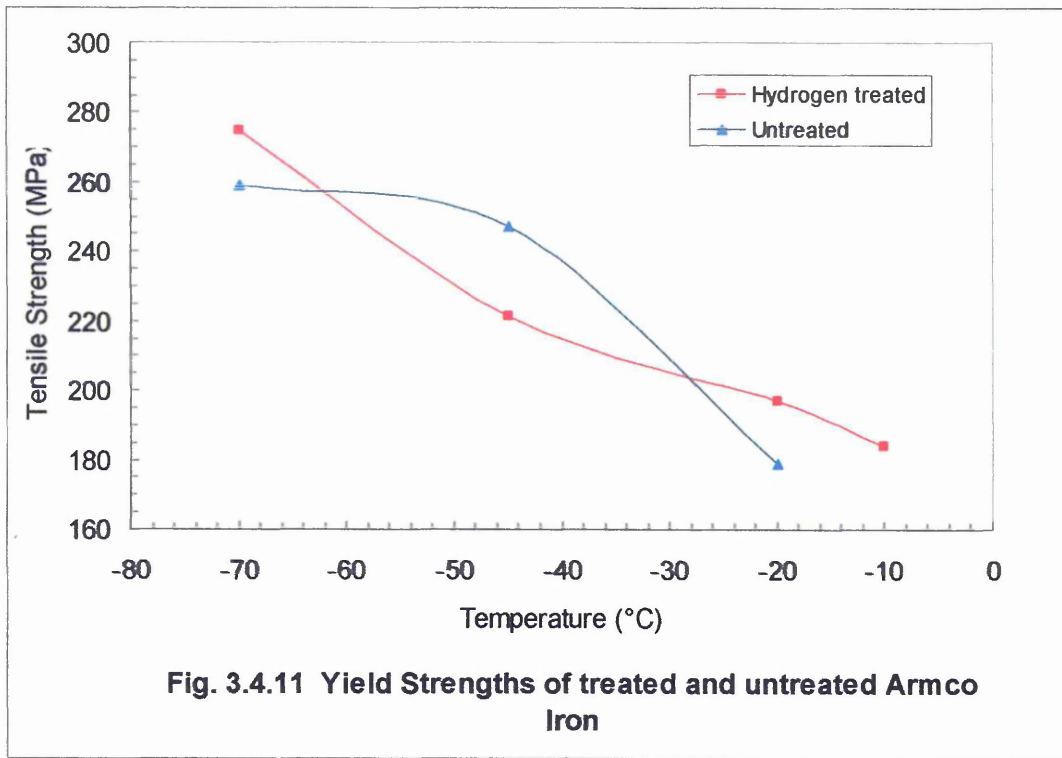


Fig. 3.4.10 Tensile Strengths for treated and untreated F8105



4.0 General Discussion

4.1 Free Nitrogen Measurements

Both nitrogen and hydrogen present problems when it comes to measuring the quantities that may be dissolved in a metal. If the metal is heated then the individual atoms can diffuse to the surface where they can combine with a similar atom to form a gas molecule which then leaves the metal. This has been the basis for standard removal treatments for hydrogen where leaving it for 24 – 48 hours at room temperature in a reasonably dry atmosphere will allow most of it to diffuse out of the metal. However, both these elements in an atomic state, as opposed to molecules are highly reactive with many of the elements found in steels.

4.1.1 Hydrogen Extraction of Nitrogen

Measurement of the change in thermal conductivity of a gas, using four electrically heated filaments arranged in a Wheatstone bridge configuration, is a standard method for measuring the relative concentrations in binary gas mixtures and is used for checking the composition of welding gas mixtures. The temperature of the wire filament depends on the thermal conductivity of the gas passing over it. Gases such as hydrogen and helium, that have high thermal conductivity, will conduct heat away from the filament at a high rate causing it to cool and so lowering its resistance. Whereas, gases with low thermal conductivity, such as carbon dioxide or ammonia, will conduct heat away at a lower rate causing the filament to rise in temperature with a subsequent rise in resistance. This type of thermal conductivity detector (TCD), as a result of the small change in resistance of a metal wire filament, is normally only used to make measurements in the percentage range, i.e. greater than 1% of the contaminant⁽¹⁵¹⁾. This is due to the fact that changes in resistance resulting from changes in temperature

are normally only in the order of fractions of an ohm per degree Celsius and this limits the sensitivity of measurement.

Replacing heated metal alloy filaments with thermistors should give an increase in the sensitivity of a TCD of several orders of magnitude as the change in resistivity of a thermistor is of the order of ohms per degree Celsius (specialised thermal conductivity analysers of this type can carry out analyses at the parts per million range⁽¹⁵¹⁾).

The actual type of thermistors used in the bridge was not recorded at the time of construction of the bridge, but based on size and availability was probably a Philips 2218 with an impedance of 4.7 k Ω at 25°C. Over the temperature range 20 to 30°C this type shows a drop in impedance of 150 Ω per °C. Based on a measured change in the potential recorded at R (see figure 3.1.3) of 1 mv, then the theoretical resolution of the temperature measuring system should be in the order of 0.0006°C. Furthermore, a change in the heat removal rate of 7 mW will cause the temperature of the thermistor to change by 1°C.

Calculations carried out after the experimental work had finished indicated that under steady state conditions at 25°C each thermistor would be dissipating 2.15 mW. A reduction in the thermal conductivity of the hydrogen – ammonia gas stream compared to the pure hydrogen of 0.26% (see section 3.1) would give a decrease in this dissipation of 0.0056 mW, an increase in temperature of only 0.0008°C, i.e. at the limit of the resolution of the detector. Furthermore, the hydrogen containing ammonia will always be at a slightly greater temperature than the incoming hydrogen as even the most efficient heat exchanger cannot be 100% efficient. This temperature difference will be greater than that resulting from the change in thermal conductivity.

It had been hoped that the ammonia formed from the free nitrogen in the steel would give rise to a detectable change in the balance of the bridge. However, it would appear from the runs using an empty boat, that the presence of the boat, in the furnace hot zone, has a variable effect on the hydrogen gas stream larger than that produced by the ammonia. This appears to be due to two effects;-

- ◆ Pushing the boat into the hot zone disturbs the gas flow through the hot zone. This disturbance may initially slightly cool the gas giving rise to the dip seen in run Blank 2, see figure 3.1.5, or the turbulence may cause more of the gas stream to come into contact with the furnace wall resulting in an increase in the temperature.
- ◆ As the boat reaches the temperature of the hot zone the increased hot surface area in contact with the gas stream increases the gas temperature. This would explain the signal increase after 20 –30 minutes seen in several of the runs.

The result of these effects was that the any variation in the bridge output due to the small amount of ammonia in the gas stream was swamped by these larger irregular variations in the temperature of the gas stream.

An attempt was made to reduce the variation in the temperature of the gas leaving the furnace by passing it through a heat exchanger but this still did not give stable measureable data.

The conclusion that has to be drawn from these tests is that as the levels of ammonia in the hydrogen gas stream are so very small, any degree of contamination by argon, methane or any other gas adsorbed on the surface of the sample and ceramic boat makes it impossible to accurately measure the ammonia content by looking for a change in the

physical properties of the exiting gas stream. This is further compounded by the virtual impossibility of getting the ingoing and outgoing gas streams passing through a thermistor bridge at exactly the same constant temperature throughout the measurement cycle.

Nitrogen in an atomic state as opposed to molecular is extremely reactive and can form very stable nitrides with elements such as titanium and niobium which have melting points of 2950°C (TiN) and 2300°C (NbN). It can also form metastable compounds such as Mg_3N_2 , which decomposes above 271°C and very unstable compound such as copper azide ($Cu(N_3)_2$) which are shock sensitive and will explode readily⁽⁴⁸⁾. This wide range of stability of metallic nitrogen compounds means that any technique for the measurement of 'free' or uncombined nitrogen in steel that involves a significant rise in temperature may result in the decomposition of nitrides that are stable at room temperature and so give an over estimate of the true free nitrogen content.

This would appear to be an inherent weakness in any method that involves the combining of the nitrogen with hydrogen to form ammonia, as in order to be carried out in a realistic time period it has to be carried out at a temperature above 400°C. As a result even a chemical measurement of the ammonia content will not give an accurate measure of the true free nitrogen content in the steel at room temperature.

4.1.2 Internal Friction Measurement

The standard internal friction technique for measuring free carbon and free nitrogen using a torsion pendulum with a fixed frequency again involves carrying out measurements at temperatures above ambient. However, this will give a much better result, than the hydrogen extraction technique, as the maximum temperatures are normally less than 200°C.

The Vibran system described in this work has the potential to give an even better result as, for most steels, the measurements can be carried out at room temperature or, in the case of the SHU modified equipment, below room temperature. This means that any nitrides that are only stable at temperatures below 100°C will not be affected by the measurements. This is particularly important if the steel is to be cold formed and the product requires a smooth surface finish.

Since this work was completed further trials have been carried out using a smaller size specimen. These tests confirmed that the specimen size is not critical, however, due to the greater torque required to twist a shorter specimen the maximum frequency that the equipment could reach was limited to 10 Hertz.

The evidence from the internal friction work appears to show that hydrogen has an effect on the peak heights of carbon and nitrogen. The effect is consistent with hydrogen reducing elastic strain as has been reported by other workers^(33, 60). This effect may give a possible method for measuring hydrogen in steel:

The specimen would be first tested in the as received condition and then heated in argon and then in vacuum to remove hydrogen and retested. If the heating is carried out below 400°C then the free carbon content should not have changed and so any reduction in the peak height would be a measure of the original hydrogen content.

4.2 Nature of Hydrogen in Steel

One of the problems of using electrolytic charging to put hydrogen into steel specimens is that it can result in plastic deformation that masks the true alloying effect of the addition. Lounamaa⁽¹⁵²⁾ had shown that for charging times of less than 6 hours there is a linear relationship between the amount of hydrogen absorbed and the charging time. In view of this, charging times used in this work were all less than 6 hours. However, as a result of a misunderstanding, the hydrogen charging technique used in all of this work would have only put relatively low amounts of hydrogen into the specimens. Serendipitously this means that the plastic deformation effects that can occur when hydrogen is electrolytically 'forced' into a steel, such as surface blistering and more importantly the loss of the yield point, have not occurred in any of these specimens.

This raises the question are the changes in the upper to lower yield ratios, seen in this work, the result of hydrogen? The answer to this would appear to be yes as the results for the Armco iron specimens used in the DSA experiments and tested above -70°C , where hydrogen was diffused into the whole of the specimen, clearly show a marked increase in the upper to lower yield ratio compared to the non-hydrogen charged specimens (see Appendix III and table 3.4.1). (At -45°C carbon and nitrogen interstitial atoms would not undergo any significant diffusion that could produce such an effect.) A similar but lesser effect can also be seen in the high and medium nitrogen mild steel DSA specimens (F8105 and F8104) tested above -70°C .

The actual value of the upper yield stress is not a fixed material property but is dependant on the characteristics of the tensile machine used for the test. However, all the tests specimens subjected to the electrical current were carried out on the same test frame (Mayes ESH 100) and the DSA tests were carried out on an identical machine. It

is therefore reasonable to compare the ratio of upper to lower yield ratios in these specimens. An examination of the upper and lower yield point reveals that in all the hydrogen treated specimens the increase in the upper yield stress appears to be the most significant effect of the hydrogen (the lower yield stresses show a varied effect suggesting that the hydrogen is not having a consistent effect and probably no effect). The effect of hydrogen on the upper yield point is unlikely to be due to hydrogen locking dislocations as the carbon and nitrogen contents of all these materials were well above the minimum of 0.003 wt% carbon needed to generate saturated atmospheres around all the dislocations in normalised materials kept at room temperature for several days⁽⁸⁾.

The current explanation for the yield effect is that it is due to the strain in the crystal structure activating new dislocation generators. The new dislocations are initially created at the upper yield point⁽¹⁵³⁾. The evidence from the work of Ferreira⁽³³⁾ and Vennett et al.⁽⁶⁰⁾ has shown that hydrogen reduces elastic strain and this is further supported by the internal friction work report here (see section 3.2.4). Therefore a possible explanation for the increase in the upper yield point is that hydrogen having reduced the elastic strain has delayed the activation of new dislocations until a higher stress has been reached, this stress giving sufficient strain to activate the generation of new dislocations.

If this is the case then an increase in the upper to lower yield ratio is a measure of an increase in the hydrogen concentration. Therefore, the experiments on the nature of hydrogen dissolved in iron have demonstrated that at low temperatures (~77K) hydrogen can be moved by an electrical potential. This can only occur if it is existing within the metal as a positively charged particle, i.e. it shows 'metallic' behaviour. The

fact that it can exist within the crystal structure as a very small charged particle with a much higher charge to mass ratio than a typical ion is a probable explanation of both the anomalously high diffusion rates that have been recorded for hydrogen and an explanation of why it diffuses to areas of high stress. This also gives an explanation for the low rate of hydrogen diffusion through an oxide layer reported by Huffine and Williams⁽⁹⁷⁾, as in an oxide which will be either covalently or ionically bonded the hydrogen would exist as an atom or a molecule but could not exist as a 'free' proton.

4.2.1 Hydrogen Transport

The evidence from internal friction measurements at low temperatures⁽⁵⁵⁾ shows that hydrogen does exist as atoms but the results from these experiments have shown that at low temperatures (~ 77K) hydrogen dissolved in iron can appear to adopt a metallic state. Whilst this is not necessarily the case at room temperature it is a possible explanation for the anomalous behaviour of hydrogen in metal.

Figure 4.2.1 show the relative sizes of a nitrogen atom and a hydrogen atom against an

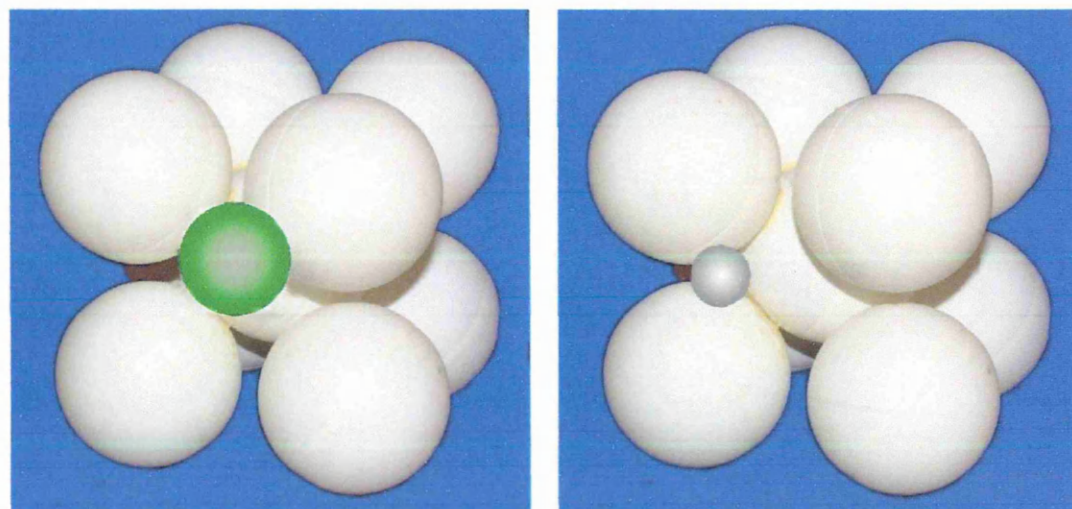


Fig. 4.2.1 Nitrogen (green) and hydrogen (silver) atom sizes relative to iron iron BCC crystal. The hydrogen atom in this picture is 93 pixels in diameter, a proton on the same scale would be one twentieth of a pixel in diameter, i.e. much smaller than

the gaps between the iron atoms. This would suggest that 'metallic hydrogen' could freely move through a metal crystal structure by releasing its electron into the electron cloud and then gaining another electron at its new location.

Cottrell in his analysis of the embedding of a hydrogen atom in a metal⁽¹⁵⁴⁾ argues that an electron from the electron cloud of the embedding metal will rapidly oscillate between the vacant 1s energy state of the hydrogen atom and the electron cloud.

Cottrell seem to assume that it is only this 'new' electron that will oscillate with the 'original' electron remaining in its 1s state. This results in the atom behaving as a negative ion with an average charge of $-0.67eV$. Cottrell appears to have based this analysis on hydrogen forming negative ions (H^-). Hydrogen does form hydrides and some of the alkali metals hydride salts in Groups I and II are ionic and do form H^- ions, however, iron does not⁽¹⁵⁵⁾. Furthermore, some metal hydrides such as uranium (UH_3) show metallic properties. The assumption that hydrogen will attract a second electron and so gain an overall negative charge would conflict with the evidence from the experimental work described in section 3.3 which is consistent with a positively charged particle. However, if both the 'new' and 'original' electrons oscillate reciprocally, this would maintain an average single occupancy of the 1s state but would allow the exchange of the 'original' electron with another from the electron cloud, i.e. metallic behaviour. Furthermore, the paired oscillation would mean that during part of the cycle there would be an overall positive balance of charge which would allow the proton to move under the influence of an electrical potential.

Heller's work⁽⁵⁵⁾, on internal friction, indicates that at low temperatures and when the metal lattice is distorted the hydrogen shows atomic behaviour. However, for a hydrogen atom existing in the metallic electron cloud undergoing reciprocal oscillation

of a pair of electrons it would be able to exchange its original electron with one from the cloud so show both atomic and metallic (ionic) behaviour.

The actual mechanism of the movement of a proton through a metal lattice will require further study. Studies of the movement of hydrogen ions (H^+) in aqueous solutions have shown that it is not a simple motion but is believed to involve the formation of complex hydrated ions⁽¹⁵⁶⁾, due to the high energy of hydration of the proton. This mechanism known as the Grotthuss Mechanism involves the rearrangement of bonds in a group of water molecules such that it results in the effective motion of a proton. This model implies that there is no coordinated motion of a proton along a chain of molecules but a sequence of very rapid low activation energy jumps between neighbouring sites⁽¹⁵⁷⁾. In a metal lattice a proton would not form hydrated molecules and so as a result of its extremely small size (approximately one eighteenth hundredth of the diameter of an octahedral site), and the evidence from Geiger and Marsden's work^(119,120), it should move relatively freely under the influence of an electrical potential without the need to jump to a limited set of specific sites.

In an ionic solution subjected to an electrical potential the diffusion or migration coefficient of an ion is related to the molar conductivity of the ion, λ (or ions), by the Nernst-Einstein equation^(158,159);

$$\lambda = z^2 \cdot D \cdot F^2 / RT$$

where z is the charge on the ion, D is the diffusion coefficient, F is Faraday's constant, R is the Universal gas constant and T is the temperature in Kelvin.

For a single ion species in a dilute fully ionised solution the molar conductivity λ is equal to the measured conductivity k divided by the concentration of the species, c .

It was noted during the running of a current through the charged specimens that in the specimen I where hydrogen was being moved along the uncharged section of the specimen, towards the notch the potential drop was less on this specimen than on specimen II where the current was flowing in the opposite direction (the same effect was noted in the subsequent tests). A calculation based on the resistivity of the two specimens gives conductivities of 1836 siemens for the specimen I and 1256 siemens for specimen II, a difference of 580 siemens.

If the following two assumptions are made;

- 1) The increased conductivity due to hydrogen ions is equal to half the change in conductivity (290 S).
- 2) The average concentration of hydrogen is 10 ppm, and assuming it all behaves metallically, this gives a molar concentration c of $\sim 80 \text{ mol.m}^{-3}$ (of hydrogen ion H^+).

Then an estimate of the migration coefficient at the temperature of liquid nitrogen (77k) can be made as follows;

$$\lambda = 290/80 = 3.625 = z^2.D.F^2 /RT$$

rearranging gives $D = 3.625.R.T /z^2.F^2$

putting in the following values

$$z = 1 (\text{H}^+), \quad F = 9.648 \times 10^4, \quad R = 8.314, \quad T = 77$$

gives a value for D of $2.49 \times 10^{-7} \text{ m}^2.\text{s}^{-1}$ a value several orders of magnitude greater than the thermal diffusion coefficient. A comparison with the value for the hydrogen ion in an aqueous solution (H^+) of $9.31 \times 10^{-9} \text{ m}^2.\text{s}^{-1}$ (158) is comparable with this value,

as for the ion in water the proton has to form hydrated molecules with the water, reducing the effective charge to mass ratio, but for a proton moving in a metallic lattice this restriction will not apply. (The sodium ion, with an even lower charge to mass ratio, in an aqueous solution has D value of $1.33 \times 10^{-9} \text{ m}^2 \cdot \text{s}^{-1}$ (158).)

However, it should be noted that there is a major difference between a normal ionic solution and a metallic solution. In a normal ionic solution the conductivity rises as the temperature rises, due to the increased mobility of the ions, whereas in a metal the conductivity decreases as the temperature rises.

The aim of this work was simply to determine if dissolved hydrogen could be moved by an applied electrical potential and so further work will need to be carried out at different potentials, different temperatures and measured hydrogen contents to obtain a better estimate for D and to determine if there is an activation energy (possibly an 'ionisation potential') for this type of movement. However, for a hydrogen atom existing within the electron cloud of a metal it was dissolved in, it would be impossible to determine for any given electron whether it originally 'belonged' to the proton or was part of the cloud i.e. changing from an atomic to a metallic state would be governed by the random motion of the electrons where the activation energy is less than the energy of the random motion.

This ability of hydrogen to behave in a metallic manner would also support the 'hydrogen shielding' model (38-41), as the presence of a large number of positively charged particles around the dislocation would have the effect of contracting the electrons around that area effectively shrinking the size of the dislocation and so reducing the strain field.

4.2.2 Diffusion of Hydrogen to a Crack Tip

Hydrogen is known to diffuse to a crack tip, Johnson et al.⁽⁹⁸⁾ proposed that the tri-axial stress field ahead of a crack tip could raise the diffusion gradient for hydrogen causing it to diffuse to that region due to lattice distortion. However, for a small sharp crack the effects of lattice strain will be limited to a relatively small volume and whilst this zone may trap any hydrogen atoms diffusing into it, it would not exert a positive attraction beyond the immediate zone.

This raises the question “if hydrogen is existing as a charged particle (a proton) could there be an electrical attractive force causing the protons to migrate towards the crack tip?” The force could be due to an imbalance in the electron cloud in an area of tri-axial stress. Such an imbalance, the presence of an excess of electrons, would exert an attractive force over a greater volume than the actual strained volume.

Coulomb’s law states that the attractive force between two equal but oppositely charged particles is inversely proportional to the square of the distance between them ⁽¹⁶⁰⁾.

In the case of the attraction between an electron and a proton spaced 10 mm apart in a vacuum this force equals 2.3×10^{-24} N which appears very small but if the electron were fixed it would give a proton, with a mass of 1.67×10^{-27} kg, an acceleration of $1,375 \text{ m.sec}^{-2}$.

The increase in resistance in a section of steel due to the presence of a crack is a well known phenomena and the change in resistance is used to monitor crack growth during fracture toughness testing.

The presence of the crack will affect the normal distribution of the electron cloud in the metal. Furthermore, the crack tip will normally suffer some plastic deformation and cold working increases the resistance of a metal.

The electron cloud can never be completely at rest as micro-currents will result from factors such as the movement of the metal through the earth's magnetic field, electromagnetic radiation and electro-chemical effects, all of which will cause movement of the electron cloud. The presence, therefore, of a crack will be a restriction to this free flow of the electron cloud in the metal. This would suggest that there will be a slight increase in the concentration of electrons around the crack tip as this will be a choke point, i.e. there will be an overall negative charge at the crack tip, a negative charge that will attract positively charged particles such as protons (metallic hydrogen).

Further possible evidence that high stresses affect the electrical behaviour of a metal comes from the fact that in high stress fracture, e.g. ball crush tests on 1%C 1.5% Cr ball bearings, a flash of light is emitted during the fracture. This appears to be the result of an electrical discharge as the imbalance reaches a critical potential (there is no evidence of frictional heating causing the light) ⁽¹⁶¹⁾.

In terms of theories of hydrogen transport as a Cottrell atmosphere around a dislocation, Tien's hypothesis ⁽⁹⁹⁾ has the lattice distortion due to the dislocation being the primary motivating force, with the hydrogen effectively being carried by the dislocation. By contrast in the King and Block model ⁽¹⁰⁰⁾ it is the effect on the hydrogen that is the main motivation force but they concluded that the attractive force would only be large enough to move the dislocation if the overall hydrogen concentration in the lattice was very high.

However, if hydrogen exists as protons this would give rise to a potential additional force, namely the electrostatic attraction of the protons to any electron concentration around the crack tip (this assumes that the overall charge on the dislocation due to the presence of hydrogen nuclei would be positive). Whilst this force is small in comparison with the stress field effect (3.2×10^{-15} N) it would be an additional contribution.

4.3 Effect of Hydrogen on Work Hardening

Even though the levels of hydrogen charged into these specimens was relatively low there is a significant difference in the appearance of the hydrogen treated tensile tested specimens compared to the untreated specimens. However, this cracking of the hydrogen specimens has not affected the tensile strength which would indicate that the maximum true stress in the hydrogen treated metal is higher than that in the untreated metal.

Again even with these relatively low levels of hydrogen the high nitrogen steels do not show any increase in the overall measured ductility as a result of hydrogen.

The results have shown that hydrogen reduces the work hardening coefficient, in the temperature range -56 to -20°C ($217 - 253\text{K}$), in Armco iron and mild steels with low and high free nitrogen contents. This is consistent with the explanation by Matsumoto et al. ⁽⁶⁸⁾ of the dislocation motion they observed i.e. a reduction in the strain fields around dislocations allowing them to move closer together under a given stress.

These results show that hydrogen is giving a strengthening effect at -70°C , with a corresponding reduction in ductility. However, the fact that the tensile and yield strength peaks in the high nitrogen steel occur at around -50°C in both the hydrogen treated and untreated steel strongly suggest that hydrogen is not generating Dynamic

Strain Ageing (DSA) in this steel. The results for the Armco iron, which has a very low free nitrogen, content do not show the same trend as the maximum measured tensile strength and yield strength in the hydrogen treated specimen occurred at -70°C , whereas in the untreated iron the maximum tensile strength occurred around -50°C . This would indicate a possible low temperature DSA type of phenomena due to hydrogen.

Unfortunately it was not possible to carry out tests at temperatures below $\sim -75^{\circ}\text{C}$ with the existing apparatus so the true position of and the maximum tensile strength of the hydrogen treated iron is not known.

Due to the limited number of tests carried out it has not been possible to determine if hydrogen produces a Dynamic Strain Ageing effect but the results do suggest that there is no effect in mild steel at temperatures down to -75°C . However, there is a possible indication that Dynamic Strain Ageing may occur in Armco iron but further work at lower temperatures would be needed to confirm this.

As similar trends were seen in the very low nitrogen Armco iron and the high nitrogen steel (F8105) it would appear there is no significant interaction between the free nitrogen and the hydrogen at temperatures below 0°C .

In conclusion had Tschischewski spoken of hydrogen, rather than nitrogen, in his 1915 paper his conclusion of its '*injurious influence*' would still be valid.

5.0 Conclusions

The following conclusions can be drawn from this work with regard to:-

5.1 Measurement of Free Nitrogen

- 1) The percentage of ammonia in the hydrogen gas stream used to extract nitrogen from a steel sample is too small to be measured by looking for a change in the thermal conductivity of the hydrogen stream.
- 2) Any method attempting to measure free or uncombined nitrogen that involves heating above 400°C is liable to give an over estimate.
- 3) A mathematical model has been developed to allow the determination of both free carbon and free nitrogen from the internal friction curves generated by a Vibran Interstitial Analyser. This allows reproducible measurements to be carried out at room temperature.
- 4) Initial results from this work indicate that the use of atomic percentages in a modified version of the ITT prediction equation produced by Mintz give a better fit to the measured values.
- 5) In freshly charged specimens hydrogen gives an increase in the internal friction peak heights for carbon and nitrogen. This is consistent with hydrogen reducing the elastic strain fields around dislocations and has potential as a method of measuring hydrogen in steel.

5.2 Hydrogen in Steel

Assuming that an increase in the ratio of upper to lower yield, for a given set of tests on a single tensile testing machine, is an indication of an increased hydrogen content, then the following conclusions can be drawn from this work:

- 1) At low temperatures hydrogen can be moved within an iron specimen by an electrical potential.
- 2) The movement is consistent with the hydrogen having an overall positive charge.
- 3) In the absence of any evidence of H^- anions the dissolved hydrogen appears to show metallic behaviour.
- 4) In the temperature range -20 to -56°C hydrogen causes a reduction in the work hardening coefficient in Armco iron and mild steel with low and high free nitrogen contents. This is again consistent with hydrogen reducing the elastic strain fields around dislocations.
- 5) In the temperature range -26 to -75°C there is no evidence that hydrogen gives rise to Dynamic Strain Ageing in mild steel with a high free nitrogen content. In Armco iron hydrogen does give a strength increase and drop in ductility at -70°C which may be a DSA effect.
- 6) In the high nitrogen steels there was no evidence that hydrogen gave any increase in the overall ductility.

6.0 Recommendations

Further work should be carried out to determine if the Vibran apparatus could be used to determine hydrogen contents.

The revised equation for the calculation of the Impact Transition Temperature using atomic % values needs to be evaluated over a large number of low alloy steels.

One implication for the finding that hydrogen dissolved in a metal is metallic is in the use of sacrificial anodes. In a structure immersed in an aqueous environment, as the anode dissolves, at some point on the structure being protected there will be a tendency to form hydrogen some of which will dissolve in the metal. As there will be a current flowing between the structure and the anode care should be taken, in the placement of the anodes, to ensure that this current is not carrying hydrogen (protons) towards any areas of high stress.

7.0 References

- 1) C.E. Stromeyer, *The Injurious Effect of a Blue Heat on Steel and Iron*, Proceedings of the Institution of Civil Engineers, vol.84, 1886, pp 114 – 137.
- 2) F. le Chatelier, *Influence du temps et de la temperature sur les essais au choc*, Review du Metallurgie, vol.6, 1909, (in French)
- 3) Mentioned in Dislocation Dynamics, A.S. Keh, Y. Nakada and W.C. Leslie, McGraw Hill, 1968, pp381-408.
- 4) G.I. Taylor, *Mechanisms of Plastic Deformation of Crystals*, Proc. Roy. Soc. A vol.145, 1934, p. 362.
- 5) E.S. Davenport and E.C. Bain, Trans. Amer. Met. Soc. 23, 1935, p.1047.
- 6) F.R.N. Nabarro, *Report on the Strength of Solids*, (London : Physical Society) 1948, p.38.
- 7) M.D. Satterlee, Final Year Project Sheffield Hallam University, 2000, p, 10.
- 8) A.H. Cottrell and B.A. Bilby, *Dislocation Theory of Yielding and Strain Ageing of Iron*, Proc. Phys. Soc. 1949, sec. A 62. p.49.
- 9) F.B. Pickering and T. Gladman, Metallurgical developments in Carbon Steels, Spec. Rep. No. 81, Iron and Steel Institute 1963. p. 10.
- 10) K.J. Irvine, F.B. Pickering and T. Gladman, *Grain-Refined C-Mn Steels*, JISI. February, 1967, p.161.
- 11) Y. Murakarmi, N. Mitamra and K. Furumura, Super TF and Hi-TF Bearings for Long Life even under Severe Lubrication Conditions, NSK Technical Journal, 652 May 1992.
- 12) N. Tschischewski, The Occurrence and Influence of Nitrogen in Iron and Steel, JISI vol.92, 1915. p.47.

- 13) L.S. Darken and R.W. Gurry: Physical Chemistry of Metals, M^cGraw – Hill, 1953.
- 14) T. Gladman: The Physical Metallurgy of Microalloyed Steels, The Institute of Materials, 1997.
- 15) W.E. Duckworth and J.D. Baird, *Mild Steels*. J. Iron Steel Inst. 207 (1969) p. 854.
- 16) B. Mintz, R.C. Cochrane and J.D. Baird, *Some Effects of Nitrogen on the Impact Properties of Ferrite / Pearlite Steels*, Scand. J. Metallurgy. 1, (1972) p. 279.
- 17) E.D. Hondros, *Interfacial Segregation of Nitrogen in Iron*, Metal Science Journal, Vol.1, 1967, p.36.
- 18) B.E. Hopkins and H.R. Tipler, Effect of heat treatment on the brittleness of high purity Iron Nitrogen Alloys, JISI, May 1954. p. 110.
- 19) B. Mintz, Influence of Silicon and Nitrogen on the Impact Properties of As-Rolled Mild and Carbon -Manganese Steel, JISI., June 1973, p. 433.
- 20) M.D. Bramhall, PhD Thesis, Sheffield City Polytechnic, 1989.
- 21) R.E. Reed-Hill, Physical Metallurgy Principles, D. Van Nostrand Company, Inc. Princeton, New Jersey. 1967, p. 234.
- 22) D.N. Crowther, *The Effect of Nitrogen on Steel Properties*, Nitrogen in Steel, Conference, Inst. of Materials, Sept. 2000.
- 23) F.B. Pickering, Physical Metallurgy and the Design of Steels, Applied Science Publishers, 1978, p. 40.
- 24) T. Gladman, *ibid.*, p.321.
- 25) J.D. Baird and C.R. MacKenzie, Effects of nitrogen and manganese on the deformation substructure of iron strained at 20°, 225° and 450°C, JISI, May 1964, p.427.

- 26) J.D. Baird and A. Jamieson, Effects of manganese and nitrogen on the tensile properties of iron in the range 20-600°C, JISI, August 1966, p.793.
- 27) B. J. Brindley and J.T. Barnby, The Effect of Nitrogen Content on Dynamic Strain-Ageing in Mild Steel, Acta Met vol. 16, 1968. p. 41.
- 28) F.B. Pickering, *Some beneficial effects of nitrogen in steel*, High Nitrogen Steels 88 Conf. The Institute of Metals, 1988, p.10.
- 29) V.G. Gavriljuk, H. Hänninen, A.V. Tarasenko, A.S. Tereshchenko and K. Ullakko: Acta Metall mater., 1995, vol. 43 No.2, p.559.
- 30) T. Zakroczymski, N. Lukomski and J. Flis, J. Electro-Chem. Soc., 1993, 140,p. 3578
- 31) B.M. Korevaar, S. Coorens, Y. Fu, J. Sietsma, and S. Van der Zwaag; Materials Science and Technology (UK), vol. 17, no. 1, pp. 54-62, Jan. 2001.
- 32) Y. Lakhtin and N.I. Sologubova, Metal Science and Heat Treatment (Russia) (USA), vol. 33, no. 7-8, pp. 518-522, July-Aug. 1991.
- 33) G. Luo, G. Zhang, S.Kou, and S. Wang, Vacuum, vol. 39, no. 2-4, pp. 279-280, 1989.
- 34) W.L. Grube, and S.R. Rouze, *The Effects of Ion-Implanted Nitrogen on the Fatigue Behaviour of Plain Carbon Steel*, Conference Proceedings - Microstructural Science, Vol. 11, Orlando, Florida., U.S.A., 18-21 July 1982. Elsevier Science Publishing Co., Inc., pp. 51-61, 1983.
- 35) P. De la Cruz and T. Ericsson, Materials Science and Engineering A (Switzerland), vol. 247, no. 1-2, June 1998, p.204
- 36) D.W. Oxtoby, N.H. Nachtrieb and W.A. Freeman, Chemistry Science of Change, Harcourt brace Jovanovich, Publishers, (1990) Orlando, Florida, p. 941.
- 37) H. C. Rogers: Acta Met., 1956, vol. 4, p.114.

- 38) P. J. Ferreira, I. M. Robertson and H. K. Birnbaum: *Acta Mater.*, 1998, vol. 46, No. 5, p.1749.
- 39) P. Sorfronis and H.K. Birnbaum, *Fatigue and Fracture of Aerospace Structural Materials*. American Society for Mechanical Engineers, Aerospace Division, 1993, **36**, p. 15.
- 40) H.K. Birnbaum and P. Sorfronis, *Material Science & Engineering A: Structural Materials: Properties, Microstructure & Processing*, 1994, **A176**, p. 191.
- 41) P. Sorfronis and H.K. Birnbaum, *J. Mech. Phys. Solids*, 1995, **43**, p. 49.
- 42) J.D. Atkinson, Z. Zhao and J. Yu, *Interactive Effect of Dynamic Strain Ageing with High Temperature Water on the Crack initiation behaviour of Reactor Pressure vessel Steels, Effects of the Environment on the initiation of Crack Growth*, ASTM STP 1298, W.A. Van Der Sluys, R.S. Piascik and R. Zawierucha. Eds., ASTM 1997.
- 43) F.B. Pickering. *Towards Improved Toughness and Ductility*, Climax Molybdenum Co. Symposium, Kyoto. 1971, 9.
- 44) L.H. Van Vlack, *Elements of Material Science*, Addison Wesley 1960. p.11.
- 45) N. Jenkins, N. and S.M. Stevens, *Determination of Nitrogen and Nitrides in Steels*, *Welding Research Bulletin* April. 1977 p. 95.
- 46) Ir. M. Vergauwens, *Heraeus Electro-Nite brochure*, 1996.
- 47) J.D. Headridge, and G.D. Long, *The Determination of Mobile Nitrogen in Steel Using an Ammonium Ion-selective Electrode*, *Analyst* Feb. 1976, vol. 101 p. 103.
- 48) J.D. Headridge, S.R. Keown, and P.A. Vergnano, *The Determination of Mobile Nitrogen in Vanadium Steels by the Extraction Method with Hydrogen*, *Analytica Chimica Acta*, 98 (1978), pp. 157 - 161.
- 49) N.N. Greenwood and A. Earnshaw, *Chemistry of the Elements*, Pergamon Press, 1984.

- 50) E.O. Hall, *Yield Point Phenomena in Metals and Alloys*, Macmillan, 1970, p.65.
- 51) G.M. Leak, *Application of Internal-Friction Measurements to the Study of Gases in Metals*, ISI Special Technical Publication, 1961.
- 52) C.A. Wert, *The Metallurgical use of Anelasticity*, in 'Modern Research Techniques in Physical Metallurgy', Cleveland, ASM. 1953, pp. 225 - 250.
- 53) T. Gladman and F.B. Pickering, *JISI.*, 1965, vol. 203, p.1212.
- 54) G. J. Couper and R. Kennedy, *Internal Friction in Iron-Manganese-Nitrogen Alloys*, *JISI.*, June 1967, p.642
- 55) W.R. Heller, *Acta Met*, 1961, vol. 9, p.600.
- 56) R. Gibala and A.J. Kumnick, *Hydrogen Embrittlement and Stress Corrosion Cracking*, ed. By R. Gibala and R.F. Hehemann, ASM, 1984, p. 61.
- 57) *Ibid.* E.O. Hall, p.157.
- 58) A.F. Wells, *Structural Inorganic Chemistry*, Oxford Clarendon Press London, 1950, p.646.
- 59) J. F. Hobson and C. Sykes: *JISI.*, 1951, vol. 169, p.209.
- 60) R. P. Fromberg, W. J. Barnett and A. R. Troiano: *Trans. ASM*, 1955, vol. 47, p.892.
- 61) A. S. Tetelman: *Fracture of Solids*, Int. Fracture Conf., Maple Valley, Wash. Interscience Publishers, New York. 1963.
- 62) R. Gilbala: *Trans. TMS-AIME*, 1967. vol. 239, p.1574.
- 63) P. Bastien and P. Azou: *Proc. First World Met. Cong.*, P. 535, ASM, Cleveland, 1952.
- 64) N. J. Grant and J.L. Lundsford: *Iron Age*, 1955, vol. 175, p.92.
- 65) A. Cracknell and N. J. Petch: *Acta Met.*, 1955, vol. 3, p. 200.

- 66) R. A. Vennett and G. S. Ansell: *Trans. ASM*, 1967, vol. 60, p. 242.
- 67) A.R. Troiano, *The Role of Hydrogen and Other Interstitials in the Mechanical Behaviour of Metals*, 34th Edward De Mille Campbell Memorial Lecture, Nov. 1959.
- 68) C. D. Beachem: *Met. Trans.*, 1972, vol. 3, p.437.
- 69) C. D Beachem, in *Stress Corrosion Cracking and Hydrogen Embrittlement of Iron Base Alloys*, NACE, Houston, TX, 1977, p.376.
- 70) T. Matsumoto, J. Eastman and H.K. Birnbaum, *Scripta Met.*, vol.15, 1981, p.1033.
- 71) H.E. Hänninen, T.C. Lee, I.M. Robertson and H.K. Birnbaum: *Corrosion Deformation Interactions*, Fontainebleau, France Oct. 1992 p. 377.
- 72) J.P. Hirth, *Effects of Hydrogen on the Properties of Iron and Steel*, *Met. Trans. A*, Vol. 11A, June 1980, p.861.
- 73) J.P. Hirth, and B. Carnahan, *Acta Met.*, vol. 26. 1978, pp. 1795 – 1803.
- 74) T. Zakroczymski, J. Flis, N. Lukomski and J. Mankowski, *Acta Mater.*, vol. 49 No. 11, 2001, p.1929.
- 75) H.C. Rogers, *Acta Met.*, 1954, 2, p.167.
- 76) K. Farrell, *Hydrogen and the Yield Point in Iron*. JISI. Jan 1965 p.71.
- 77) A.M. Adair and R.E. Hook. *Acta Met.* 1962, vol. 10 p.741.
- 78) Sheffield Hallam University Laboratory notes (Wang 1997).
- 79) E. Lunarska, *Effects of Hydrogen on the Plastic Properties of Iron Single Crystals, Whiskers and Polycrystals*, in *Hydrogen Degradation of Ferrous Alloys*, ed.R.A.Oriani, J.P.Hirth and M.Smialowski, Noyes Publications, 1985, p.332.
- 80) Private Communication W. Cook, BSC Swinden Laboratories, 1990.
- 81) K.B. Grove and J.A. Charles, *Hydrogen and Dynamic Strain-Ageing in Ferrite*, *Metal Science*, 1974, vol. 8, p.367.

- 82) K.B. Grove and J.A. Charles, *A New High Temperature Microhardness Tester*, Metallurgist 1974, vol.6, p.119.
- 83) B.A. Willcox, W.A. Brisbane and R.F. Klinger, Trans. Am. Soc. Metals, 1962 vol 55, 179. quote in E.O. Hall.
- 84) D. Hardie and P. McIntyre, The Low-Temperature Embrittlement of Niobium and Vanadium by Both Dissolved and Precipitated Hydrogen, Met. Trans. vol.4, May 1973, p. 1247.
- 85) Private Communication, J.D. Atkinson, Sheffield Hallam, University, 2007.
- 86) A.H. Priest: Fatigue Crack Growth and Fracture Resistance of Steels in High Pressure Hydrogen Environments, Commission of the European Communities, EUR No. 8191. p.47, 1983.
- 87) M. Cain and A.R. Troiano, *Petroleum Engineer*, 1965, p.78.
- 88) P.G. Marsh, and W.W. Gerberich, Influence of Microstructure and Texture on Fatigue Crack Initiation in HSLA Steel in Hydrogen and Nitrogen Atmospheres, The Minerals, Metals & Materials Society (TMS) (USA), pp. 287-292, 1993.
- 89) WP. Kedzierzawski, *Diffusivity of Hydrogen and Its Isotopes in Iron Alloys*, in Hydrogen Degradation of Ferrous Alloys, p.253.
- 90) *Ibid.* L.H. Van Vlack, p.29.
- 91) *Ibid.* E.O. Hall, p.67.
- 92) *Ibid.* L.H. Van Vlack, p.295.
- 93) J. A. Donovan, Accelerated Evolution of Hydrogen from Metals during Plastic Deformation, Met Trans A Vol. 7A Nov 1976 pp 1677 - 1683.
- 94) M.R. Louthan, Jr., G.R. Caskey Jr., J.A. Donovan and D.E. Rawl, Jr., *Hydrogen Embrittlement of Metals*, Mater. Sci. Eng. 10 (1972), pp. 357-368.
- 95) www.chm.bris.ac.uk/webprojects2000/plewis/Whatis.html

- 96) D.I. Phalen and D.A. Vaughan, *The Role of Surface Stress on Hydrogen Absorption by 4340 Steel*, Corrosion - NACE, vol. 24, No. 8, August 1968, p. 243.
- 97) C.L. Huffine and J.M. Williams, *Hydrogen Permeation through Metals, Alloys and Oxides at Elevated Temperatures*. Corrosion - NACE, vol.16, Sept. 1960, p.102.
- 98) H.H. Johnson, J.G. Morlet and A.R. Troiano. *Hydrogen Crack Initiation and Delayed Fracture in Steel*. Transactions of the Metallurgical Society of AIME, 212, 1958. p. 528.
- 99) J.K. Tien, A.W. Thompson, I.M. Bernstein and R.J. Richards, *Hydrogen Transport by Dislocations*, Met. Trans.A, vol.7A, June 1976, p.821.
- 100) J. King and R. Block, *Hydrogen Induced Dislocation Motion*, Scripta Met. Vol.19, 1985, p.337.
- 101) J.L. Lee and J.Y. Lee, A theoretical model on the generation of the hydrogen induced defects during cathodic charging, Scripta Metallurgica, vol. 19, No.3, 1985, p.341.
- 102) J.P. Hirth, *Hydrogen-Defect Interactions*, in *Hydrogen Degradation of Ferrous Alloys*, ed.R.A.Oriani, J.P.Hirth and M.Smialowski, Noyes Publications, 1985, p.138.
- 103) H.H. Podgurski and R.A. Oriani, Met. Trans. 3, 1972, p.2055..
- 104) Private Communication, W. Rudd, Corus, Swinden Technology Centre.
- 105) P.H. Pumphrey, CEGB Memorandum, TPRD/L/MT0211/M84.
- 106) W.Y. Choo, and J.Y. Lee, *Thermal Analysis of Trapped Hydrogen in Pure Iron*, Met Trans A., vol. 13A, January 1982, p. 135.
- 107) H. Hargi, Y. Hayashi and N. Ohtani, Trans JIM. vol. 20, 1979, p.349.
- 108) E. Wigner, and H.B. Huntington, *On the Possibility of a Metallic Modification of Hydrogen*, Journal of Chemical Physics, vol. 3, 1935, p. 764.
- 109) www-phys.llnl.gov/H_Div/GG/metalhydrofact.html 1996.

- 110) Reported in Omni, vol.1. no. 11 August 1979, p.39.
- 111) www.giwi.edu/research/planetary_science.
- 112) B. Militzer and W.B.Hubbard, *Implications of shockwave experiments with precompressed materials for giant planet interiors*, in Shock Compression of Condensed Matter – 2007, M.Elert et al. eds., pp 1395 – 1398, AIP Conference Proceedings 995, American Institute of Physics, Melville N.Y. 2007.
- 113) <http://physicsworld.com/cws/article/news/5307>
- 114) P. Loubeyre et al. 2002, Nature 416 613
- 115) S.T. Weir, A.C. Mitchell, and W.J. Nellis, *Metallization of Fluid Molecular Hydrogen at 140 GPa (1.4Mbar)*, Physical Review Letters, 1996, vol. 76, no. 11, pp. 1860 - 1863.
- 116) R.Q. Hood and G. Galli, *Insulator to metal transition in fluid deuterium*, J. Chemical Physics, vol. 120, 12. March 2004, p.5691.
- 117) R. Gibala, Stress Corrosion Cracking and Hydrogen Embrittlement of Iron based Alloys, Conf. France 1973, NACE, 1977. p. 244.
- 118) M.A. Cavanaugh, T.P. Felner, J.A. Kargol and N.F. Fiore, Scripta Met. 1982, vol. 16, pp.709 – 712.
- 119) M. Nelkon and P. Parker, Advanced Level Physics, Heinemann, 1964, p.1043
- 120) <http://ganymede.nmsu.edu/tharriso/ast301/class20.html>
- 121) V.G. Gavriljuk, V.N. Shivanyuk and B.D. Shanina, Change in the electron structure caused by C, N and H atoms in iron and its effect on their interactions with dislocations, Acta Mater. 53 (2005) p. 5017 – 5024.
- 122) D. Hull, Introduction to Dislocations, Pergamon Press, 1968, p. 129.
- 123) <http://www.matter.org.uk/matsci/drom/manual/di.html>
- 124) A. Gourmelon, Mem. Sci. Rev. Met. 72: 475 (1975). Quoted by Lunarska ref 73.

- 125) *Ibid.* E. Lunarska, p.324.
- 126) G.D. Long, PhD thesis, Sheffield University, Oct. 1976.
- 127) G.F.C. Rogers and Y.R. Mayhew: *Engineering Thermodynamics*, Longmans, 1962.
- 128) www.engineeringtoolbox.com/ammonia-d_971.html
- 129) J.D. Waldram: *The Theory of Thermodynamics*, Cambridge University Press, 1985.
- 130) Kannuluik and Carmen quoted in Waldram p.226
- 131) S. Chapman and T.G. Cowling, *The Mathematical Theory of Non-uniform Gases* Cambridge University Press, London, 1952, second edition.
- 132) M.M. Elafify, K.M. Elawadly and S.G. Elsharkawy, *Prediction of the Thermal Conductivity of Gas Mixtures using Direct Simulation Monte Carlo Method*, Information Technology Journal , 3 (1): 2004, p.23.
- 133) E.A. Mason, and S.C. Saxena, *Approximate Formula for the Thermal Conductivity of Gas Mixtures*, Phys. Fluids vol.1, no.5, 1958, p.361.
- 134) M.P. Sakena and S.C. Saxena, *Thermal Conductivity of Polyatomic Gas Mixtures and Wassiljewa Form*, Applied Scientific Research, vol.17, no. 4-5, July 1967, p.326.
- 135) T.L. Ibbs and A.A. Hirst, *The Thermal Conductivity of Gas Mixtures*, Proc. Roy. Soc. A. vol.123, no.791, 1929, p.134.
- 136) U. Sokolov, *Analysis of Binary Gas Mixtures by Thermal Conductivity*, Hebrew University of Jerusalem, August 1965.
- 137) www.sensortecinc.com/docs/technicalresources
- 138) <http://www.efunda.com/DesignStandards/sensors/thermistors>
- 139) I.G. Ritchie and Z.-L. Pan, 33rd MWSP Conf. Proc., ISS-AIME XXIX, (1992).

- 140) K. Elroot and J. Dilewijns, Calculation of the Effect of texture on the Snoek Peak Height in Steels, ISIJ 1997. pp. 610 – 614.
- 141) T. Gladman and I.D. McIvor, *Scandinavian Journal of Metallurgy*, 1 (1972) pp.247 - 253.
- 142) M.R. Corrigan, PhD thesis SHU2007.
- 143) *Fracture*, H. Liebowitz, ed., vol.1, Academic Press, 1968, p.397.
- 144) J.F. Knott, Hatfield Memorial Lecture, *Quantifying the Quality of Steel*, Ironmaking and Steelmaking, 2008, vol.35 no. 4 p.277.
- 145) **Data from E.O. Hall, p91.**
- 146) J. Heslop and N.J. Petch, *Phil. Mag.*, 1956, 1. p.866.
- 147) *Ibid.* E.O. Hall, p. 44 – 45.
- 148) **Private Communication, R.G. Williams, Corus Swinden Technology Centre.**
- 149) W. Beaty, *Speed of Electricity*, 1996,
<http://www.amasci.com/miscon/speed.html>
- 150) A. Karimi Taheri, T.M. Maccagno and J.J. Jonas, *Dynamic Strain Ageing and the Wire Drawing of Low Carbon Steel Rods*, ISIJ International, vol.35 (1995), No. 12, p.1532.
- 151) D. Richarson, *Gases and Welding Distributor*, Nov-Dec, 2003.
- 152) K. Lounamaa, Hydrogen pick-up by different methods of charging used in steel embrittlement studies, *JISI*. February 1965, p.183.
- 153) *Ibid.* T. Gladman, p20.
- 154) A. Cottrell, *Concepts in the Electron Theory of Alloys*, IOM Communications Ltd., 1998, p.18.
- 155) *Ibid.* Greenwood and Earnshaw, p. 71-73.
- 156) W.J. Moore, *Physical Chemistry*, Longmans, 1957, p.441.

157) P.W. Atkins, Physical Chemistry, Oxford, sixth edition, 1999, p.741.

158) *Ibid.* p. 749

159) Diffusion and Conductivity: the Nernst-Einstein Equation,

http://www.tannerm.com/diffus_conduct.htm

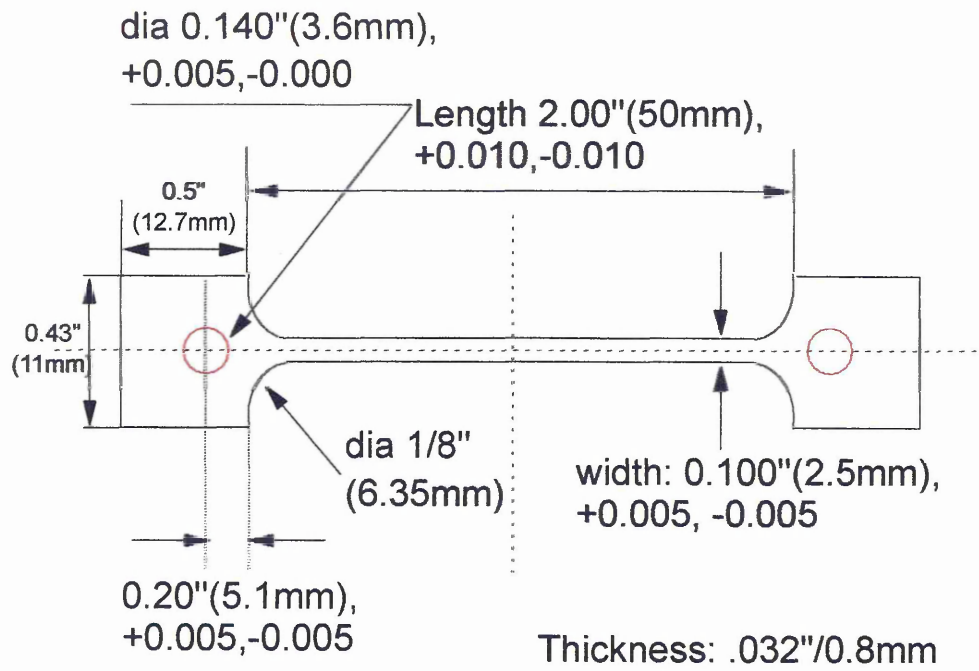
160) *Ibid.* M. Nelkon and P. Parker, p.773.

161) Observations by the author and colleagues at NSK's European Technology

Centre when conducting ball crush tests. 1990.

APPENDIX I

A.1 Vibran Specimen

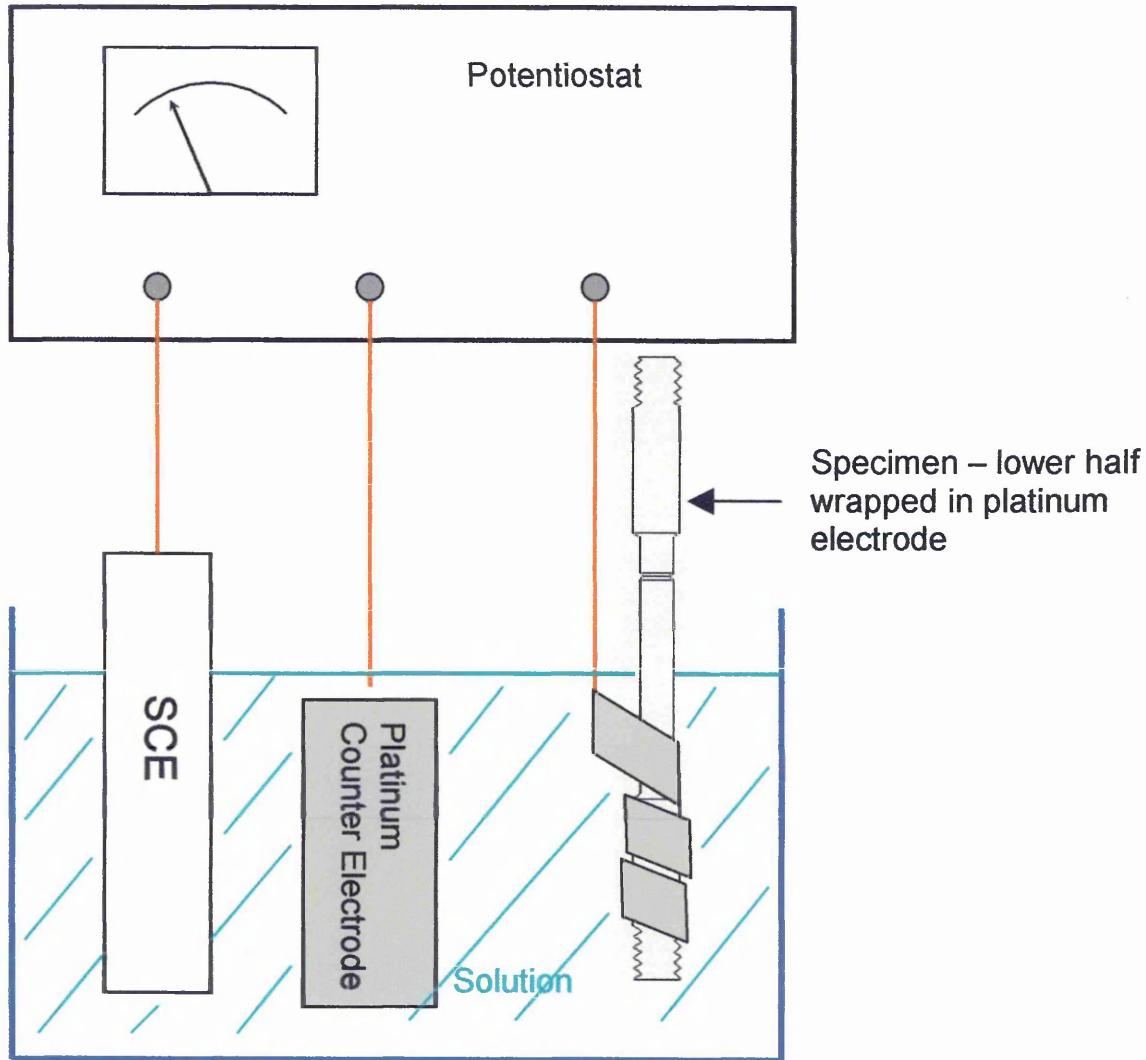


A. D. Higgins March 2004

APPENDIX II

A.2 Electrochemical Hydrogen Charging

Figure below is a block diagram for the set-up used for the electrochemical hydrogen charging of specimens.



SCE: Saturated Calomel Electrode – reference electrode.

Platinum Counter Electrode : used to accelerate the establishment of the equilibrium between the molecular and atomic forms of hydrogen.

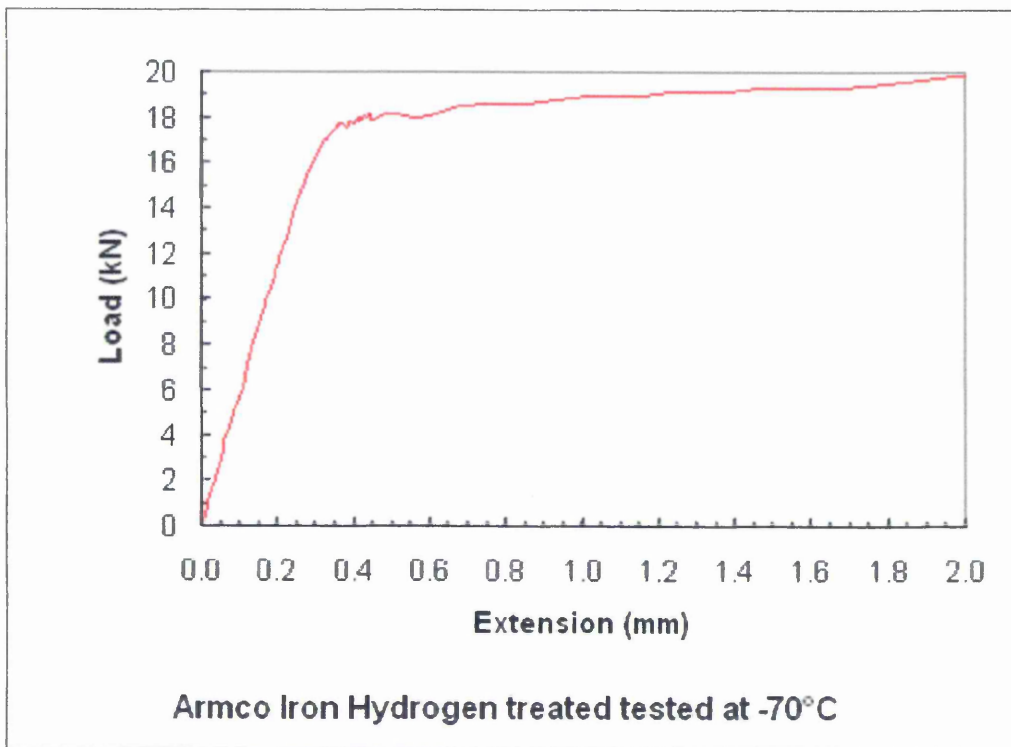
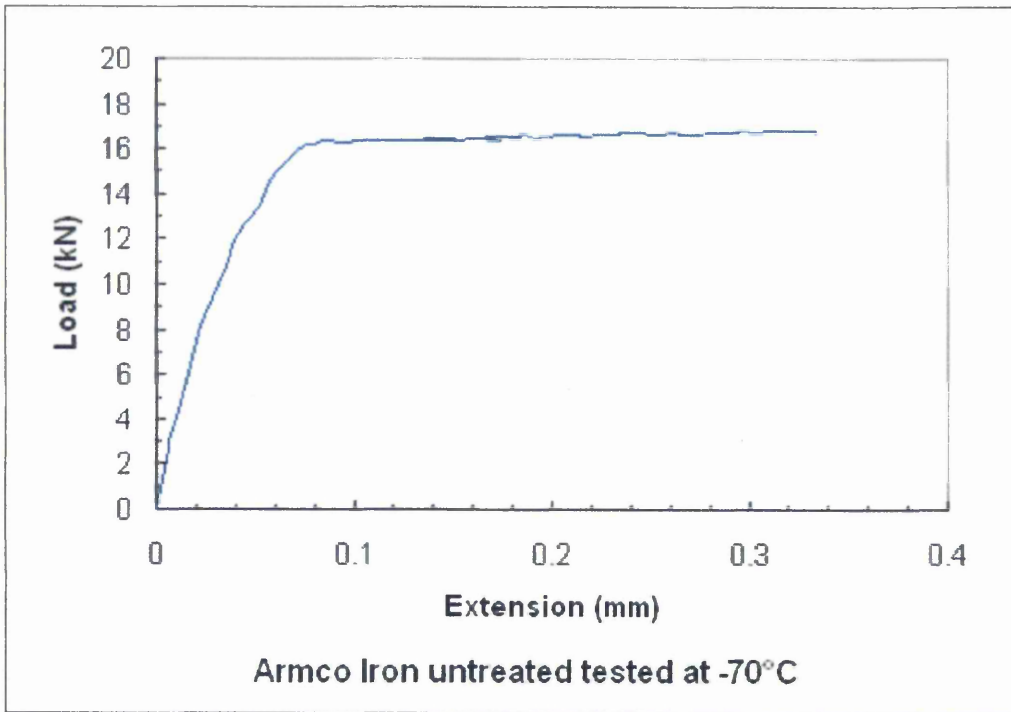
Specimen : wrapped in a platinum foil (the working electrode).

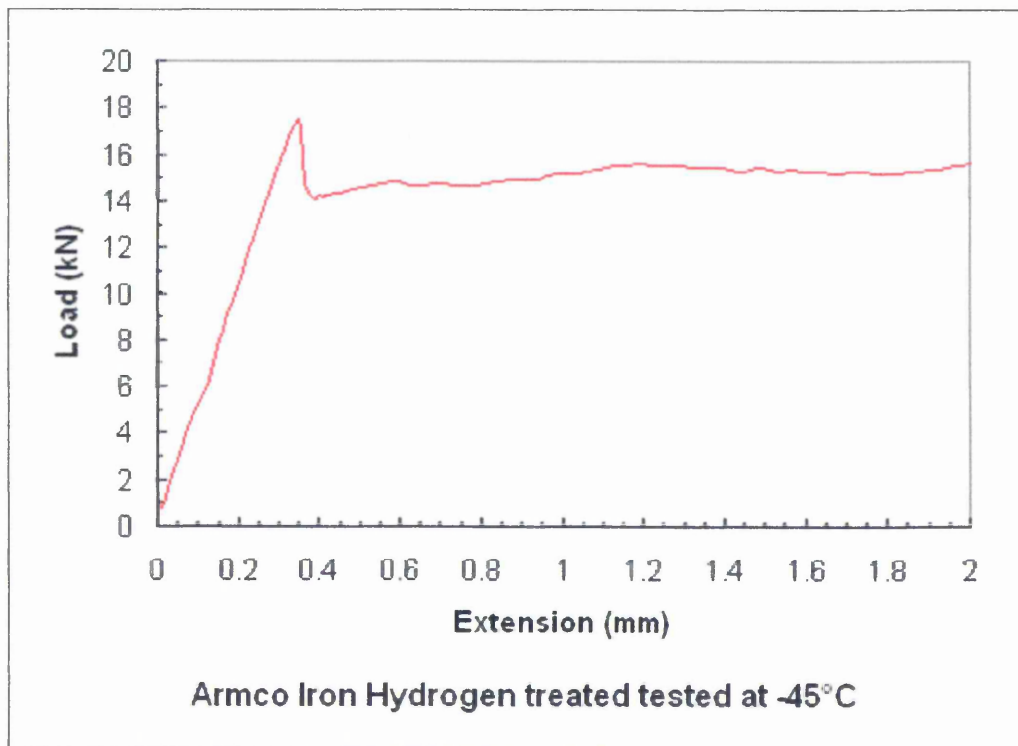
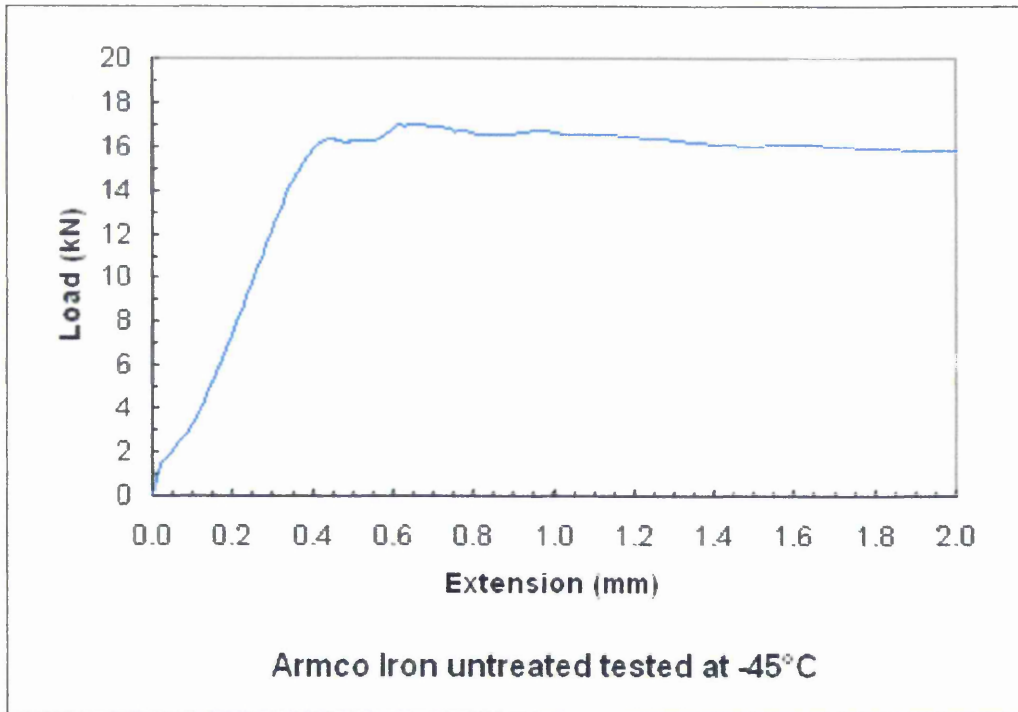
Solution : 1.0M Sulphuric acid
3.5% Sodium Chloride
10g/l Thiourea

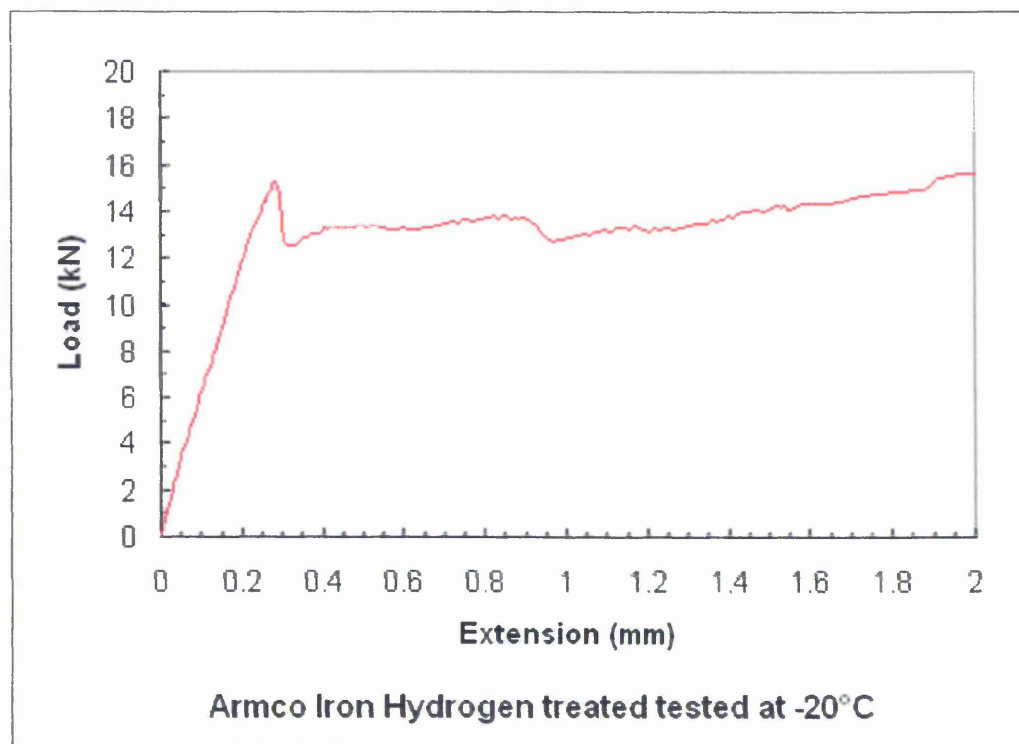
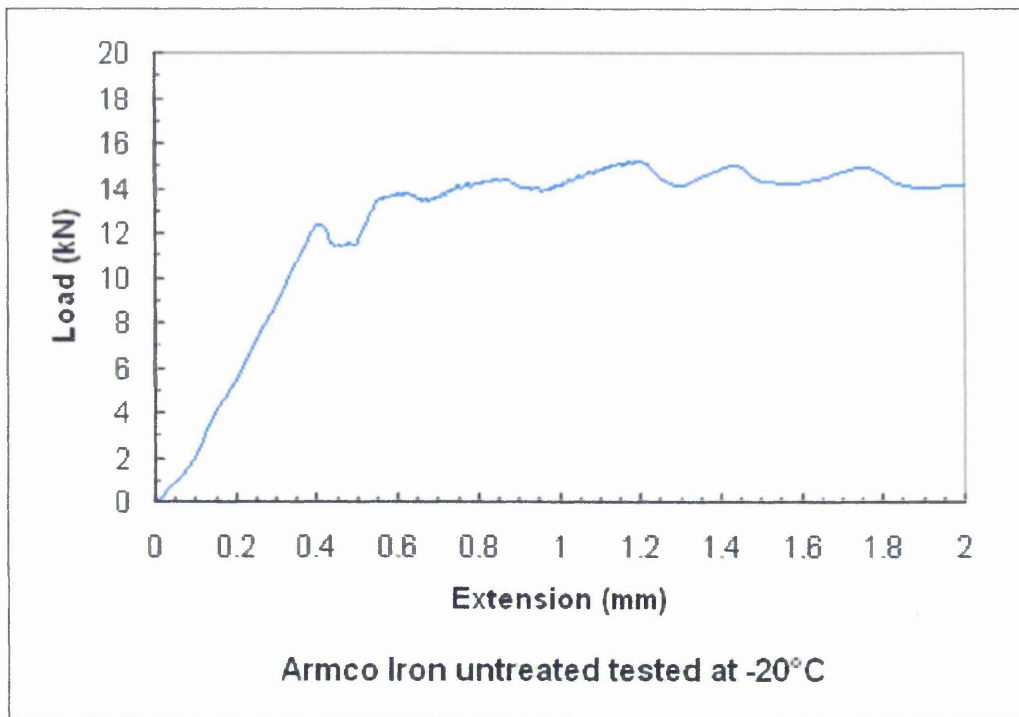
Potential : -1.2v SCE

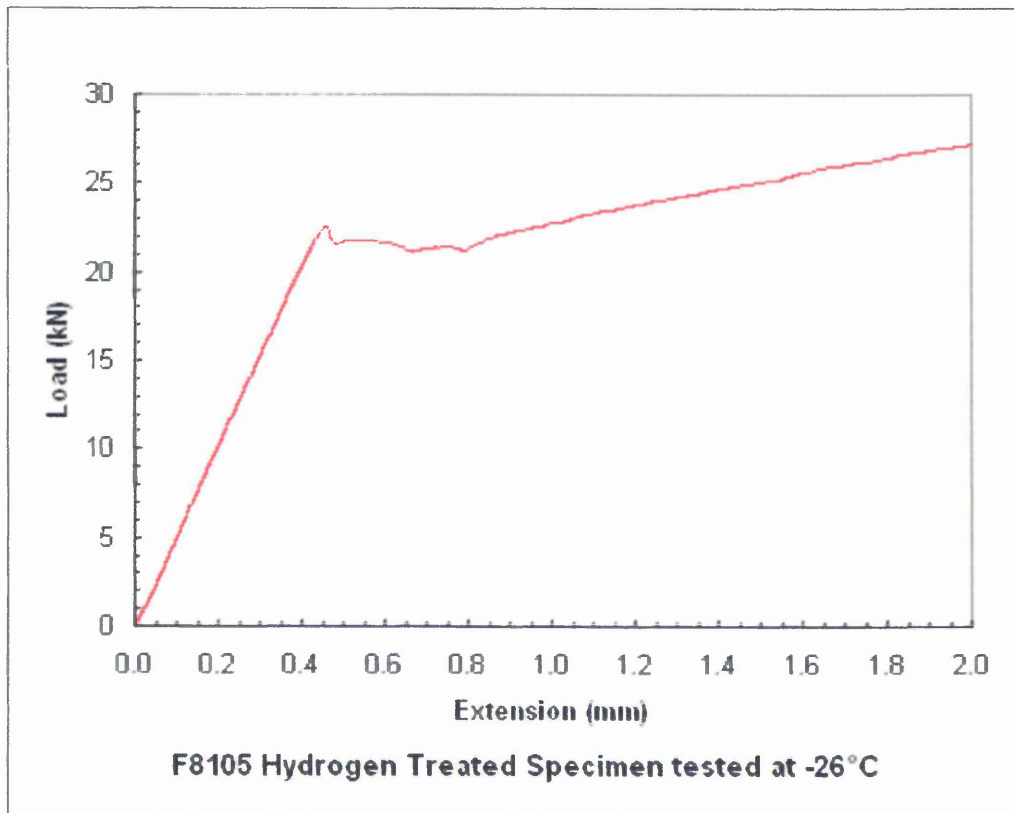
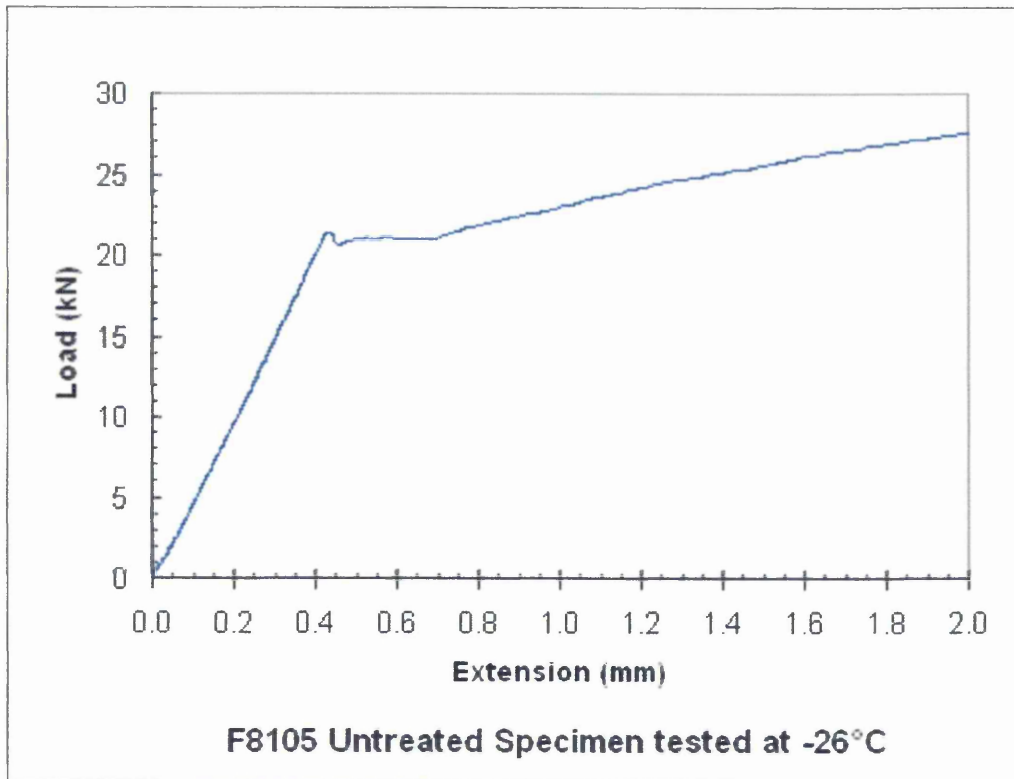
APPENDIX III

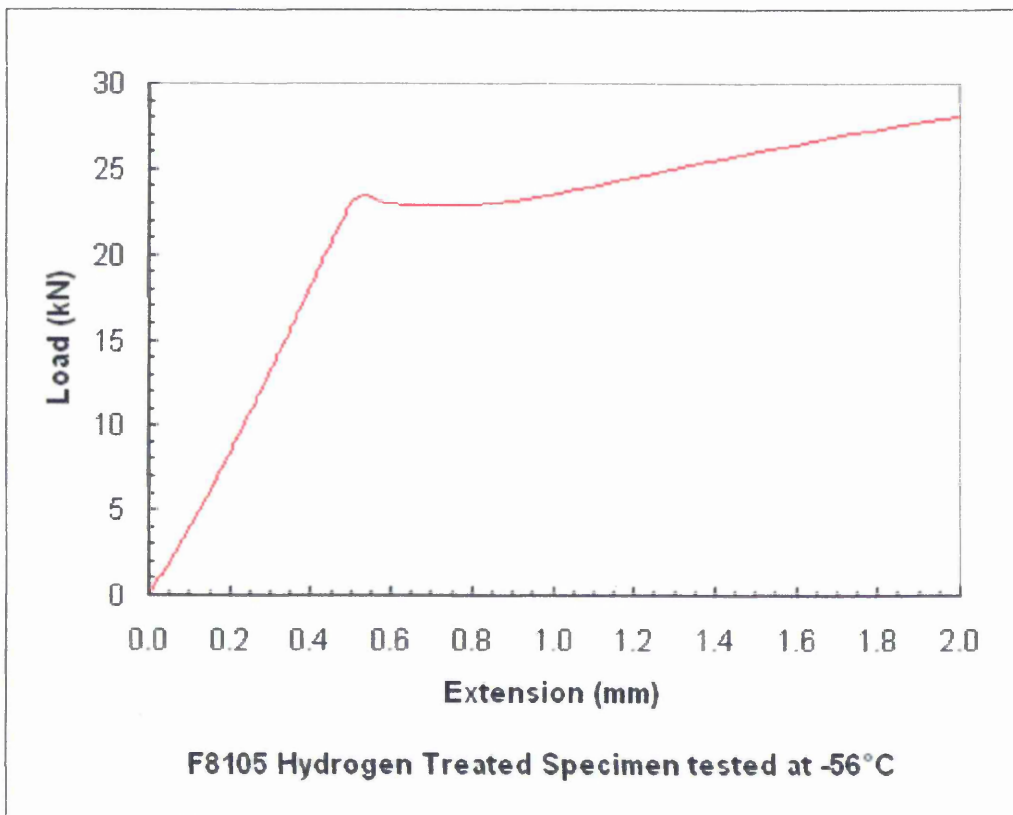
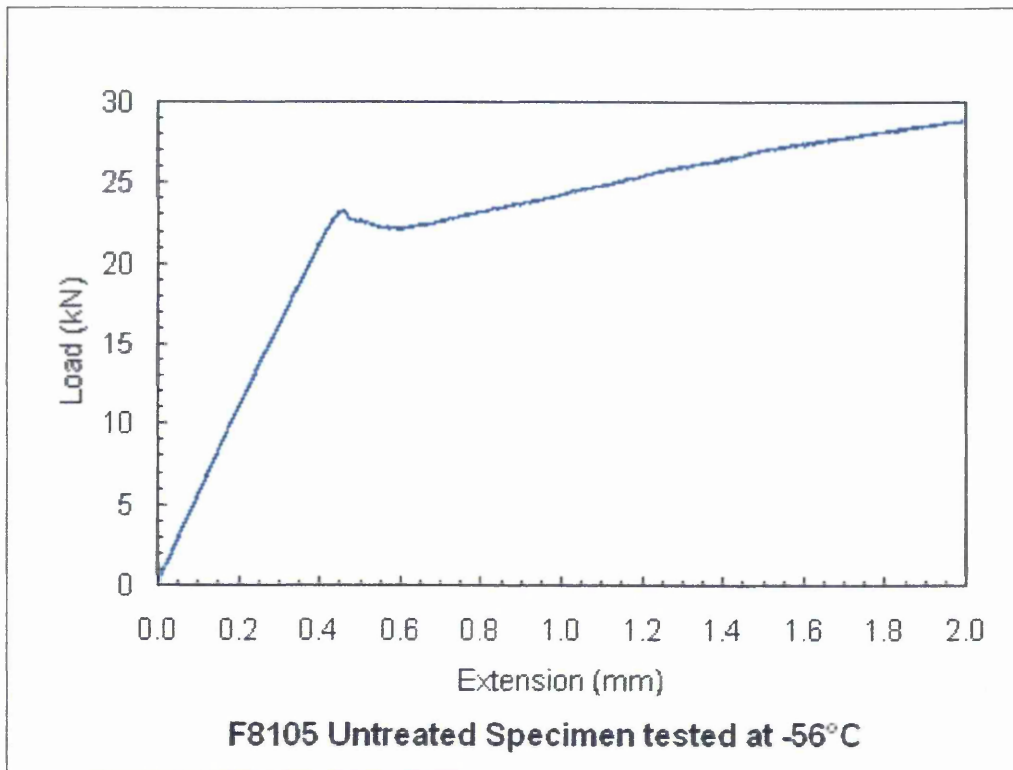
Load Extension Curves for Hydrogen treated and Standard Steel Specimens

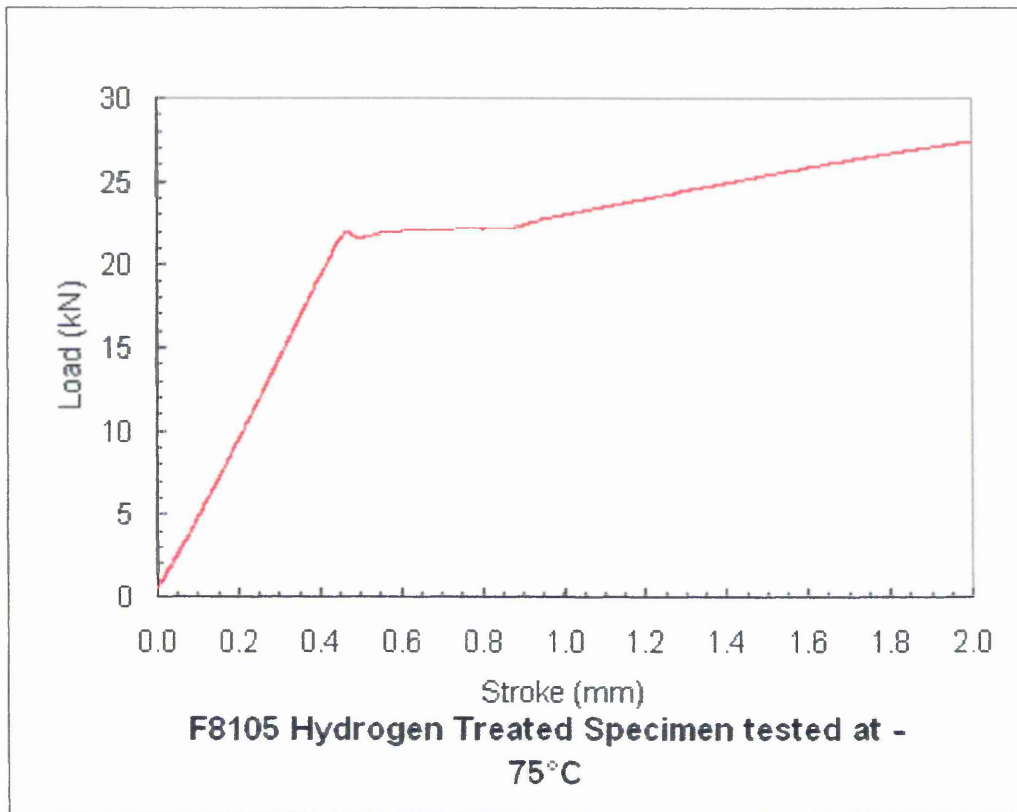












Data file for the untreated F8105 specimen was accidentally lost.

